

CHARACTERIZATION AND IMPLEMENTATION OF A DECELLULARIZED PORCINE
VESSEL AS A BIOLOGIC SCAFFOLD FOR A BLOOD VESSEL MIMIC

A Thesis Presented to the Faculty of
California Polytechnic State University, San Luis Obispo

In Partial Fulfillment of the requirements for the Degree
Master of Science in Biomedical Engineering

By
Aubrey Nichole Smith

May 2011

© 2011

Aubrey N. Smith

ALL RIGHTS RESERVED

COMMITTEE MEMBERSHIP

TITLE: Characterization and
Implementation of a
Decellularized Porcine Vessel as a
Biologic Scaffold for a Blood
Vessel Mimic

AUTHOR: Aubrey Nichole Smith

DATE SUBMITTED: May 27, 2011

COMMITTEE CHAIR: Kristen O'Halloran Cardinal, PhD

COMMITTEE MEMBER: Trevor Cardinal, PhD

COMMITTEE MEMBER: Lily Laiho, PhD

Abstract

CHARACTERIZATION AND IMPLEMENTATION OF A DECELLULARIZED PORCINE VESSEL AS A BIOLOGIC SCAFFOLD FOR A BLOOD VESSEL MIMIC

Aubrey Smith

Every 34 seconds, someone in the United States suffers from a heart attack. Most heart attacks are caused by atherosclerotic build up in the coronary arteries, occluding normal blood flow. Balloon angioplasty procedures in combination with a metal stent often result in successful restoration of normal blood flow. However, bare metal stents often lead to restenosis and other complications. To compensate for this problem, industry has created drug-eluting stents to promote healing of the artery wall post stenting. These stents are continually advancing toward better drug-eluting designs and methods, resulting in a need for fast and reliable pre-clinical testing modalities. Dr. Kristen Cardinal recently developed a tissue engineered blood vessel mimic, with the goal of testing intravascular devices. However, the scaffold component of this model exhibits several physiological limitations that must be addressed to create a truly biomimetic BVM. The current model uses expanded poly(terafluorethylene) [ePTFE] or poly(lactic-go-glycolide) [PLGA] as the choice material for the scaffold. ePTFE has several advantages as it is a widely recognized biomaterial. However, ePTFE is very expensive and lacks native mechanical properties. PLGA is another polymer that is created in-house to produce a uniquely tailored scaffold for use in the BVM; resulting in a cheaper alternative scaffold material. However, PLGA again lacks the necessary native mechanical properties to properly mimic an *in-vivo* artery. The creation of a biological scaffold will provide a unique biomimetic material to most accurately recapitulate the artery *in-vitro*.

Decellularization is the process of removing all cellular components from a tissue, leaving an acellular structure of extracellular matrix. Understanding the clinical problem and the

potential of the BVM, the aim of this thesis is to develop the decellularization process for the creation of a biologic scaffold as a replacement to the non-physiologic polymer scaffolds for the BVM. The first phase of this thesis was to develop and optimize an acceptable protocol for the decellularization of porcine arteries. The use of a 0.075% sodium dodecyl sulfate detergent was sufficient for complete removal of all vascular cell types, without significant degradation to the scaffold wall. In the second phase of this thesis, the decellularized scaffolds were mechanically tested to ensure retention of their native properties. The longitudinal and radial properties of the scaffold were found to be similar to the native artery, indicating the decellularized scaffold improves several physiologically aspects when compared to a polymer scaffold. These mechanical attributes improve the testing environment when evaluating stent deployment or new balloon angioplasty devices; as the decellularized scaffold has an physiological compliance. The final phase of this thesis examined the cellular adhesion capacities of the scaffold through recellularization with human umbilical vein endothelial cells (hUVECS). Fluorescent microscopy analysis suggests uniform attachment of cells along the length of the scaffold creating a monolayer. These results indicate this new scaffold type can develop an endothelium to complete the ideal, most physiologically relevant BVM system. Further optimization of the decellularization procedures could enhance the ability of the scaffold to be cultured for long-term interaction with intravascular devices.

Acknowledgements

I would like to thank Dr. Kristen O'Halloran Cardinal for her undying support and guidance; without her encouragement and passion for the tissue engineering field, this thesis would not be possible. I have been so fortunate to have you as an advisor, a mentor, and a friend. Without you Dr. Cardinal, I would not have pushed myself to excel through all my college endeavors. I would also like to thank my thesis committee members, Dr. Trevor Cardinal and Dr. Lily Laiho. You both have continually supported me and encouraged through this process. Additionally, Dr. Black from the Biological Sciences Department was integral to some the test preformed.

I would like to thank my fellow Tissue Engineering Lab members, Dimitri E. Delagrammaticas, Colby James, Chris Miracle, Dalton Chavez, and the rest of the team; it has been wonderful to work with and learn from all of you. I would especially like to thank Dimitri for starting my work in the lab and for laying the foundation of my thesis work. Colby, you were my go to guy when I first started in the lab. Dalton, you have always been a huge help with all my experiments. Finally Chris, thanks a million for all the help you have given me.

Additionally I would like to recognize my parents, Bill and Joni, whose love and continual support have helped me through college. I am truly blessed to have two parents who continually listen to and encourage me through my trials and tribulations. To Bryan, thank you for being my foundation, for supporting and loving me through these trying times; you are simply the best.

TABLE OF CONTENTS

LIST OF TABLES	xii
LIST OF FIGURES	xiii
LIST OF EQUATIONS	xvi
CHAPTER 1 – INTRODUCTION	1
1.1 Motivation	1
1.2 Cardiovascular Disease	2
1.3 Treatment of Coronary Artery Disease	3
1.3.1 Coronary Artery Bypass Grafting	4
1.3.2 Angioplasty and Stenting	8
1.4 Tissue Engineering Blood Vessels	12
1.4.1 Highlights of Tissue Engineering Blood Vessels	12
1.4.2 Synthetic Scaffold for TEBV	15
1.5 Biologic Scaffolds for TEBVs	19
1.5.1 The Use of a Decellularized Biologic Scaffold	20
1.6 Purpose of a Blood Vessel Mimic	23
1.6.1 The BVM Scaffold	24
1.7 Overview and Aims of the Thesis	25
CHAPTER 2 – DEVELOPMENT AND EVALUATION OF DECELLULARIZATION	
PROTOCOL	28
2.1 Introduction	28
2.2 Methods for Decellularization	31
2.2.1 Protocol Development	31

2.2.1.1	Static Decellularization Methods	32
2.2.1.2	Perfusion Decellularization Methods	32
2.2.2	Protocol Assessment	34
2.3	Results	35
2.3.1	Static Decellularization Results	35
2.3.2	Perfusion Decellularization Results	37
2.4	Discussion	39
CHAPTER 3 – CHARACTERIZATION OF DECELLULARIZED VESSELS		43
3.1	Introduction	43
3.2	Methods	44
3.2.1	Structural Evaluation	44
3.2.1.1	Hematoxylin and Eosin Staining	44
3.2.1.2	Scanning Electron Microscope Imaging	46
3.2.2	Mechanical Evaluation	48
3.2.2.1	Tensile Testing	48
3.2.2.2	Burst Pressure Evaluation	52
3.2.3	Biological Evaluation	53
3.3	Results	54
3.3.1	Structural Evaluation	54
3.3.1.1	Hematoxylin and Eosin Staining	54
3.3.1.2	Scanning Electron Microscope Imaging	56
3.3.2	Mechanical Evaluation	58
3.3.2.1	Tensile Testing	58

3.3.2.2	Burst Pressure Evaluation	61
3.3.3	Biological Evaluation	62
3.4	Discussion	64
3.4.1	Structural Evaluation	64
3.4.2	Mechanical Evaluation	66
3.4.2.1	Tensile Testing	66
3.4.2.2	Burst Pressure Evaluation	67
3.4.3	Biological Evaluation	67
CHAPTER 4 – USE OF DECELLULARIZED VESSELS IN THE BLOOD VESSEL MIMIC		69
4.1	Introduction	69
4.2	Methods	72
4.2.1	Short-Term Cultivation – Trial 1	72
4.2.2	Long-Term Cultivation – Trial 2	74
4.2.3	Dual Sodding Proof of Principle – Trial 3	77
4.2.4	Analyzing Images	82
4.3	Results	86
4.3.1	Short-Term Cultivation – Trial 1	86
4.3.2	Long-Term Cultivation – Trial 2	88
4.3.3	Dual Sodding Proof of Principle – Trial 3	91
4.4	Discussion	95
4.4.1	Short-Term Cultivation – Trial 1	95
4.4.2	Long-Term Cultivation – Trial 2	98
4.4.3	Dual Sodding Proof of Principle – Trial 3	100

CHAPTER 5 – DISCUSSION AND CONCLUSIONS	102
5.1 Overview and Summary	102
5.2 Challenges and Limitations	105
5.3 Future Work	107
5.4 Conclusions	109
LIST OF REFERENCES	110
APPENDIX A - ABBREVIATIONS	120
APPENDIX B – PROTOCOLS AND EXPERIMENTAL DETAILS	121
Appendix B.1 Determining the Optimal Concentration for Decellularizing Porcine	
Arteries	121
Appendix B.2 Perfusion Decellularization	124
Appendix B.3 Final Perfusion Decellularization	127
Appendix B.4 Histological Staining	130
Appendix B.5 SEM Preparation	132
Appendix B.6 Tensile Testing Protocol	133
Appendix B.7 Burst Pressure Protocol	135
Appendix B.8 Bacterial Evaluation	138
Appendix B.9 Tensile Testing Evaluation	140
Appendix B.10 Original Sodding Protocol	145
Appendix B.11 Acute 3T3 Sodding	148
Appendix B.12 Making the BBI Stain	151
Appendix B.13 Procedure for BBI Evaluation of Cell-Sodded Scaffolds	152

Appendix B.14 Long-Term Testing of Decellularized Vessels with hUVSMCs	155
Appendix B.15 Long-Term Testing of Decellularized Vessels with HUVECs	158
Appendix B.16 Cell Tracker Staining	162
Appendix B.17 Analyzing Cell Tracker Images	164
 APPENDIX C – Extra Data	 170
Appendix C.1 Higher Magnification Decellularization Pictures	170
Appendix C.2 Sample Tensile Testing Data	171
Appendix C.3 Summary Table of Raw Tensile Testing Data	176
Appendix C.4 Images and Average Cell Counts for 3T3 Sodding	177
 APPENDIX D – CIRM Translational Project	 180
D.1 Introduction	180
D.2 Methods	183
D.2.1 Decellularization Coating	183
D.2.2 Sodding scaffolds	184
D.2.3 Analysis	185
D.3 Results	188
D.4 Discussion	192

LIST OF TABLES

Table 1.1. The Clinically Used Synthetic Graft	8
Table 1.2. Comparison of Biologic Grafts	8
Table 1.3. The Comparison of the Biologic Verses the Synthetic Scaffolds	19
Table 2.1. Summary of Classifications for Each Concentration Sample	37
Table 3.1. Summary of Scaffold Classifications	56
Table 3.2. Summary of the Average and Standard Deviation	60
Table 3.3. Summary of Experimental Burst Pressures	62
Table 3.4. Summarized Averages Found in Literature	67
Table 4.1. Summary of Experiments From this chapter	81
Table 4.2. The Quantitative Characterization of the 3T3 Fibroblasts	88
Table 4.3. Average Number of hUVECs on Each Vessel	91
Table 4.4. Concentration for the Brightest Fluorescent Intensity	93
Table 4.5. 3T3s Visualized Pre and Post Trypsinization	93
Table 4.6. Skills Developed Through Experimentation with 3T3 Fibroblasts	97
Table 4.7. Summary of the Results from Recellularization the Decellularized Scaffold	101
Table C.1. Summary of Young's Modulus and Critical Yield for Tensile Tests	176

LIST OF FIGURES

Figure 1.1. Development of plaque in the coronary artery	3
Figure 1.2. The procedure for bypass grafting	5
Figure 1.3. The angioplasty procedure	9
Figure 1.4. Stenting procedure	10
Figure 1.5. Restenosis	11
Figure 1.6. Completely biological vessel	14
Figure 1.7. The BVM system	24
Figure 2.1. Scanning electron microscope (SEM) image of ePTFE	29
Figure 2.2. Luer lock barbs sutured to the scaffold	33
Figure 2.3. Peristaltic pump and orbital shake table utilized for decellularization	34
Figure 2.4. Images of static decellularized porcine arteries at various concentrations of SDS ...	36
Figure 2.5. Perfusion decellularization	38
Figure 2.6. Successful perfusion decellularization	39
Figure 3.1. Intact vs. not intact	45
Figure 3.2. A diagram for how an SEM operates	47
Figure 3.3. The TM3000 Tabletop Microscope used for imaging	47
Figure 3.4. A visual depiction of the cutting preparations for a tensile test	51
Figure 3.5. A representative image of the longitudinal cut made	51
Figure 3.6. The complete set up of pressure transducer, syringe, barbs, and scaffold	53
Figure 3.7. Scaffolds classified as ‘Intact’	55
Figure 3.8. Scaffolds classified as ‘Not Intact’	55
Figure 3.9. SEM images illustrate decellularized arteries	57
Figure 3.10. Images of intact native porcine arteries, with endothelial cell lining	58

Figure 3.11. Sample stress versus strain graph	59
Figure 3.12. The Young's modulus of native and decellularized vessels	60
Figure 3.13. Comparison of the critical yield for native and decellularized scaffolds	61
Figure 3.14. The TSA plate bacterial culture	63
Figure 3.15. Broth culture	64
Figure 4.1. Model of the bioreactor setup for the BVM system	71
Figure 4.2. Longitudinal cut of the recellularized scaffold	74
Figure 4.3. A setup of decellularized scaffold with the peristaltic pump and BVM	75
Figure 4.4. This image represents the six-well plates used in experiment 3	81
Figure 4.5. Top is a representative image of a Ronchi ruling	84
Figure 4.6. Trial 1 with 3T3 fibroblasts sodded	87
Figure 4.7. Trail 2, Experiment 1 with hUVSMC sodding	89
Figure 4.8. Trial 2, Experiment A H and E staining	89
Figure 4.9. Trial 2, Experiment B sodded with hUVECs	91
Figure 4.10. Comparison of cell distribution on vessels A and B	91
Figure 4.11. Cell Tracker Green intensity at various concentrations over a 7-day duration	92
Figure 4.12. Dyed 3T3 cells with and without trypsinization	94
Figure 4.13. Staining using Cell Tracker Green and Red	95
Figure B.1. Burst Pressure Images set up	137
Figure B.2. Microscope anatomy	153
Figure B.3. QCapture Pro control panel	154
Figure C.1. Higher magnification of decellularization	170
Figure C.2. Bottom A: BBI	177
Figure C.3. Top A: BBI	178

Figure C.4. Bottom B: BBI	178
Figure C.5. Top B: BBI	179
Figure D.1. The improvement of skeletal myoblasts on decellularized skeletal matrix	182
Figure D.2. The procedure for creating the decellularized coating matrix	184
Figure D.3. Scaffold sections	187
Figure D.5. H and E images of the cellularized ePTFE scaffold	190
Figure D.6. BBI images of the non-coated scaffold	190
Figure D.7. BBI images of the coated scaffold	190
Figure D.8. BBI cell counting	191
Figure D.9. Live and Dead stains on the ePTFE scaffolds	192
Figure D.9. Viability comparison of live HUVECs on ePTFE	192

LIST OF EQUATIONS

$\frac{Load(N)}{Extension(mm)} = \frac{N}{L}$	Equation 3.1	49
$E(Pa) = \frac{\sigma}{\varepsilon}$	Equation 3.2	49
$\sigma = \frac{Load(N)}{Area(mm^2)} = \frac{N}{t * w}$	Equation 3.3	49
$\varepsilon = \frac{Extension(mm) + length(mm)}{Length(mm)} = \frac{L + L_o}{L_0}$	Equation 3.4	49
$circularity = 4\pi \left(\frac{Area}{Perimeter^2} \right)$	Equation 4.1	82
$\frac{\text{Number of Vertical Lines}}{\text{Number of Pixels in the x direction}} = \text{the length of that side}$	Equation 4.2	84
$\frac{\text{Length of side 1}}{\text{Pixels on side 1}} = \frac{x}{\text{Pixels on side 2}}$	Equation 4.3	85

Chapter 1 - Introduction

1.1 Motivation

In 2010 in the United States, the occurrence of cardiovascular disease (CVD) has recently reached an all time high, affecting more than 81.1 million people per year according to the American Heart Association (1). Atherosclerotic build up in coronary arteries (known as coronary artery disease, or CAD) contributes to the majority of heart disease sufferers; about 17.6 million people in the U.S. (1). Since 1987 the development of metallic stents has greatly improved the effectiveness of traditional balloon angioplasty as a treatment for CAD (2). Stent design is an ever-improving technology. Specific areas of improvement include stent architecture, drug-eluting designs, deployment methods, and adjuvant drug therapies (3). Current methodologies for testing stents and other intravascular devices require the use of *in-vivo* animal models. The use of animal models requires money, time, and resources. As new stent designs develop daily, there is an increased need for a fast and reliable form of testing to bridge these devices to market. One potential solution is to create and implement a living *in-vitro* test model that serves as a conduit to represent a simplified human vessel.

The recently developed “blood vessel mimic” (BVM) has been shown to successfully evaluate the endothelialization of bare metal and coated stents, by using specific tissue engineering techniques to create a living *in-vitro* model (4, 5). Although most tissue engineered blood vessels are created with a goal being a treatment of CAD by creating bypass or replacement grafting, there is great potential for the use of engineered blood vessels as a consistent, accurate, and relevant pre-clinical testing modality for intravascular devices. The implementation of such a testing modality would improve the cost and accuracy of pre-clinical testing and potentially reduce the number of animal studies.

Previously, the BVM system was created using a synthetic polymer scaffold lined with human microvessel endothelial cells (HMVECs). However, this model has several limitations with regard to its physiological and mechanical properties. The ‘gold standard’ for the polymer scaffold material in the BVM has been, and is currently, expanded poly(tetrafluoroethylene), which is non-degradable and biocompatible. The ePTFE scaffold has been well characterized to support the development necessary to mimic the native vessel’s endothelium. It is however, subject to several disadvantages such as high cost, poor mechanical compliance, and inability to mimic the native extracellular (ECM) microstructure (physically and chemically). Therefore, the purpose of this thesis was to create a biologic scaffold to serve as an alternative scaffolding material to improve the BVM model.

The following sections of this Introduction will provide the background and foundation on which this thesis is based. A summary of coronary artery disease and treatments, including bypass grafting, angioplasty, and stenting will be provided. A review of tissue engineered vascular grafts (TEVGs) will be presented, with an emphasis on scaffolding. The Introduction will also include a review of the decellularization process, including the theory and methodology specific to TEVG development. The Introduction will conclude with the aims and overall goals of this thesis.

1.2 Cardiovascular Disease

The leading cause of death in the United States is heart disease, claiming more than 2300 lives per year (1 in every 2.9 American deaths) (1). On average 1 in 3 Americans is affected by one or more types of cardiovascular diseases (CVD) (1). CVD is an umbrella term for many specific types of heart and artery problems such as heart attacks, congenital heart defects, heart failure, stroke, CAD, peripheral artery disease (PAD), and some arrhythmias. High cholesterol,

poor diet, inactivity, high blood pressure, and obesity contribute to a person's increased risk for the occurrence of CVD (1). CAD is one of the most common types of heart disease, claiming approximately 1 in every 6 CVD patients and costing an average of \$11.7 billion per year (1). CAD occurs when there is plaque build-up in an isolated area of the artery as illustrated in Figure 1.1. When the plaque builds to the extent pictured in Figure 1.1B, a restriction of the blood flow occurs, which can cause angina, shortness of breath, heart attack, stroke and often death (6).

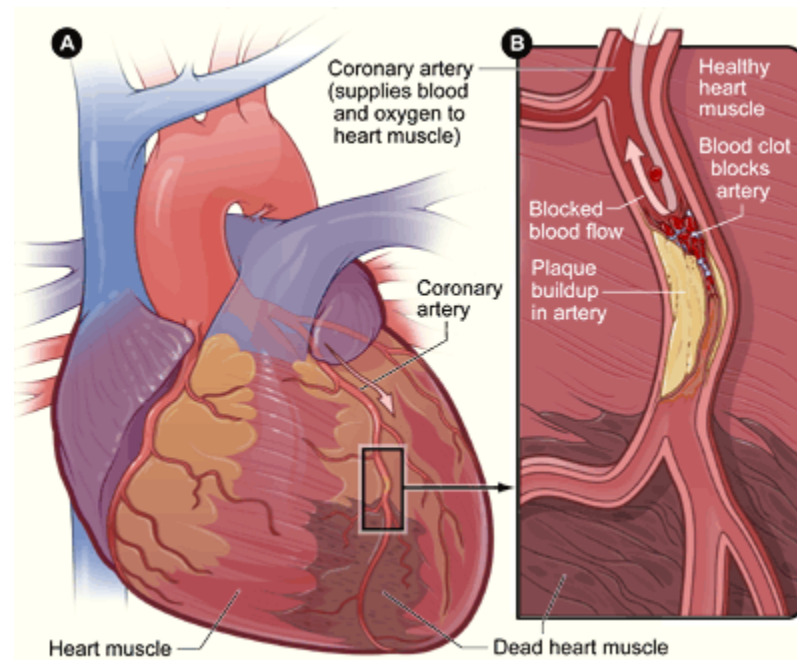


Figure 1.1. Development of plaque in the coronary artery. This type of blockage leads to CAD (7).

1.3 Treatment of Coronary Artery Disease

Common approaches and therapies used to treat CAD include changes in life style, drugs, a stent, or bypass surgery (8). Life style changes include a better diet, increased exercise, and quit smoking, or drinking. Drugs can be taken to help treat heart disease, by lowering blood pressure such as, hydrochlorothiazide and atenolol (9). A stent can be inserted into the occluded artery to re-open the artery to restore normal blood flow. Bypass surgery is performed only in

the worst case scenarios to create a new flow path for the blood around the blockage. All of these therapies can help to treat different severities of the disease. Due to their relevance to this thesis, bypass surgery and stenting will be reviewed in greater detail in the subsequent sections.

1.3.1 Coronary Artery Bypass Grafting

From 1996 to 2006 the number of cardiovascular operations and procedures increased by 33% annually, according to the American Heart Association's *Heart Disease and Stroke Statistics* in 2010 (1). Over 176,138 coronary artery bypass graft (CABG) surgeries were performed in 2007 (1). A bypass surgery aims to use an artery from the patient to use as a graft on the heart to redirect blood flow around the blocked portion of the artery, as illustrated in Figure 1.2. This procedure is the most common type of open-heart surgery, and is highly invasive to the patient (10). While CABG is expensive and requires a long recovery time, it has been successful long term with a lower rate of mortality, angina, and revascularization procedures than alternative methods (11).

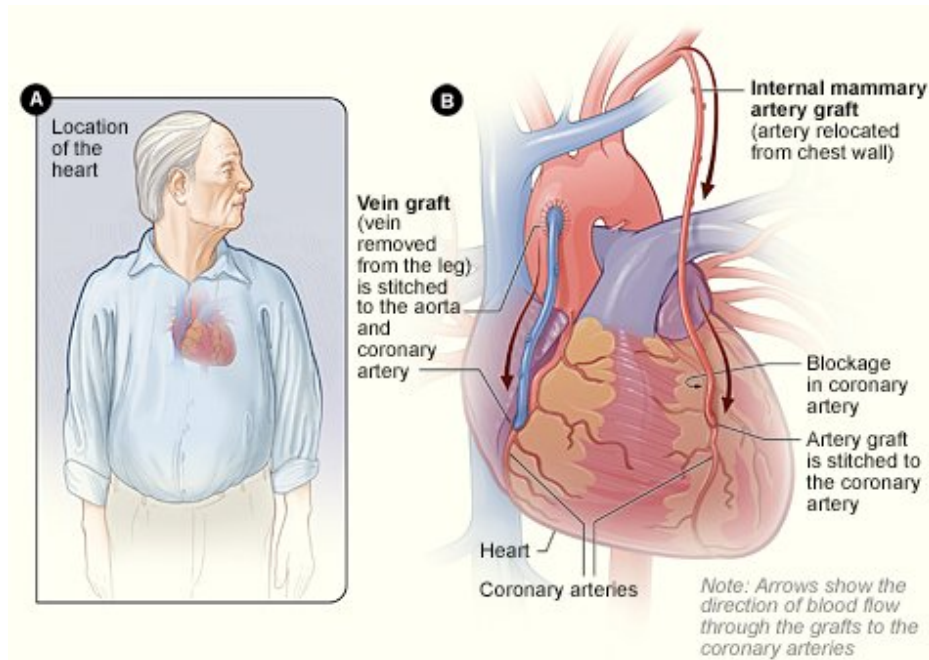


Figure 1.2. The procedure for bypass grafting. The graft is connected from the aorta to the distal part of the epicardial coronary arteries to redirect flow around the blocked portion of the coronary artery (10).

There are three main classifications for a biological bypass graft: autografts, allografts, or xenografts. Autografts utilize one's own vessels, usually the internal mammary artery or the greater saphenous vein. Less commonly used are the radial artery and lesser saphenous vein along with a few others (12). In any of these cases, bypass surgery is performed by isolating the graft from the host's leg, arm, or chest. It is then connected proximally and distally to the blockage in order to reroute the blood flow as shown previously in Figure 1.2. The chance of an immune response is low since the graft is from the host's body. Unfortunately only 60% of patients needing bypass surgery have suitable vessels for grafting (13). In most cases the patient suffers from a number of pre-existing cardiovascular diseases and therefore may have

atherosclerotic build up rendering any possible autologous vessels non-viable for grafting (13). If this is the case, either allografts or xenografts must be used.

The next most commonly utilized vessel type is an allograft, where the vessel is donated from an individual of the same species. Although donors are matched with a host, allografts have an increased risk for immune rejection, and patients will normally be placed on immunosuppressants to increase the graft's success (14). This is a suitable alternative for a native vascular graft, but the number of donors is in short supply. Finally, with the shortage of donor allografts and viable autologous vessels there has been an increase in exploration into xenogenic grafting. A xenogenic graft is donated from a different species, usually porcine. Pig vessels closely mimic the human physiology and size, but will elicit an immune response from the host (15, 16). This rejection is just as severe as allograft responses and will require the patient be on immunosuppressants (16, 17). Due to the limitations of xenogenic grafts, along with other biologic grafts, a synthetic graft is another plausible alternative to be utilized for CABG.

Synthetic grafts are well characterized for use in peripheral locations in the body and can be scaled up for high-throughput clinical uses. These types of grafts are commonly used for the larger diameter bypass procedures, but are currently not viable options for CABG, which requires a small diameter graft. For over 50 years, synthetic grafts have primarily been made of poly(ethylene terephthalates) [Dacron] and expanded poly(tetrafluoroethylene) [ePTFE] (18). Both of these materials have been used clinically for peripheral applications and have become well characterized and clinically tested with successful outcomes for large diameter (>6 mm) vessels (18). Although a synthetic material is a seemingly suitable choice for an alternative CABG material, there are several disadvantages regarding the lack of physiological attributes. Synthetic

grafts lack the appropriate endothelium, have little to no compliance, and have high thrombosis rates in small diameter grafts (19). Specifically, the lack of an effective endothelium contributes to the onset of intimal hyperplasia and thrombus formation, rendering the graft not functional for use in CABG grafting procedures (20-22). To improve the functionality of the graft, the development of a surface endothelialization of Dacron and ePTFE has shown a reduction of the thrombogenic effects normally seen *in-vivo* (23). There are several other treatments that can be performed on synthetic grafting material such as chemical modifications, heparization and protein coatings to improve the functionality of the graft (24). These treatments do help in short term, *in-vivo* applications, but still tend to end in a graft failure via hyperplasia or thrombosis long term evaluation (24, 25). Table 1.1 and 1.2 summarize the potential bypass grafts for synthetic grafts (Table 1.1) and a comparison of biological grafts (Table 1.2). To summarize, the use of either a synthetic or natural graft as a CABG material has specific individual limitations, resulting in a high demand for new materials and/or alternative treatments for CAD.

Table 1.1. The Most Clinically Used Synthetic Graft (18).

<i>Vascular substitute choice</i>	Vascular regions				
	Large-caliber arteries (≥ 8 mm)	Medium-caliber arteries (6-8 mm)	Small-caliber arteries (≤ 6 mm)	Venous reconstructions	Hemodialysis arterio-venous access
	Aorta, arch vessels, iliac and common femoral arteries	Carotid, subclavian, common femoral, visceral and above-the-knee arteries	Coronary, below-the-knee, tibial and peroneal arteries	Superior and inferior vena cava, ilio-femoral veins, portal vein, visceral veins	Upper > lower extremity
<i>1st choice</i>	Prosthesis (Dacron, ePTFE)	Prosthesis or autograft (equal)	Arterial or venous autograft	Saphenous spiral vein graft, deep venous autograft	Native material
<i>2nd choice</i>	Allograft, deep venous autograft	Prosthesis or autograft	Composite graft, vein interposition, prosthesis (ePTFE, Dacron), allograft, biosynthetic	Allografts, ePTFE, Dacron, biografts	ePTFE, PU, xenografts, biografts, TEBV (clinical trial)

ePTFE (expanded polytetrafluoroethylene), PU (polyurethane), TEBV (totally-engineered blood vessels).

Table 1.2. Comparison of Biologic Grafts (18).

	Autografts		Allografts (homografts)		Xenografts (heterografts)
	Arterial	Venous	Arterial	Venous	
<i>Advantages</i>	Closest approximation, less diameter mismatch, internal mammary artery anatomically nearby, excellent function	Durable and versatile, good results, infection resistance, relative availability	Off the shelf availability, better resistance to infection, transplant-recipient patients		
<i>Disadvantages</i>	Availability, vasospasm (radial artery), donor site morbidity	Availability, harvest injury, vein graft disease	Antigenicity, graft deterioration, early occlusions, chronic rejection, intake of drugs, infection risk		
<i>Healing</i>	Intimal thickening, myointimal hyperplasia (radial artery)	Endothelial desquamation, vein dilation, wall thickening, arterIALIZATION, re-endothelialization	Endothelial denudation, immune response, fibrotization		
<i>First use</i>	Jaboulay and Briau 1896	Goyannes 1906	Gross <i>et al.</i> 1948	Linton 1955	
<i>Review e.g.</i>	Nezic <i>et al.</i> 2006	Cooper <i>et al.</i> 1996	Fahner <i>et al.</i> 2006	Dardik <i>et al.</i> 2002	Schmidt and Baier 2000

1.3.2 Angioplasty and Stenting

There is one procedure that is commonly performed on CAD patients that does not require open-heart surgery and can open a partially blocked artery to restore normal blood flow.

This procedure is called angioplasty and it is mainly used on CAD patients who have not reached a life threatening point. It has been performed in over 1,300,000 patients in the United States, in 2006 according to the American Heart Association (1, 26). To perform angioplasty, a balloon catheter is inserted into the patient's heart via their femoral artery near the groin. The balloon is expanded at the blockage area, compressing all the plaque to the outer most diameter of the vessel, and re-augmenting restoring proper blood flow, as illustrated in Figure 1.3 (27).

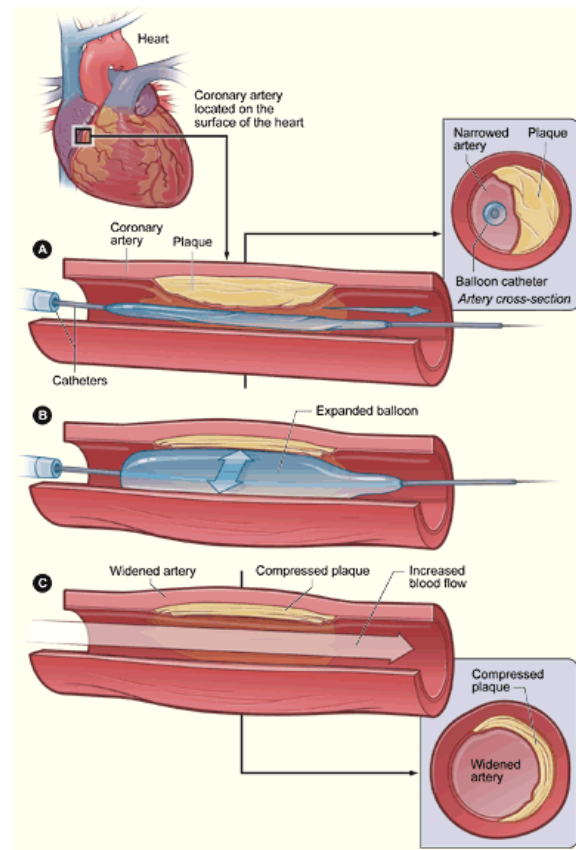


Figure 1.3. The angioplasty procedure. A balloon catheter is inserted to the blocked area(A), expanded to compress the plaque (B), then deflated and removed (C) (27).

Unfortunately, this procedure restores blood flow temporarily, this simple compression does not maintain long lasting results; and restenosis, narrowing of the artery, commonly occurs. To augment a longer compression on the plaque, a bare metal support (stent) was developed to deploy with the help of the balloon during angioplasty (26, 27). When deployed, the metal stent

expands to its full diameter, it pushes the blockage radially towards the wall of the vessel, reopening flow through the artery, as illustrated in Figure 1.4 (26). This stent would remain in place permanently to keep the vessel open. Since 1987 approximately 80% of all angioplasties incorporated the deployment of a stent, consequently the restenosis rate was reduced by 50 % (1).

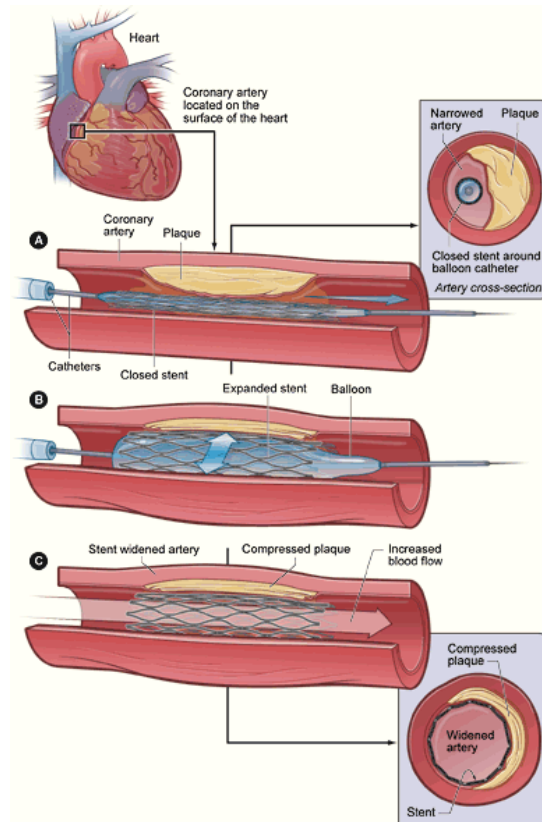


Figure 1.4. Stenting procedure. The balloon catheter with a collapsed stent is placed in the area of the blockage (A). The balloon is expanded along with the metal stent to deploy the stent, (B).

Then the balloon is deflated and removed while the stent remains in place (C) (27).

While the use of a stent extends the effects of the angioplasty procedure, in-stent restenosis is a common complication with bare metal stents (26). In-stent restenosis occurs when plaque starts to re-form near and around the stent, recreating the original blockage problems (26, 27). This process is illustrated in Figure 1.5, the bare metal stent displaces and

disrupts the normal layer of plaque and the endothelium of the vessel causing an increase in inflammation. The inflammation expands the vessel wall and becomes extremely sticky causing components in the blood stream to attach to the build up and cause further narrowing of the vessel.

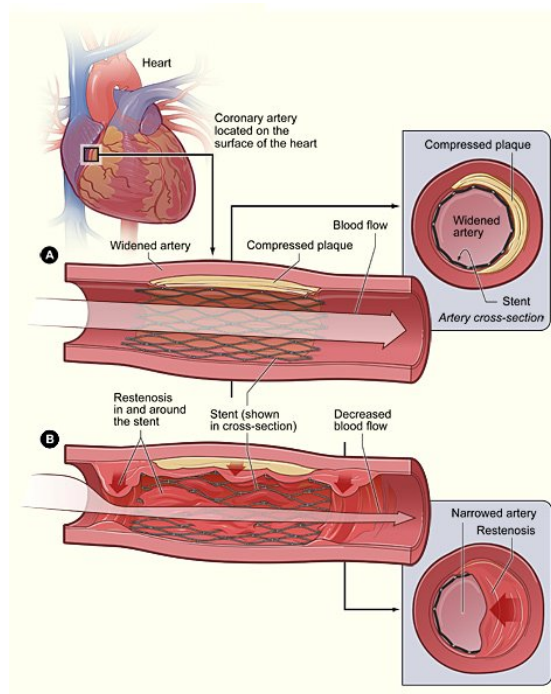


Figure 1.5. Restenosis. The stent remains in place throughout time (A), but the endothelium becomes inflamed and restenosis occurs (B) (27).

To reduce restenosis, researchers have recently improved the bare metal stent by coating it with a time-releasing drug, known as a drug-eluting stent (26). The released drugs typically prevent cell proliferation, thereby inflammation. Through this specific, localized application of the drugs to the intima of the blood vessel, the responses to stenting have become more successful. Additionally, researcher's focused on the characterization and development of the specific drugs and their elution profiles, as well as the acute and chronic healing responses. To encourage the continued advancement with the stenting technology, these devices should be

carried through for FDA approval for use in the clinical setting as quickly as possible. Thus, the development of a high throughput, consistent *in-vitro* testing modality could serve as a primary way to assess the utility of these specific and unique stents in a timely manner.

1.4 Tissue Engineered Blood Vessels

In the past 10 – 15 years there has been extreme progress in cell biology and cell culture, leading to the creation of the tissue engineering field (28). As tissue engineering is newer science, many human tissues have recently been researched and developed; to name a few, TEBV, skin, bladder, heart valves, and cartilage (29). Tissue engineers have focused on these areas not only because of the large clinical need, but also because they have relatively simple structures that can be mimicked with synthetic or natural scaffolds. The main goal of tissue engineering is to recreate functional tissues and organs with cultured human cells for the production of replacement tissues (28). In the case of a TEBV, the goal is to create an autologous vascular graft for bypass surgery. However, as previously mentioned, it is also possible to engineer a blood vessel for use in preclinical device evaluation. Tissue engineering manipulates material properties to produce a unique configuration to mimic a specific tissue and help thousands (4).

1.4.1 Highlights of Tissue Engineered Blood Vessels

The development of tissue engineered blood vessels made its debut in published literature in the 1980's, with vessels utilizing a synthetic (Dacron) or biologic (collagen) scaffold (30, 31). As TEBVs have developed, the addition of endothelial cells (ECs), smooth muscle cells (SMCs), and fibroblasts have modeled a more physiologically relevant scaffold, representing the various layers of a blood vessel (4, 19, 32). In 1986, Weinberg and Bell were the first to develop a vessel composed primarily of biological components: bovine aortic ECs

(BAECs), SMCs, and fibroblasts on a layer of collagen (33). The collagen and SMCs were jelled together using a casting media in a tubular mold with a centrally located mandrel, to represent the media of a vessel. Then a Dacron sleeve was placed around the exterior of the tissue engineered 'media' and drip seeded with fibroblasts to enhance mechanical properties of vessel and mimic the adventitia. After one week of culture, the central mandrel was removed to present a lumen to be pressure seeded with BAECs. The mechanical strengths along with the scaffold structure of this vessel mimicked the mammary muscular artery, representing the first TEBV with increased physiological relevance and durability (31).

Soon after Weinberg and Bell's biologic scaffold, Foxhall et al. experimented with the application of endothelial cells on Dacron grafts (30). In attempts to simplify the development of a TEBV, Foxhall et al. worked with different coatings to promote endothelization. Collagen and fibronectin were coated on the luminal surfaces of Dacron resulting with a surface that significantly increased the proliferation of endothelial cells (30). This synthetic scaffold was thought to have a greater potential for use as a small diameter vascular graft (30). Results indicated that the scaffold had similar *in-vitro* properties as a mammalian muscular artery and could be used to study the cellular interactions with a vascular ECM.

In 1998 L'Heureux et al. developed a construct to improve upon Weinberg and Bell's mostly biological scaffold (28). This scaffold utilized a simple collagen sheet which was seeded with human vascular SMCs and wrapped around a small mandrel, to represent the media of a vessel. Then a similar sheet seeded with fibroblasts was wrapped around the exterior of the SMCs, to mimic the adventitia, as seen in Figure 1.6. Finally, the mandrel was removed and the lumen was seeded with ECs (28). The L'Heureux et al. vessel was completely biologic and had the potential for natural remodeling and reduced foreign body reactions. Unfortunately, this model had limited mechanical strength and tears would occur when used on its own (28). The

development of these and several other scaffold types created the ground work for future TEBVs. These scaffolds have many basic qualities, such as the proper cell type, natural shape, and a microstructure that increased the scaffold's physiological relevance (34). With these strong foundations, many researchers branched out to create countless types of tissue engineered grafts with the goal of transitioning these models into clinical applications for CABG.

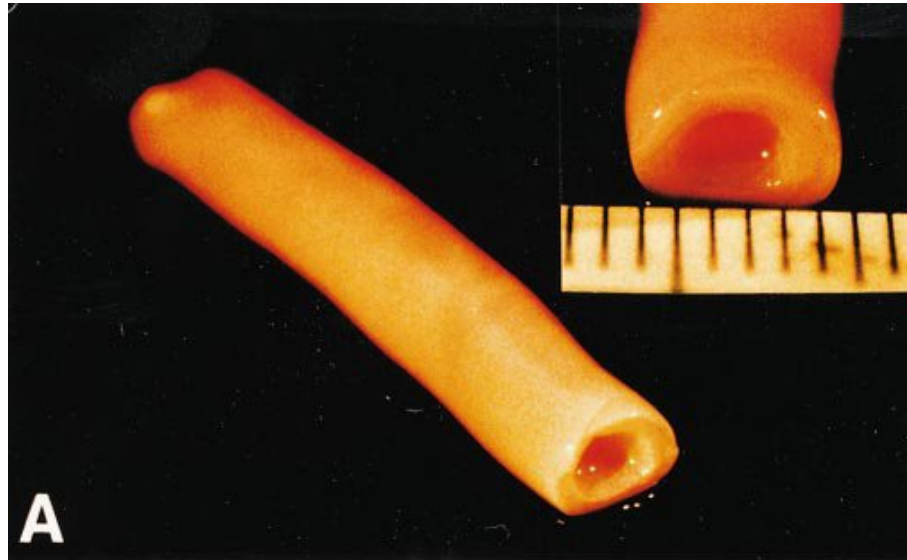


Figure 1.6. Completely biological vessel (28).

Through the development of TEBV, several qualities have been identified to be extremely important to the graft function. The development of the microstructure is one of the most important aspects to be taken into consideration during the scaffold selection process. To create a comfortable 'living environment' for cells, the microstructure of a TEBV scaffold should have small fibers that are randomly interconnected to create a unique porous scaffold. Having the proper structure onto which the cells can anchor will encourage strong cell adhesion, and contribute to the ability of the cells to proliferate and express normal endothelial cell markers, to communicate with the surrounding tissues for potential remodeling, thus increasing the scaffolds overall physiological relevance (18). These are achieved by having a microstructure that closely mimics the native ECM (18). The ECM for native blood vessels is

constructed of nanofibers about 100 nm that are layered in random orientation, eventually producing a porous wall (29, 35-37). Blood vessel ECM consists of mostly collagen, fibronectin, glycoaminoglycans, elastin, and laminin (29). These components will interact with the ECs to aid in cell adhesion, integration with neighboring tissues as well hemodynamic interactions (35). To create a TEBV, the graft which best represents the native microstructure and components will be the most advantageous for a successful vessel.

1.4.2 Synthetic Scaffolds for TEBV

Synthetic scaffolds have been most frequently used in recent history for clinical and investigational applications of a TEBV(18). The material properties for synthetic scaffolds are generally well characterized with reproducible and consistent results when tested for the ability to physically function as a graft (28). Synthetic scaffolds have a high but acceptable burst strength, positive surgical handling, and is usually biocompatible (28). Non-degradable synthetic polymers which are most often utilized in a TEBV are poly(ethylene terephthalates) [Dacron] and ePTFE (4, 18, 28). Dacron and ePTFE are both a highly crystalline and hydrophobic materials, that reduce the overall elusion of particles (contributing to the overall biocompatibility) and structural integrity (18, 32). The widespread use of synthetic scaffolds occurs because the material characteristics have widely accepted microstructure, reproducibility, and biocompatibility (32). Scaffold properties can be changed by specifically manipulating given components of the polymer makeup, thus changing the microstructure (32). For example, ePTFE can be manufactured to have varying intermodal distances by knitting the basic polymers together (32). This manipulation will contribute to the way the cells interact with the scaffold; knitting the polymers will produce a microstructure with a large surface area increasing the ability for coatings and cells to anchor to the material (32). The knitted construction of the

scaffold increases the intermodal distance from the well characterized 30 μ m to an experimental 60 μ m (32). Although cells adhere better to these more porous surfaces, the mechanical properties are weakened, causing the scaffold to undesirably kink (32). Even though these materials are well characterized, many researchers are trying to improve upon the basic design to create new scaffolding material.

In addition to the non-degradable scaffolds summarized above, there are also other degradable synthetic scaffolds, such as polyglycolic acid (PGA) (32), which have quickly become more prevalent than non-degradable materials for TEBV. PGA along with other degradable scaffolds can be manufactured to have unique microstructures. Scaffold microstructure alterations may include increased porosity for better cell adhesion, a variety of degradation profiles for drug delivery or integration with the host, as well as specific mechanical properties for improved surgical handling or overall strength improvement (32, 38). These are only a few select examples of scaffold properties that may be manipulated to tailor the capabilities of a particular scaffold. The properties of synthetic scaffolds have encouraged their wide spread acceptance as a tissue engineering material and will continue to be used for TEBV.

While synthetic scaffolds are extremely controllable, predictable, and reproducible, there are still downfalls in their fundamental construction. For example, ePTFE does not contain a media or adventitia layer, which contributes greatly to the scaffold's ability to mimic an artery. This downfall limits the physiological relevance of the scaffold, because it has an inability to remodel and react to signals sent by the endothelium (4, 32, 39). The inability to have a communication with the cells on the scaffold will limit the abilities of the scaffold to naturally heal and change with the environment, if used in a CABG procedure (39). The lack of communication may lead to an increase in the foreign body response and chronic inflammation (28). Low performance as a physiological scaffold will increase the rate at which an *in-vivo*

vessel will have thrombogenic occurrences (40). Some of these downfalls of a synthetic material can be improved by conditioning or coating the scaffold with native proteins (such as collagen or fibronectin) or molecules (such as nitric oxide or adhesion molecules) to improve cellular interaction with the material (32). To address the limitations of synthetic materials biologic materials have been explored and developed for TEBV.

The production of a combination scaffold aims to combine the best of a synthetic and biologic material. These scaffolds are fabricated by combining a synthetic material with a biologic component (usually collagen) to produce a tubular vascular scaffold. There are several different manufacturing processes to create different mechanical properties of the material and can be a highly controlled process. This control will directly influence the mechanical properties, as well as the cellular interface with the biologic components (32). These improvements help to improve the physiological relevance of the scaffold. The production of these types of scaffolds relies heavily on creating a unique, intricate, porous scaffold as a structural foundation. One way researchers have been able to create these types of scaffolds is through a process termed electrospinning (32). Electrospinning is the process of charging a solution as it is pushed out of a syringe towards a spinning mandrel, which is grounded as a collector for the polymer/biologic solution (32). This process creates a tubular scaffold that can have micro to nano-sized fiber diameter with randomly orientated porous walls (32). While the composition and core development of the scaffold is more ideal than other synthetic materials, there are ways to improve the basic structure to better mimic the ECM. In the case of electrospinning, altering the voltage charge on the syringe or the distance between the source and the collected will alter the fiber diameter of the scaffold (41). Electrospinning has produced nanofibers that have enhanced mechanical properties while maintaining biocompatibility (41). However, the process for determining the right combination and concentration of the blend is

difficult, time consuming, and can become quite costly. If the electrospun scaffold has the proper fiber size, porosity, and mechanical strength, the fibers may still have limited cell adhesion, migration, proliferation, and differentiation properties due to the unique material made up of the scaffold (41). Continued research with the various combinations of parameters may produce a better scaffold. While the combination of biologic and synthetic materials produces a scaffold with more physiological attributes, the more biologic components that are incorporated can only improve the capabilities of the scaffold. The biological components are derived from natural growth factors and proteins, which mimic the ECM and should be maximized for the most physiologically relevant scaffold.

As will be described in more detail in the next section, there are several methods to create a biological scaffold or manipulate a synthetic scaffold. However, the most efficient and pertinent construction of a scaffold will depend on the desired properties and applications of the scaffold. To narrow the choices down, many properties of the scaffold should be considered including mechanical strength, biocompatibility, porosity, and cellular interaction to better classify the material. Identification of the properties that are crucial to the functionality of the scaffold's final application is imperative to select the most appropriate scaffolding material. To better understand the information previously described, Table 1.3 represents a summary of the essential differences between a biologic scaffold and a synthetic scaffold. Once a scaffold material is selected, it can be used for many different applications, all leading towards improving knowledge and treatments for CVD.

Table 1.3. The Comparison of the Biologic Verses the Synthetic Scaffolds.

Characteristics	Mechanical Properties	Ability For Structural Manipulation	Compliance	Protein Interactions	Immune Response	Small Diameter Potential	Repair and Remodeling Potential	Consistency
Synthetic	Strong	Strong	Weak	Weak	Weak	Weak	Weak	Strong
Biologic	Weak	Weak	Strong	Strong	Strong	Strong	Strong	Weak

1.5 Biologic Scaffolds for TEBVs

Although synthetic scaffolds have certainly demonstrated significant progress and success for use in TEBV research, another significant scaffold choice for a TEBV is the use of biologic material. A biologic scaffold, is commonly composed of materials naturally found in the ECM of vessels or arteries, such as collagen or fibrin (32, 42, 43). These scaffolds can be composed of the entire ECM by decellularizing a native vessel, or contain a combination of a polymer and biologic components as discussed earlier (32). Once again the desired properties of the scaffold will determine which of these methods may best be utilized for the proper result. The following is a brief overview of the development of various biologic scaffolds.

As discussed previously in the history of TEBV, Weinberg and Bell along with Foxall in 1986 were among the first to develop a TEBV composed of biological components using ECs, SMCs, and fibroblasts mixed with collagen (30, 33). This ground work provided a solid foundation for other researchers such as Yuan et al. in 1994 and L’Heureux et al. in 1998 to develop similar constructs (28, 33). While these scaffolds improved the biological interfaces compared to synthetic materials, the man-made completely biologic vessel lacked the mechanical strength to be used *in-vivo* (28). In attempts to increase the mechanical strength and overall construction of a biologic vessel, researchers looked into isolating the primary tissue source and removing all of its cellular components (40). This cellular removal process is known as decellularization and has been utilized to develop a scaffold that maintains its structural integrity,

while retaining its native biological components (40). The use of primary tissues as a scaffold was first developed in the 1960's when researchers thought that by cross-linking the tissue, the immunogenic effects would be reduced enough to create a viable scaffold source (44). The lowered immune response occurred through crosslinking, but mechanical properties were lost and cell death occurred (44). Laka et al. in 1989 decided to use a detergent to break cellular bonds from the ECM, leaving an acellular, biological graft (44, 45). This chemical decellularization process provided more desirable mechanical results without the detrimental effects of fixation (45). From this original paper, many other researchers further developed the decellularization process (44). There are many applications for which decellularization may be utilized; essentially any tissue that can be isolated can be decellularized. The major benefit of decellularization is not only the potential to create scaffold with ideal microstructure and mechanical properties, but also its reduction to the basic biological components that are seen throughout the animal kingdom, thus limiting immunogenic effects of a graft while increasing the potential tissue sources (45, 46).

1.5.1 The Use of a Decellularized Biological Scaffold

Utilizing a decellularized scaffold may improve the current issues with 'man-made' TEBV. As described in the previous section, decellularization is the systematic removal of all cellular and nuclear components from tissues to leave the complex mixture of functional and structural proteins that form the native ECM (47). The removal process is gentle enough to minimize its effects on the composition, biological activity, and mechanical integrity of the remaining ECM (47). When the cellular components are removed from the native ECM, most of the protein material that remains is conserved among species (47). Having a native structure that

is tolerable across many species opens a huge field for the potential to use xenogeneic and allogeneic grafts, which makes scaffold sources easily and widely available (47).

The process of decellularization usually entails physical agitation and a chemical treatment. Trypsin, ionic solutions, or detergents can be utilized to disrupt cellular membranes and their bonds to the ECM (47). Physical agitation is usually performed via sonication, mechanical pressure, or a freezing and thawing cycles in order to pull cells away from the scaffold once the cellular bonds are broken (47). Once all of the cells are removed the extracellular matrix of the original tissue is all that remains. Through this relatively simple process, a scaffold with the native microstructure and protein make-up can potentially serve as an ideal scaffold to engineer new tissues.

To elaborate on the widespread used of decellularization in the creation of tissue engineered materials, the following will briefly describe a few applications of this process. Ott et al. have worked to decellularize an intact rat heart. Perfusing a sodium dodecyl sulfate (SDS) solution, a common detergent, through dissected rat hearts produced an enacted acellular rat heart (48). After numerous rinses to remove excess SDS, the heart scaffold was recellularized with neonatal cardiac cells, and contractions occurred with an electrical stimulus (48). This work effectively showed how the decellularization process can be utilized to create tissues with the most accurate native architecture, encouraging this process's continued used. The development of a decellularized vessel can be seen through Schanner et al.'s work in 2004 (49). The protocol used SDS to break cellular bonds from a porcine carotid blood vessel to produce a natural scaffold, composed only of blood vessel ECM. Another example of decellularization for tissue engineering can be seen with decellularized bladders, where the native viscoelastic behavior of the scaffold is vital to the overall function of the bladder (50). Through declularization, the architecture of the scaffold remains intact and thus enables the bladder to maintain the

mechanical strength needed for contraction and relaxation (50). Though these are only a few specific examples of decellularized tissues, the overarching idea behind decellularizing tissues is to keep the essential properties of that tissue intact to produce the most physiologically relevant scaffold.

Although the potential attributes are numerous, there are some disadvantages to using the decellularization process. The production of the scaffold tends to be a more laborious process while not consistently showing improvement over many synthetic scaffolds (40, 47). The decellularization process is a time consuming treatment to perform on a tissue, but is similar to the time needed to specifically manipulate synthetic grafts which encompass similar microstructural properties. There may also be trace amounts of the decellularization chemicals on the scaffold, potentially affecting the scaffold's ability to house cells. While these are some potential limitations of a decellularized scaffold, the advantages of proper mechanical properties and essential biologic components typically outweigh the risks and make it a highly desirable material for TEHV.

After decellularization, several components of the ECM remain in the scaffold (51). A decellularized blood vessel has the tissue specific components and the unique capacity to interact with intravascular devices, such as a drug-eluting stents, the cellular monolayer, enabling the material to mimic an artery. This scaffold type also maintains a native microstructure throughout various treatments, making it well-suited to house cells and to culture an effective endothelium. Additionally, a decellularized scaffold has a unique composition that is unmatched by other scaffolding material. It innately houses all the layers of an artery and can be used to study the inflammation pathway found during restenosis. Together these properties encourage the use of a decellularized scaffold in the BVM because it's a simplistic way to mimic a native blood vessel.

1.6 Purpose of a Blood Vessel Mimic

As summarized previously, researchers have developed several different kinds of stents, including bare metal and drug eluting stents, and degradable stents, which are currently emerging. With new devices being developed at a rapid rate, there is a need for improved methods of testing. Currently, there are two main modes for evaluating the functionality of stents. Testing can be done either in a highly controlled, usually two-dimensional, *in-vitro* environment or in the environment of *in-vivo* animal models. *In-vitro* environments and animal models can both potentially provide highly effective and reliable methods for evaluating key properties of stents and other intravascular devices. Tests that are conducted within *in-vitro* environments typically lack physiologic conditions, and tend to focus on one aspect of the material properties such as, toxicity, proper expansion, and mechanical strength (52, 53). *In-vivo* animal testing provides vital information about the device's interactions and integration with the body; focusing on biocompatibility, healing responses, biodegradation, inflammatory responses, and elusion profiles (54, 55). To create a bridge between the *in-vitro* and *in-vivo* testing Dr. Kristen O'Halloran Cardinal has developed an *in-vitro* 'blood vessel mimic' (BVM) for the purpose of testing intravascular devices (4, 5).

The purpose of the BVM is to create a living model of a blood vessel with the goal of creating a more physiologic *in-vitro* preclinical testing system (4, 5). The BVM enables a platform for high throughput analysis of newly developed intravascular devices, intravascular imaging modalities, and drug delivery systems, (4, 5). The model consists of a cylindrical scaffold with an intimal endothelial cell lining housed in a biochamber, and luminal perfusion with media via a peristaltic pump (Figure 1.7) (4). The intimal cell lining acts as a living human tissue for physiologic interaction with a device (4). This interaction allows for the potential assessment of various coatings and configurations of intravascular devices, providing more data for the identification of

the best candidates to proceed to further evaluation (4). Thus, this methodology has the capabilities to improve the traditional methods of preclinical testing (4).

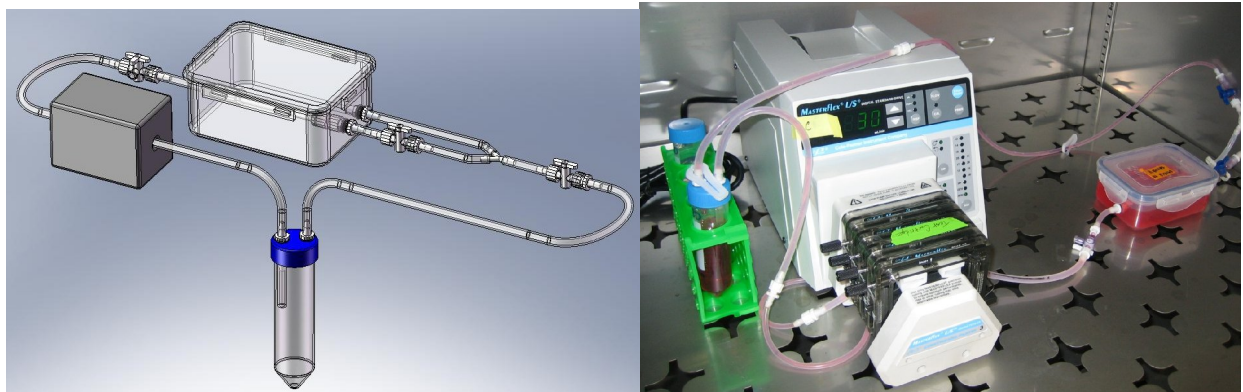


Figure 1.7. The BVM system. The solidworks model of the current BVM system (Left). The actual set up of the BVM in an incubator (Right).

1.6.1 The BVM Scaffold

To create a physiologically relevant bioreactor system several aspects of the scaffolding must be considered, such as size, orientation, material, microstructure, and biocompatibility. The BVM design allows for variations to the overall composition of the scaffold and bioreactor system. A scaffold's size can be varied from 3 mm to 4 mm inner diameter, and from 3 cm to 5 cm in length via exchangeable lure lock fittings. Also, through some configuration alterations, the bioreactor can house scaffolds with more natural curvatures, such as 90 degree or 180 degree bends and bifurcations for more native orientations. Changes in orientation of a scaffold may increase the physiological aspects of the BVM, while presenting more realistic geometries to evaluate newly developed intravascular devices. These versatile components make the BVM design a promising preclinical testing method. The scaffold plays a critical roles in the over function and physiological relevance of the BVM system.

The physical orientation of the scaffold is an important attribute of the BVM, but the scaffold choice is a key aspect as well. As previously described, there are several types of scaffold materials that can be utilized in a TEBV. Currently in Dr. Cardinal's research, ePTFE has been the gold standard for use in the BVM. The synthetic scaffold is well known and characterized for its use as a TEBV, and will continue to be a consistent choice for countless testing applications. Although the properties of ePTFE are not ideal, lacking in radial compliance and native porosity, ePTFE has the ability to support the development of an endothelium. The question remains if the scaffold can be made better? A scaffold that has a native porosity, essential proteins of the ECM, native mechanical properties, and the potential to grow and develop would be a more physiologically relevant option for the BVM. Based on current work in the TEBV field, as summarized previously, decellularized scaffolds present a potential option that has not been previously explored for the BVM. Through the decellularization of porcine arteries, all of these properties are possible.

1.7 Overview and Aims of the Thesis

This Introduction has described the background for which this thesis is based. The clinical problem of CVD is prevalent in the United States, where CAD is one of the most commonly treated disorders. As described previously, the development of a metallic stent device has been widely used to treat CAD, by effectively re-opening the blood flow through the vessel. New stents are being developed constantly to greatly improve the long-term results of stenting. To enable the most promising new devices make it to clinical applications, new methods for preclinical, informative evaluation are required. Thus, a highly specialized testing modality, the BVM, has been created to provide preliminary endothelialization data in an *in-vitro* setting.

As stated, the purpose of the BVM is to create a simplified physiological representative model of a human blood vessel with the intention of testing intravascular devices. In the current BVM model, the scaffold must primarily be able to support a functional endothelium. Thus, the specific characteristic of supporting an endothelium is vital to fulfilling the BVMs main goal. To achieve this, the scaffold must support cell adherence, proliferation, and phenotypic expression. The scaffold's ability to maintain the endothelium will improve the BVM's capabilities (46). Once the development of a strong endothelium is ensured, the mechanical properties of the scaffold become the next characteristic for consideration. Mechanical properties of the scaffold will determine its capacity to withstand the stent deployment (29). The radial compliance is a major aspect to investigate when choosing a scaffold material (20, 46). A scaffold with little to no compliance may prevent the stent from deploying properly, or if it's too compliant the stent may not interact with the wall in an ideal manner. Currently, the ePTFE scaffold lacks physiologic compliance and a new scaffold may have the potential to improve these limitations. In addition to the mechanical relevance of a decellularized scaffold, integral for stent deployment, it can be used to improve knowledge of sent interactions with the smooth muscle cells of an artery to develop knowledge regarding the common problem of restenosis. Further more, a decellularized scaffold may help to develop novel imaging modalities, as it is a unique composition and light can penetrate through the material.

Based on published use of decellularized tissues as biologic scaffolds, and specific successes in the use of decellularized vessels for TEBVs, this thesis explored the development of decellularized porcine vessels for use as a scaffold in Dr. Cardinal's BVM. To investigate the potential use of this scaffold in the BVM, there were three main aspects of this thesis: establishment of a decellularization protocol, mechanical characterization of the decellularized scaffold, and finally re-cellularization of the scaffold. These experiments characterized the

decellularized scaffold's potential to be used in the BVM system. The mechanical properties and the ability to support an endothelium will provide the basic proof of concepts needed to support further investigation into the consistent use of decellularized blood vessels.

The following is a summary of the specific aims pursued in this thesis.

- Aim 1: Establish a decellularization protocol for the complete decellularization of porcine arteries and evaluate the success of the decellularization protocol using histology.
- Aim 2: Determine the ability of the decellularized scaffold to maintain the native mechanical properties by assessing Young's Modulus and Critical Yield via tensile testing. Evaluate burst pressure for the radial compliance of the treated vessel.
- Aim 3: Create a protocol for seeding the vessel with cells and evaluate the re-cellularized scaffold.

In conclusion, this thesis will provide documentation of the previously mentioned experiments to support the potential for a decellularized porcine scaffold to be utilized as a specific scaffold testing modality for the BVM.

Chapter 2 - Development and Evaluation of Decellularization Protocol

2.1 Introduction

As described in Chapter 1, a range of synthetic polymeric materials exist for various biomedical applications. One of the widely used polymers previously mentioned, ePTFE, is a readily used biomaterial for several *in-vitro* and *in-vivo* applications. Polytetrafluoroethylene (PTFE), commonly known as Teflon, was discovered in 1937. Teflon is an inert material and is considered to be one of the most ideal electrical insulating materials currently on the market (56). The polymer is composed of highly crystalline and hydrophobic molecules. This particular combination of molecules prevents hydrolysis from occurring to keep the polymer as an intact structure (56). One of the first medical uses of PTFE was in the early 1960's as an implanted heart valve (56). In 1969, a company called Gore patented an expanded version of the polymer (ePTFE), which became known as Gore-tex (56).

To create ePTFE, the polymer is manufactured differently than just PTFE. The polymer is put through a series of stretching and extruding processes, in a heated environment to produce a microporous, non-woven material (56). Through this manufacturing process along with the biostable molecules and electronegative surface, ePTFE is capable of supporting tissue adhesion (Figure 2.1) (56). The tubular ePTFE grafts are manufactured via stretching the material over a solid polymer shaft. This stretching causes the non-woven material to crack, creating the micropores (56). This manufacturing process is well defined leading to a predictable microstructure; there will be node-fibril structures running parallel on the length of the tube (Figure 2.1) (56). The node-fibrils are approximately 30 μ m apart with interconnecting fine fibrils (Figure 2.1) (56).

EPTFE was manufactured to be used for vascular grafting, because once created the resulting combination of the molecules and expanded micro-porous structure closely mimics the

native structure of a blood vessel. This material has been used during vascular surgeries for large diameter bypasses such as aneurysms and aortoiliac occlusive disease, (57). There is a 5-year lifetime of this scaffold, which is a large improvement compared to the widely used Dacron and even the Gelatin coated Dacron grafts (57). Today, ePTFE is the gold standard for large diameter vascular prostheses in clinical practice. However, when ePTFE is used for small diameter vascular prostheses, thrombosis occurs within a few months due to the low polymer compliance (56, 58).

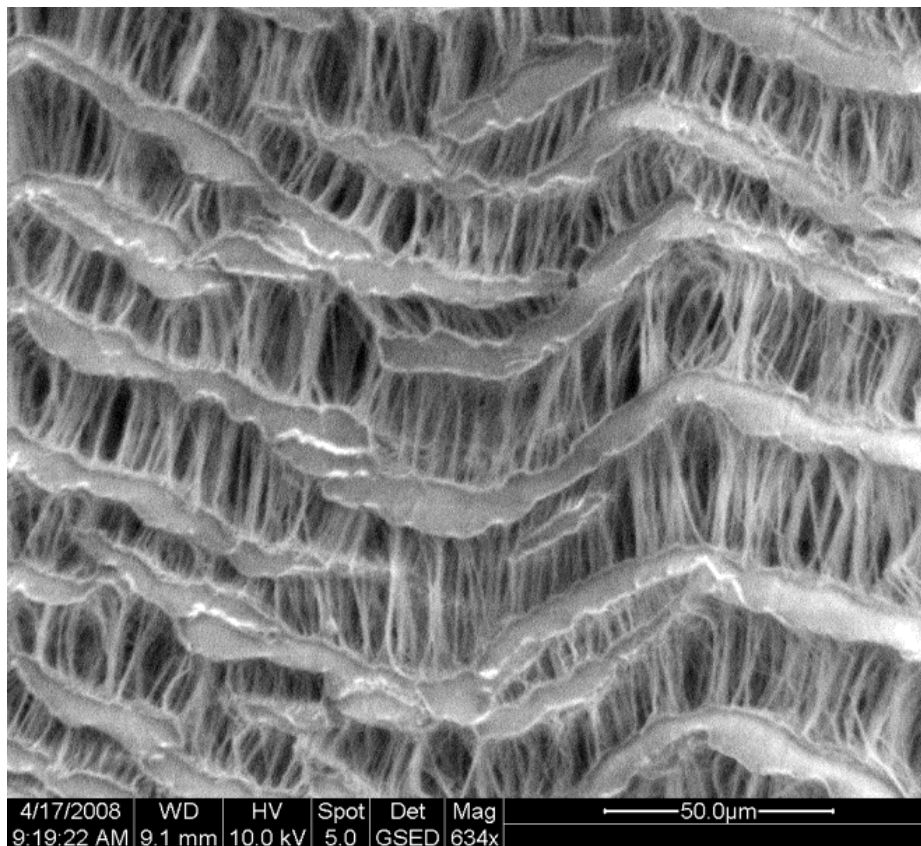


Figure 2.1. Scanning Electron Microscope (SEM) image of ePTFE. The microporous structure, with nodes running horizontally, parallel to the tubing length and the internodal fibers run vertically (59).

Also as described in Chapter 1, ePTFE has also found use in the BVM as the primary scaffold material. The goal of the BVM model is to create a pre-clinical testing system to

evaluate intravascular devices. This *in-vitro* model aims to be high-throughput, cost effective, reliable, and physiologically relevant to simulate an *in-vivo* environment. The use of ePTFE in the BVM model has many advantages. Some of these include the extensive existing pre-clinical and clinical data on the endothelialization on ePTFE, the ability to be autoclaved or gas sterilized, good biocompatibility, non-biodegradability, proper EC orientation encouraged via the unique microstructure, and it's availability in several different dimensions. The fabrication methods of ePTFE produce a consistent scaffold and hence more consistent results. Although this is an appropriate material for the development of a high throughput system, ePTFE is costly, dependent on the suppliers, and has non-native mechanical or physical properties. Simply, the ePTFE is a limited material that cannot be easily tailored to incorporate specific properties to further advance the BVM model. The production of a new scaffold which is created in house scaffold could improve the cost effectiveness and the physiological relevance of the BVM model. One such scaffold that, which is the focus of this thesis is created through decellularization of a native tissue.

The production of a decellularized scaffold could potentially result in the production of a more physiologically relevant scaffold, improving the ePTFE scaffold. In 2004, Schaner et al. produced a completely decellularized vessel that maintained its native structural properties (49). This work became the basis for the development of the biologic scaffold for the BVM, using the decellularization on porcine vessels (49).

The decellularization of arteries for tissue engineering has been used for over two decades and was first utilized by Malone et al. in 1984 where autologous small diameter carotid arteries were decellularized and then implanted in dogs (60). These scaffolds were found to function properly 80% of the time. Since this first experiment, the process of decellularization has grown exponentially and is now recognized as a legitimate method for the creation of

scaffolds for uses both *in-vivo* and *in-vitro* (61). This thesis intends to further investigate the use of decellularized scaffolds for *in-vitro* use specifically. The development of a decellularization protocol will aid in determining the potential utility of a decellularized biologic scaffold for use in the BVM.

2.2 Methods for Decellularization

2.2.1 Protocol Development

All vessels were harvested from pigs at the Cal Poly swine unit or at Creston Valley Meats. Pigs about 2-6 months old were sacrificed and vessels were harvested within one hour of death. The jugular vein, carotid artery, arteries from the brachiocephalic trunk, subclavian vein and artery, femoral artery and vein, as well as other superficial arteries throughout the body were the choice vessels during harvesting. The locations of these vessels are relatively well known, but the differences between an artery or vein, and the precise locations were not always clear. Harvested vessels were taken to the lab for cleaning, or the removal of all the connective tissue using a scalpel, razor blade, and scissors. Extra attention was focused on removing only the connective tissue, not the adventia of the vessel wall. Care was also taken to ensure the vessel was not 'nicked' by the cutting instrument. Vessels were then cataloged based on their outer diameter; smaller than 2 mm were recorded as small, from 2-5 cm were recorded as medium, and larger than 5 cm were recorded as large vessels. Vessels were then stored in a -20°C freezer within 8 hours of harvesting and remained usable for up to two years. In preparation for decellularization, vessels were thawed in a 37°C water bath until the structure was malleable. At this time the vessel was able to be used for any experimentation.

2.2.1.1 Static Decellularization Methods

The preliminary decellularization parameters were based on the work of Schaner et al., including the duration of decellularization and concentration of SDS (49). Primary experiments focused on determining the ideal concentration of SDS, as was done in Schaner et al.'s. work (49). To optimize the decellularization protocol, different concentrations of SDS, ranging from 0% to 0.125%, were evaluated on the ability to remove all cells from the tissue without altering the native properties of the vascular wall ECM. A high concentration of SDS, it results in the degradation of the vessel wall structure. Conversely, a low concentration of SDS will leave all of the existing cells on the vessel may not be removed. The other experimental parameters were taken directly from Schaner et al.; the decellularization process took place for 15 hours on a Daigger orbital shake table (model SH 06050597). The experimental procedure is provided in Appendix B: B.1, which describes the detailed steps for decellularization. The first test evaluated concentrations of 0%, 0.075%, 0.1%, and 0.125% SDS to elucidate the optimal concentration for complete decellularization. The ideal concentration from this experiment optimized the static decellularization protocol. For these studies, small and medium sized vessels were utilized.

2.2.1.2 Perfusion Decellularization Methods

Once the vessels were found to be decellularized, further experimentation was required to evaluate the potential for use as a scaffold in the BVM. The lumen of the vessel needed to remain open in order to perform these additional experiments. However, during static decellularization, the vessel became swollen and the lumen was lost in the remaining connective tissue and adventia. Therefore, to ensure the lumen remained accessible, it was essential to keep

the lumen open during the decellularization process. A male luer lock barb was inserted into the lumen. The luer lock barbs were sutured onto either ends of the vessel just after thawing or during the “clean-up” portion of the harvesting (Figure 2.2). The protocol was further altered by adding a Thermo Fisher Scientific Masterflex L/S 3 roller peristaltic pump (model 7519-05), to perfuse the lumen during the decellularization process, rather than the orbital shake table for mechanical agitation. The change in mechanical agitation is to keep the lumen open was the only modification to the static decellularization protocol (0.075% SDS for 15 hours). This modified perfusion protocol is in Appendix B: B.2. The SDS solution perfused the lumen at 140 rpm for 15 hours.

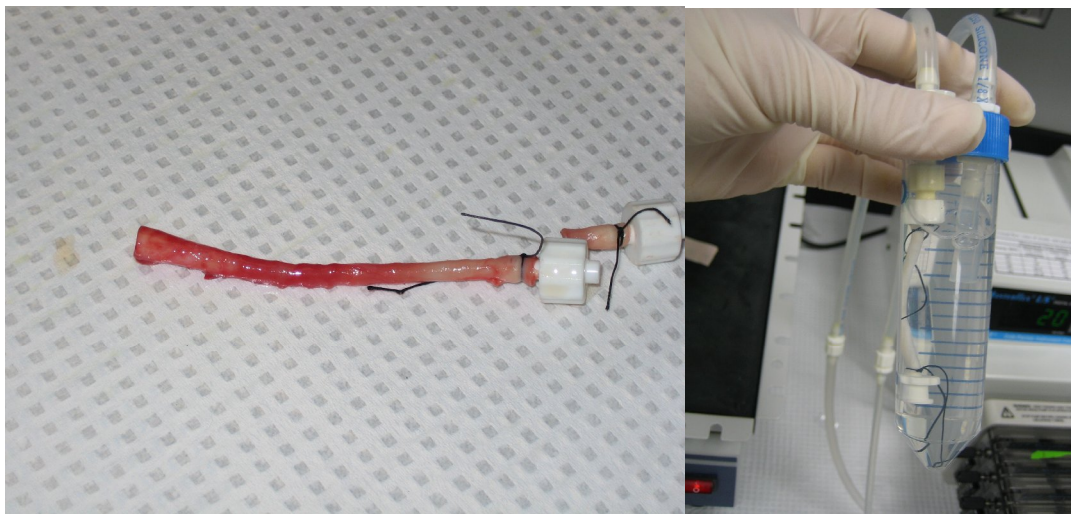


Figure 2.2. Luer lock barbs sutured to the scaffold. Sutured during cleaning (right) and during decellularization (left),

The consequent experiments to improve the perfusion decellularization, the flow rate of SDS through the lumen was optimized. The perfusion rate through the vessel with SDS was lowered to 20 rpm. Also, the use of a shake table was reinstated to improve decellularization by providing two types of agitation to the vessel wall. The final protocol used a 3-roller peristaltic

pump at 20 rpm for 20 hours on a shake table rotating at 30 rpm (see Appendix B: B.3). The final set-up with the shake table and peristaltic pump, is pictured in Figure 2.3.

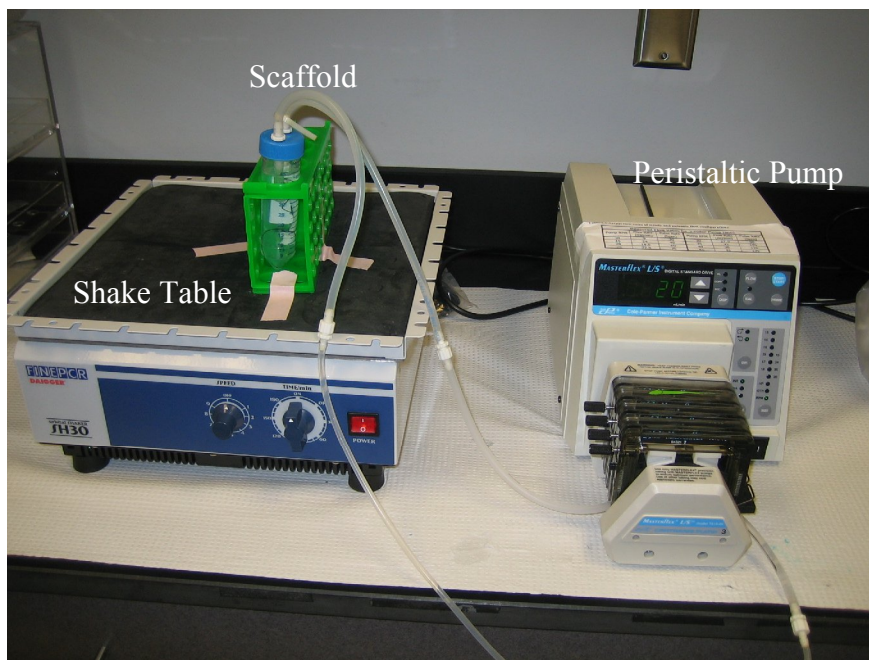


Figure 2.3. Peristaltic pump and orbital shake table utilized for decellularization.

2.2.2 Protocol Assessment

For both static and perfusion decellularization, histology was used to evaluate the decellularization process. Samples were fixed in histochoice overnight to ensure the proteins in the sample were crosslinked. Samples were then processed using a Thermo Scientific, Shandon Excelsior ES tissue processor and then embedded in paraffin wax via a Thermo Scientific EC350 embedding center. Samples were embedded with a cross sectional orientation to view the scaffold lumen. Sections approximately 6 μ m thick were cut from the block, using a Lyca RM 2255 microtome. Samples were stained with hematoxylin, a purple nucleic dye, and eosin, a pink cytoplasmic and collagen dye (hematoxylin from Fisher Scientific 7211 and eosin from Fisher Scientific 7111). This staining process is called H&E staining and the full protocol is in Appendix B: B.4 Histology Staining. Stained and cover slipped slides were imaged using white

light on an Olympus BX41 Microscope at 10x magnification. The primary evaluation to assess decellularization consisted of nuclei identification within the image. Secondly, the status of the tissue was evaluated for any noticeable degradation from the SDS solution. Degradation was evaluated based on a visual evaluation of the vessel wall structure.

The evaluation of the decellularization was based on the classification of the histological pictures. There were three classifications of the vessel status: not decellularized, decellularized, and degraded. A not decellularized scaffold had similar nuclei and wall structure as the control. A decellularized scaffold had similar wall structure as the control but no nuclei are present. Finally, a degraded scaffold had no nuclei and an altered structure from the control. With these classes, all of the images from each sample concentration were evaluated.

2.3 Results

2.3.1 Static Decellularization Results

In Figure 2.4, two images from each concentration of SDS are compiled together. All sections were stained with H&E and imaged at 10x magnification (higher magnification pictures are in Appendix C: C.1). Table 2.1 summarizes the classifications given to each sample. A concentration of 0.075% SDS was considered to be the optimal concentration for decellularization without degrading the vessel wall.

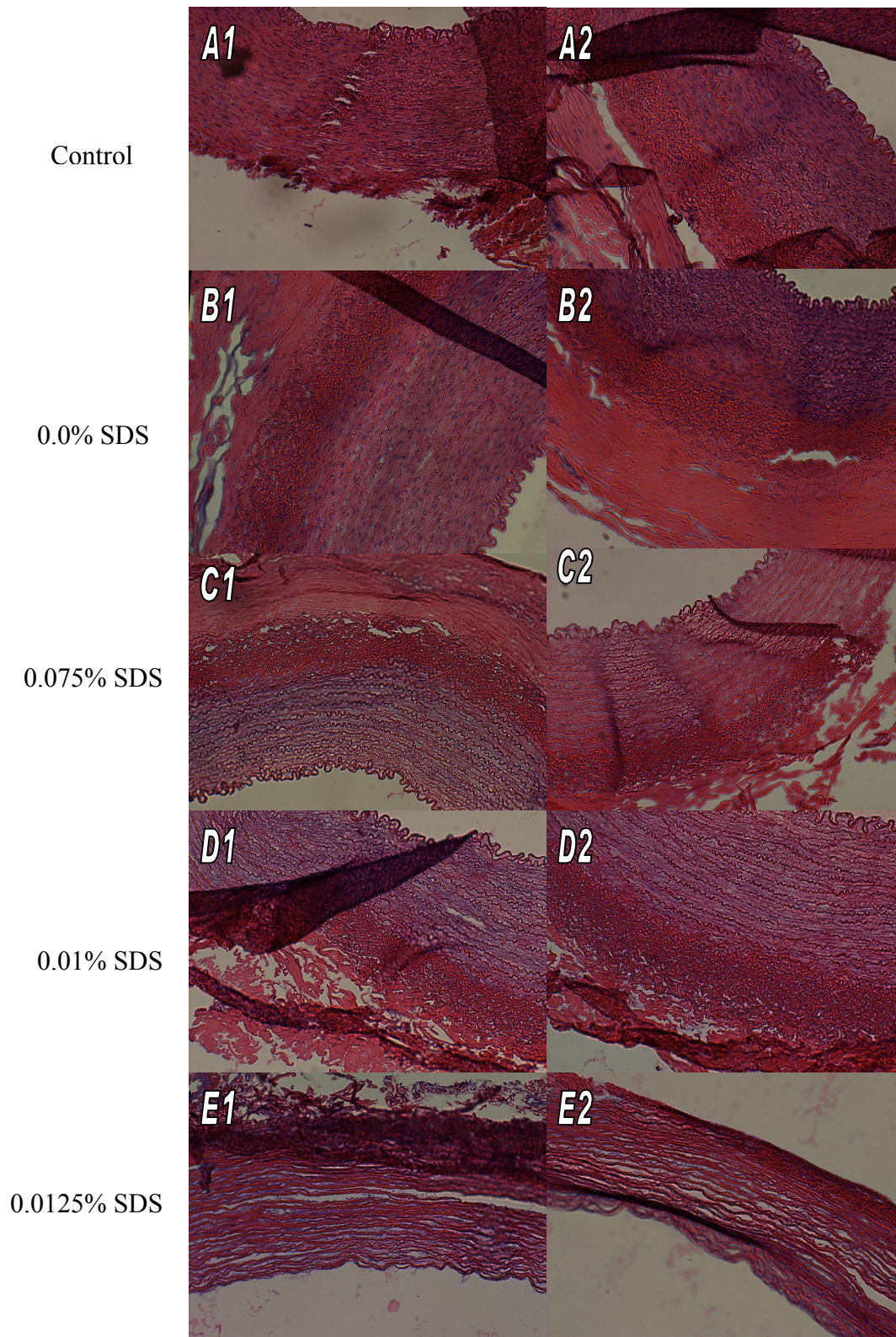


Figure 2.4. Images of static decellularized porcine arteries at various concentrations of SDS.

Higher magnification images in Appendix C.1.

Table 2.1. Summary of Classifications for Each Concentration Sample.

Sample	SDS	Classification
A	Control	Not decellularized
B	0% SDS	Not decellularized
C	0.075% SDS	Decellularized
D	0.1% SDS	Decellularized, Degraded
E	0.125% SDS	Degraded

2.3.2 Perfusion Decellularization Results

To optimize the decellularized scaffold for use in the BVM (or for any use requiring access to the lumen) the protocol was altered to keep the lumen of the vessel open. The protocol alteration included the addition of a luer lock barb, which is easily integrated into a simple 50mL conical bioreactor. The conical bioreactor enables decellularization via luminal perfusion. The static shaking method focuses on decellularizing from the outside of the vessel into the lumen; where as perfusion methods have a particular focus on decellularization in the reverse direction, from the lumen to the outside of the vessel. Using this theory, mechanical agitation by an orbital shake table from the static protocol was changed in the perfusion protocol. This experiment used a 0.075% solution of SDS to perfuse the lumen at 140 rpm for 15 hours. Figure 2.5 are the images from the resulting histological analysis from the perfusion procedure. The vessels were again scored with the same three classifications: not decellularized, decellularized, and degraded. Overall, the perfused vessel was scored as ‘not decellularized.’ The flow rate was too high for the given application and considered to be the main problem with the protocol since it was the only altered from the working static protocol.

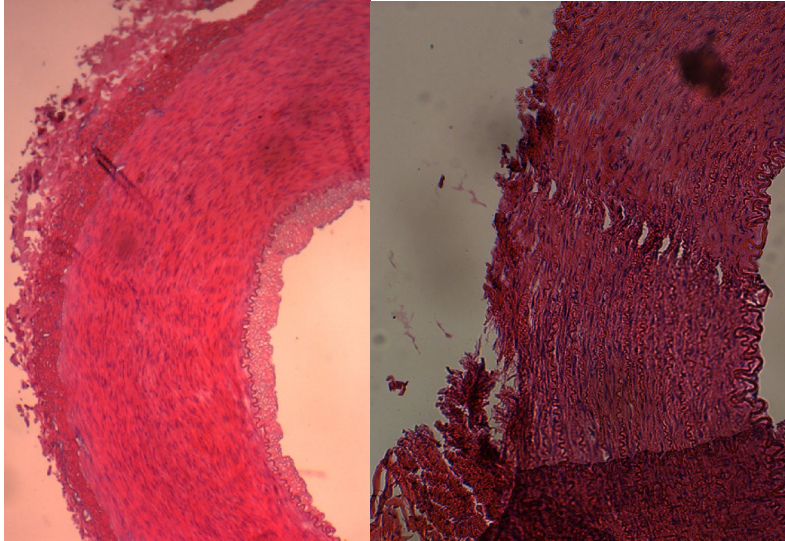


Figure 2.5. Perfusion decellularization. Perfusion decellularization scaffold (left) and control vessel (right).

Investigations into the literature revealed that a lower flow rate, for a longer duration would allow the SDS to better interact with the scaffold, and improve the decellularization of tissue. Also, a combination of the rotary shake table and perfusion methods was determined to be the ideal mode of mechanical agitation for complete decellularization. Therefore, the final decellularization protocol perfused the lumen of the vessel at 20 rpm for 20 hours while on an orbital shake table (Appendix B: B.3 Final Perfusion Decellularization). Figure 2.6, is the histological results from this new method compared to a native control and a statically decellularized vessel. This final protocol was successful for the complete decellularization of a porcine artery and vascular wall, while maintaining the opening of the lumen. Further verifying the efficiency of this protocol, the same protocol was repeated over ten times with a similar result. It is important to note, that with the addition of the luer lock barb the whole tissue was not decellularized. Through H and E analysis, the portion of the scaffold which was sutured to the barb was not completely decellularized and the scaffold was always cut from the barb before further processing.

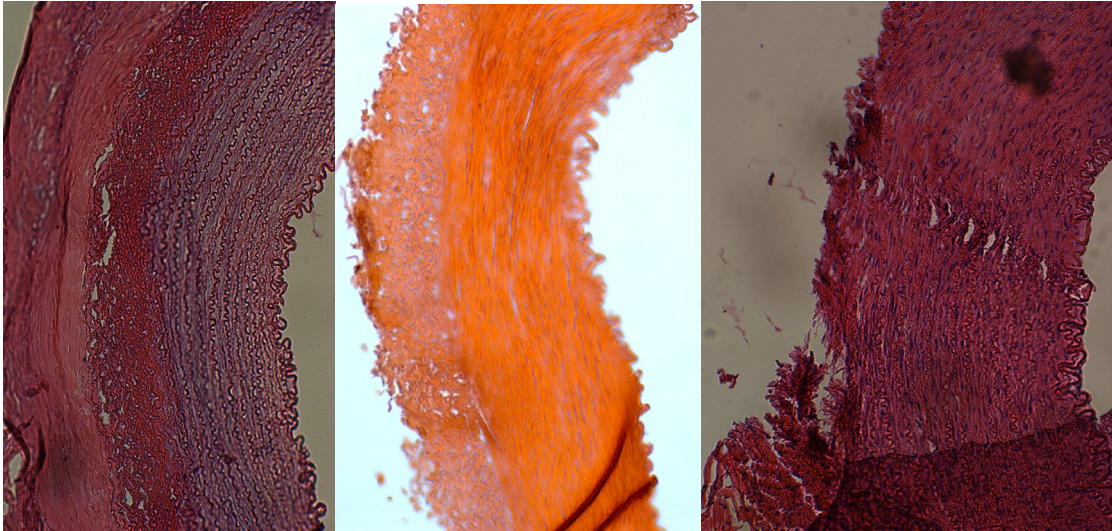


Figure 2.6. Successful perfusion decellularization. Static decellularized scaffold (right), perfusion decellularized scaffold (center), and native control vessel (left).

2.4 Discussion

Several groups have done static decellularization using similar methodologies; where various methods of agitation were applied to the tissue, helping to remove all the cellular debris. Singelyn et al. utilized a stir bar to continuously move the tissue in an SDS solution for several days for full decellularization (51). Lichtenburg et al. suspended tissue in an Erlenmeyer flask with a stir bar to move the solution of SDS continuously around the tissue. The decellularized scaffold was then re-suspended in a similar manner to for all other *in-vitro* testing (62). The methodology from Shanner et al. is the bases for the static protocol used in this experimentation, where scaffolds were physically submerged repeated times into a SDS solution as the main form of agitation for cellular removal. This method worked well for decellularization, but all other *in-vitro* tests preformed by this group did not require access to the lumen (49). These groups and others have demonstrated that static decellularization is possible with simple agitation methods, but the ultimate goal of the research will tailor what methodology works best. In some applications the structure of the scaffold may remain intact, while for other applications, the

structure can be lost. Thus, the most vital parameters of any decellularization protocol include only the concentration of the SDS and some means of agitation to the tissue.

Static decellularization was found to successfully remove all cellular components at a concentration of 0.075% SDS. It could be debated whether the concentration was best at 0.075% or at 0.1% SDS, because both were fully decellularized with little damage to the vessel wall. By looking at several other sections of the different concentrations, 0.1% SDS had more apparent degradation of the adventia layer of the vessel wall. Also, limiting the amount of SDS present in the process would be ideal if this scaffold is to be used in biologic experiments. Thus, the lower and most successful concentration of 0.075% SDS was chosen to be part of the optimal static decellularization protocol. The other variables of the protocol had been determined through the literature and were repeated in this experiment. Thus, there was no reason to perform additional experimentation for the optimization of these parameters.

After successfully establishing a static protocol for decellularization, using 0.075% SDS and an orbital shake table to agitation, the next phases of *in-vitro* testing needed to be evaluated. These alternative *in-vitro* tests required access to the luminal space. Specifically, to mechanically evaluate the scaffold is cut open and laid flat to determine its elastic modulus. In addition when then scaffold is used in the BVM the scaffold to be sutured into the system and lumenally pressure sodded with cells. Therefore, it would be ideal to alter the decellularization techniques to provide luminal access for down stream testing.

During static decellularization, the vessel became swollen and structures were unidentifiable from one another thereby rendering the lumen inaccessible. By adding lure locks and perfusion step to the decellularization process, the vessel lumen could remain open for future experimentation. By inserting the male lure lock barb into the vessel lumen of a frozen or fresh vessel, the lumen would remain opened throughout storage and decellularization. The perfusion

step ensures the lumen is exposed to SDS and with the combination of the shaker have the mechanical agitation enabled complete cellular debris removal.

Perfusion methods have been used in literature to decellularize scaffolds where keeping an intact the macrostructure is imperative. Ott et al. was the first group in 2008 to decellularize an intact rat heart using the perfusion methods. The rat hearts were carefully dissected from the animals, then the chambers of the heart were perfused (following the path of blood flow) with PBS and SDS for several days (48). Using the perfusion method, most of the macrostructures remained intact, including: ventricles, atriums, coronary arteries, Purkinje fibers, atrioventricular, and semilunar valves (48). Keeping these macrostructures intact was important for whole heart decellularization because the scaffold maintains its complexity and intricacy, which is currently impossible for any man-made scaffold. The end goal for a whole heart decellularization is to reach the clinic, where it is promised to one day improve the organ transplant process (48). For this goal, having all of the complexities and intricacy of a normal heart is vital to the usability for this type of scaffold. Overall, this perfusion method enables the decellularization from the inside out, without drastically harming the macro- or microstructure. Using a similar perfusion method to decellularize a single artery, should retain the native macrostructure intact. This has been performed in the vascular decellularization literature; produce a physiologically relevant scaffold (40, 49, 63). Thus in theory and as shown in these experiments, the established perfusion decellularization protocol maintains the scaffold structure very similar to that of a native artery.

To further evaluate the perfusion decellularization protocol, the reproducibility of the protocol was evaluated. Reproducibility of a scaffold was designated by efficiently and repeatedly decellularizing scaffolds of all sizes. Small, medium, and large sized vessels were decellularized using the final perfusion decellularization protocol (Appendix B: B.3). Over 50 vessels have been decellularized in this fashion, with continued successful results. To further

investigate the potential for this procedure transition to a high throughput model, three scaffolds were successfully decellularized at once time.

In summary, perfusion decellularization did not remove the cells as efficiently as the static decellularization methodology had done previously. Without changing the concentration of SDS, the duration of the SDS rinse was extended and the flow rate was decreased in order to increase the exposure time to the detergent. Finally, a combination method including both perfusion and rotary agitation was discovered to be ideal at not only for decellularization, but also for the set-up of future *in-vitro* testing. Essentially, the final protocol is reproducible, effective at maintaining an open lumen, efficient at decellularization, and leaves the microstructure intact. Maintaining the native structure is vital to ensuring the conservation of all native properties; mechanical for compliance, integral for sent deployment, and biologic composition, critical for stent-wall evaluations or vascular pathway modeling of disease.

Chapter 3 - Characterization of Decellularized Vessels

3.1 Introduction

Chapter 2 determined the optimum decellularization protocol for complete removal of cellular material, without apparent harm to the integrity of the ECM. The goal of the next investigation was to quantitatively evaluate the condition of decellularized vessels post decellularization. It was necessary to evaluate the damages sustained to the ECM during the decellularization treatment, as it may lower the physiological relevance of the vessel scaffold. Excessive scaffold degradation can prove problematic because the lack of a porous, intact scaffold wall could hinder endothelium growth and viability in both the short and long term (61). Currently, one of the key limitations of cell-based tissue engineering is the lack of mechanical strength within the scaffold wall, resulting in the subsequent reliance on synthetic scaffold materials (64). The development of a decellularized scaffold promises to bridge the gap between weak cell-based or biologic scaffolds and synthetic materials. In order for a scaffold to be incorporated into the BVM, the mechanical, structural, and basic biological properties of the scaffold should not differ from that of a native vessel. Therefore, the evaluation of the scaffold's mechanical properties prior to its use in the BVM is important. The scaffold must effectively fulfill the goal of the BVM, by maintaining the structural stability necessary to support an endothelium throughout the course of an intravascular device evaluation.

The structural properties were visually analyzed by Hematoxylin and Eosin staining, as well as with scanning electron microscopy (SEM). These images were used to examine if the decellularization treatment had any lasting effects on the wall structure, which is important to the overall functionality of the scaffold. To evaluate scaffold mechanics, tensile and burst pressure evaluation were performed on both native and decellularized vessels. The mechanical testing

methods utilized were modeled from the work done by Montoya et al. in 2009 for the evaluation of a decellularized scaffold (65).

In addition to structural and mechanical assessment, biological evaluation of the decellularized scaffold examined its bacterial content post harvesting and post decellularization. These results provided information regarding the sterility of the harvest and decellularization process. These experiments characterize and support the ability of the decellularized protocol to efficiently remove all cellular components from a blood vessel without disrupting its natural structure, which further demonstrates its potential to be incorporated into the BVM. All scaffolds used in this investigation were prepared following the final protocol described in Chapter 2 of this thesis (Appendix B: B.3).

3.2 Methods

3.2.1 Structural Evaluation

3.2.1.1 Hematoxylin and Eosin Staining

Two imaging techniques were utilized to visualize the potential effects of the decellularization process on the structural integrity of a scaffold. As discussed in Chapter 2, Hematoxylin and Eosin (H and E) staining can be used to visualize cross-sections of the vessel wall for specific identification of cell nuclei as well as other macro-structures in the vessel (66). The H and E staining provides a basic image for comparisons between pre- and post-decellularization; regarding not only the presence of cells as in Chapter 2, but also for the maintenance of basic structures.

As described in Chapter 2 section 2.2.1.2 ('Perfusion Decellularization Methods'), decellularization was performed by perfusing SDS through the lumen while simultaneous shaking for 20 hours. Once decellularized scaffold sections were fixed in histochoice to fix the

sample. Then samples were process and embedded in paraffin wax. Sections approximately 6µm tick were taken from each sample and stained with H and E, as discussed in Chapter 2 section 2.2.2 ('Protocol Assessment').

The images were again scored based on the amount of degradation present within the vessel wall. The scoring system for degradation coincides with the decellularization scoring, as the two evaluations are similar. There were two classifications of the vessel status: not intact or intact. All of the images evaluated were considered to be properly decellularized. The classifications are further described as either an intact vessel wall, where the wall of the vessel is continuously touching and each pink collagen line remains within close proximity to its neighboring fiber, or not intact, where the pink collagen lines of the vessel do not retain their close proximity and continual interaction. Examples of "intact" versus "not intact" are provided in Figure 3.1. The evaluated scaffolds followed the decellularization protocol listed in Appendix B: B.3.

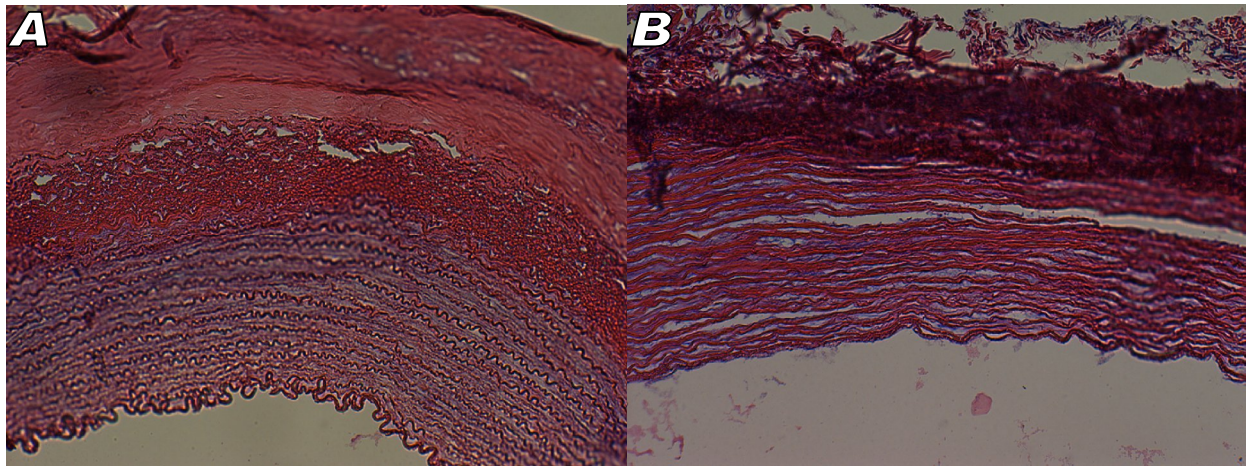


Figure 3.1. Intact vs. not intact. Decellularized scaffold classified as intact (A). Decellularized and classified as not intact (B).

3.2.1.2 Scanning Electron Microscope Imaging

A scanning electron microscope (SEM) provides a micro- or nano- scale view of a material's surface topography (67). SEM images produce an image of the material's surface at 10-20,000 times magnification (67, 68). This high resolution imaging technique reveals information regarding the material's porosity, fiber diameter, and composition (67). SEM images were used to visualize the luminal structure of the decellularized artery; specifically looking at the fiber topography and possibility of cellular presence. The combination of SEM and H and E images helped to define the structure of the scaffold pre and post decellularization, to assess any damage to the scaffold wall from the decellularized treatment.

To obtain an SEM image, the sample was placed in a vacuum, then a high powered electron beam was directed on the sample. The width of the beam can be altered by the coils to increase or decrease the magnification (68). The electrons that were not absorbed by the sample were scattered back towards the walls of the SEM (68). The walls have several detectors to absorb the backscattered electrons; the angle at which deflected electrons hit the detector and are computed into topographical image of the sample's surface (68). Figure 3.2 depicts the procedure for SEM imaging. The samples were dehydrated prior imaging to ensure quality images and a functioning SEM. Dehydration is an essential step for SEM images as the electron beam will heat up any water molecules present in the sample, causing damage to the sample and potentially to the sensitive instruments within the SEM. The exact dehydration protocol is provided in Appendix B: B.5. SEM images were acquired using a Hitachi High Technologies' TM3000 Tabletop Microscope (Figure 3.3)

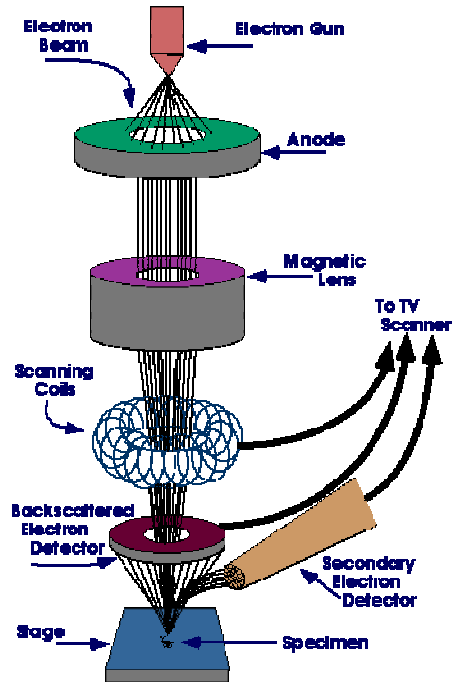


Figure 3.2. A diagram for how an SEM operates. Depicting the electron beam, scanning coils, and backscattered detectors (69).



Figure 3.3. The TM3000 Tabletop Microscope used for imaging.

3.2.2 Mechanical Evaluation

3.2.2.1 Tensile Testing

The decellularization process requires strong chemical agitation, which may degrade components of the ECM and weaken the structure. Tensile testing a sample will determine the elastic modulus and yield strength for a decellularized vessel compared to a control vessel. The elastic modulus describes the amount of elasticity in a material, while the yield strength determines the point at which the material begins plastic deformation (70). These results quantitatively describe how the decellularization treatment affects the mechanical strength of the vessel wall. All tensile testing was performed on an Instron In-Spec 2200 Portable Tester with PDA Data Management Software equipped with a 250 N (50 lb) load cell tensile machine for data collection.

Samples were placed in the tensile testing machine and stretched until failure. The machine pulls the sample 1 mm every 0.1 seconds and records the resistance of them material every stem. Equation 3.1 below describes the relationship graphed between extension and load. The extension of the sample is the distance stretched during the test and the load is the amount of resistance felt by the machine as it increases the length of the sample. Using the raw data (extension versus load measurement) and measured specifications (surface area and width) of the sample, stress and strain was plotted and were then used to calculate the elastic modulus. The relationship between stress and strain is known as “Hooke’s Law” (seen in Equation 3.2 (70)) and is derived in the following equations (equations 3.3 and 3.4) (70). The elastic modulus (E) seen in Equation 3.2 is the relationship between stress (σ) and strain (ϵ) (70). Stress in Equation 3.3 is the load from the raw data divided by the cross-sectional area of the sample (thickness*width). Strain in Equation 6 is given by the change in length of the sample over the original length of the sample. Equations 3.1-4 were used to determine the elastic stress and

strain curve for any given point of the experiment. Young's Modulus and yield strength were then calculated for all the raw data points using these stress and strain values. The elastic modulus was measured by the linear portion of the stress versus strain curve, while the yield strength was taken where elastic deformation ended and plastic deformation began (just after the linear portion) (70).

$$\frac{Load(N)}{Extension(mm)} = \frac{N}{L} \quad \text{Equation 3.1}$$

$$E(Pa) = \frac{\sigma}{\varepsilon} \quad \text{Equation 3.2 (70)}$$

$$\sigma = \frac{Load(N)}{Area(mm^2)} = \frac{N}{t * w} \quad \text{Equation 3.3 (70)}$$

$$\varepsilon = \frac{Extension(mm) + length(mm)}{Length(mm)} = \frac{L + L_o}{L_0} \quad \text{Equation 3.4 (70)}$$

To tensile test samples, a control group was first cut from each native vessel. Then samples were decellularized using the protocol from Appendix B: B.3. Samples were cut into pieces approximately 5cm in length (Figure 3.4). The smaller samples were then cut longitudinally and laid flat for placement in the tensile tester (Figure 3.5). From Figure 3.5, the sides indicated by “width” were placed in the clamps of the tensile tester. Once samples were cut into a flat section, they were oriented longitudinally and edges were placed in the clamps of the tensile tester. About 1 cm of the sample was aggressively clamped down on either end. The sample was then stretched until taught; the machine was calibrated at this point to zero for force and length. The original length (between the two clamps), width, and thickness of the sample were recorded for later calculations of Young's Modulus and yield strength. Finally, the tensile tester was started; samples were pulled 1mm per second, producing a slow and consistent longitudinal pulling force on the sample, until the sample was broken. For more detailed

methods see Appendix B: B.6 Tensile Testing Protocol. The stress and strain was calculated from the raw data using a macro program (full macro program Appendix B. B.7). A two-sample T test was used to evaluate the statistical significance of the Young's Modulus for the control and decellularized scaffolds. Significance is given by a p-value less than 0.05, with six samples for each group (n=6).

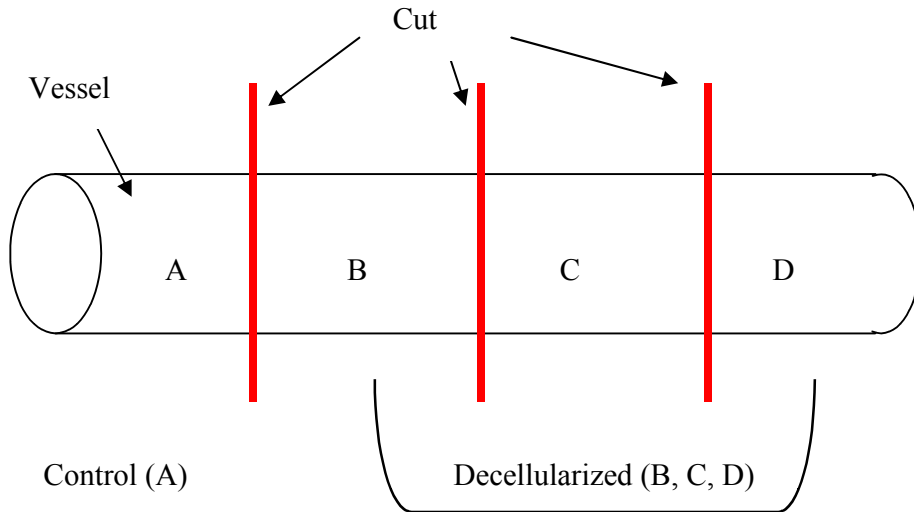


Figure 3.4. A visual depiction of the cutting preparations for a tensile test. Sections A, B, C, and D are approximately 5 cm long each.

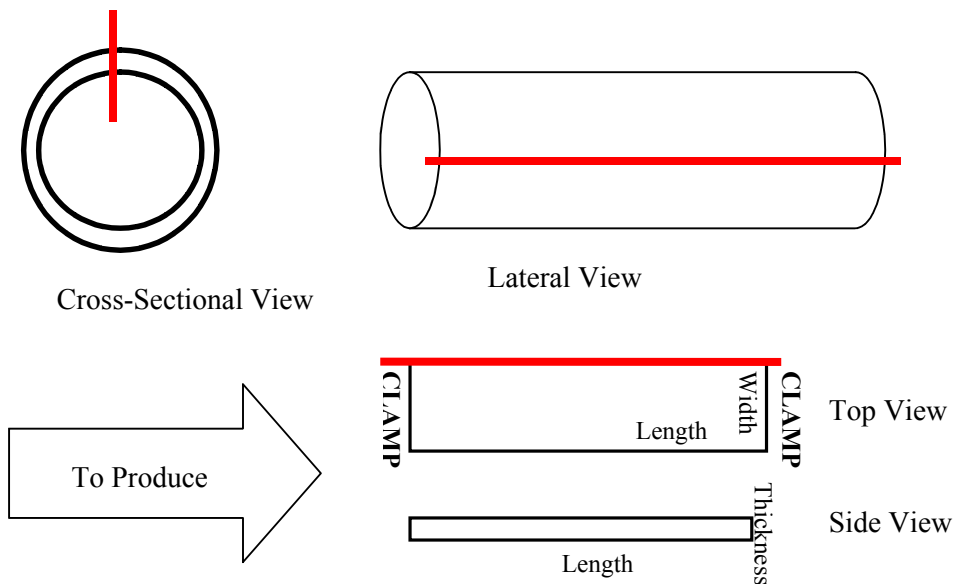


Figure 3.5. A representative image of the longitudinal cut made (seen in red on the top images) to each of the samples for preparation in the tensile tester. The bottom images show the flat sample of tissue placed in the tensile tester, again red indicates the side of the sample that was cut. The sides indicated by “width” were placed in clamps to produce a longitudinal tensile force.

3.2.2.2 Burst Pressure Evaluation

A burst pressure evaluation was used to further evaluate the mechanical integrity of the scaffold post decellularization treatment. Burst pressure measures the maximum circumferential stress that a scaffold can maintain. The scaffold should at minimum be able to withstand normal physiological pressures from 70 to 150 mmHg (71). Burst pressure was measured via a pressure transducer. The pressure transducer equipment was controlled using Data Acquisition Software (ADQ) and AD Instruments (ADI). Samples went through a three-staged process for testing the maximum burst pressure of the scaffold. Stages included calibration, scaffold set-up, and burst procedure.

The pressure transducer was calibrated first using the ADI system, a pressure transducer, blood pressure cuff, and Lab Chart. To calibrate, see Appendix B: B.8 for the detailed steps. Decellularized and native scaffolds were then connected to the system, one at a time. The distal end of the sample was capped off and the proximal end was connected to a pressure transducer (all decellularized scaffolds followed the protocol in Appendix B: B.3). On the transducer side, extra tubing and a stop cock was attached a water-filled syringe that supplied the pressure into the scaffold (Figure 3.6). The transducer was also attached to the ADI system to record the pressure changes throughout the experiment. Finally, the burst pressure was tested by slowly injecting fluid into the lumen of the decellularized scaffold until it burst open, and the maximum pressure was recorded. The detailed protocol for this procedure is in Appendix B: B.8.

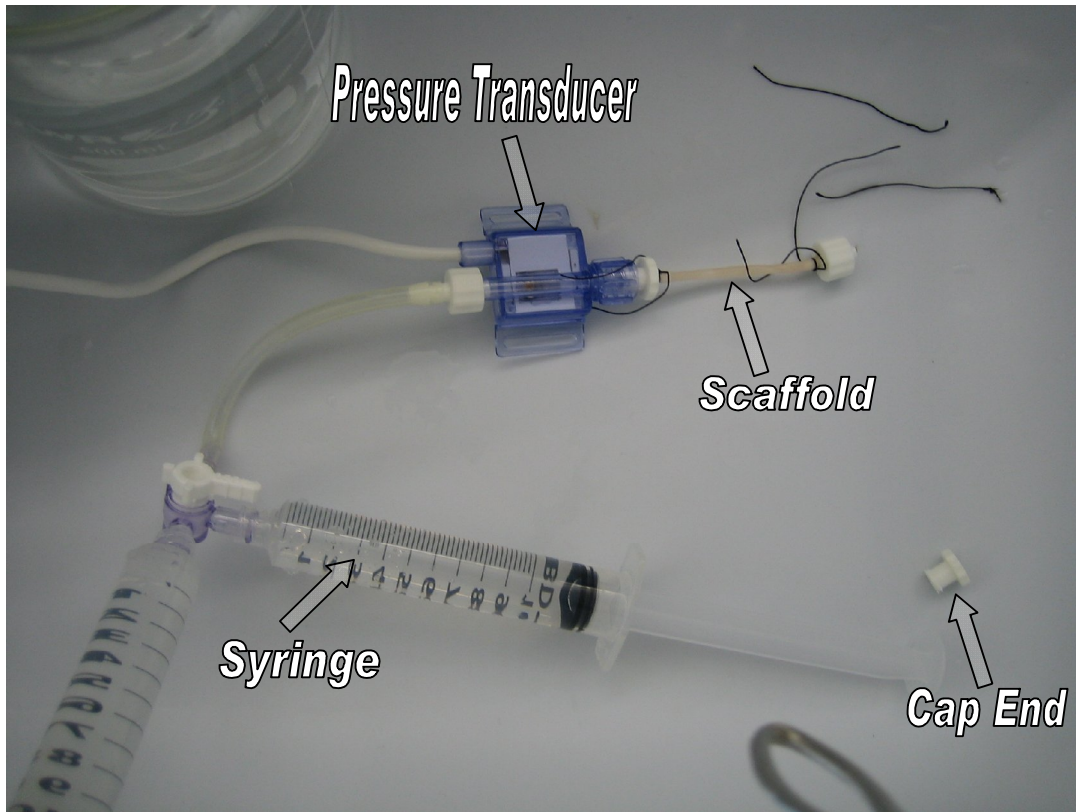


Figure 3.6. The complete set up of pressure transducer, syringe, stop cock, cap end, and scaffold

3.2.3 Biological Evaluation

To evaluate the potential contamination of the sample post harvest from the pig and post decellularization, a bacterial assay was performed. The harvesting process was not performed in a sterile environment, thus it is important to assess any level of contamination that may have occurred. If these scaffolds are to be used in the BVM system and eventually seeded with cells, thus an aseptic scaffold is ideal. Therefore, determining the amount of biological contamination was imperative to understanding the scaffold's potential use in the BVM.

Trypticase soy agar (TSA) plates and lysogeny broth (LB broth) tests were utilized for this bacterial content assay. The detailed procedures for these tests are provided in Appendix B: B.9. This assay was conducted with four variables: pre and post decellularization, as well as pre and post decellularization with 1% penicillin:streptomycin (penstrep). The 1% penstrep is a

common antibiotic used to prevent bacterial growth. These variables described the condition of the scaffold post harvesting and post treatment, as well as the potential strength of the antibiotic, in case there was contamination did occur during the harvesting process. Each of the four samples were placed on TSA plates and in the LB broth. Evaluation was performed by visual inspection of the bacterial contamination; if contaminated bacterial colonies will formed on the TSA plate and the LB broth will become cloudy, if no contamination then both medias will remain clear.

3.3 Results

3.3.1 Structural Evaluation

3.3.1.1 Hematoxylin and Eosin Imaging

Hemotaoxylin stain was useful for visualizing decellularization (by staining the nuclei), while the Eosin staining was useful for the structural analysis (by staining the structural components). The H and E images were then used again to evaluate the changes in the scaffold wall from the decellularization treatment. Figures 3.7 and 3.8 are images that represent the each of the classifications ('Intact' or 'Not Intact'); Figure 3.7 were 'Intact' scaffolds and Figure 3.8 were 'Not Intact' scaffolds. Please note, these images are meant only for comparison purposes; as these images were taken after further processing and not after the decellularized treatment alone. Table 3.1 is a summary of the number of scaffolds found to be 'Intact' verses 'Not Intact'. Interestingly, there was some correlation between the size of the scaffold and the classification of the scaffold; the larger the scaffold the more likely it was classified as 'Not Intact'.

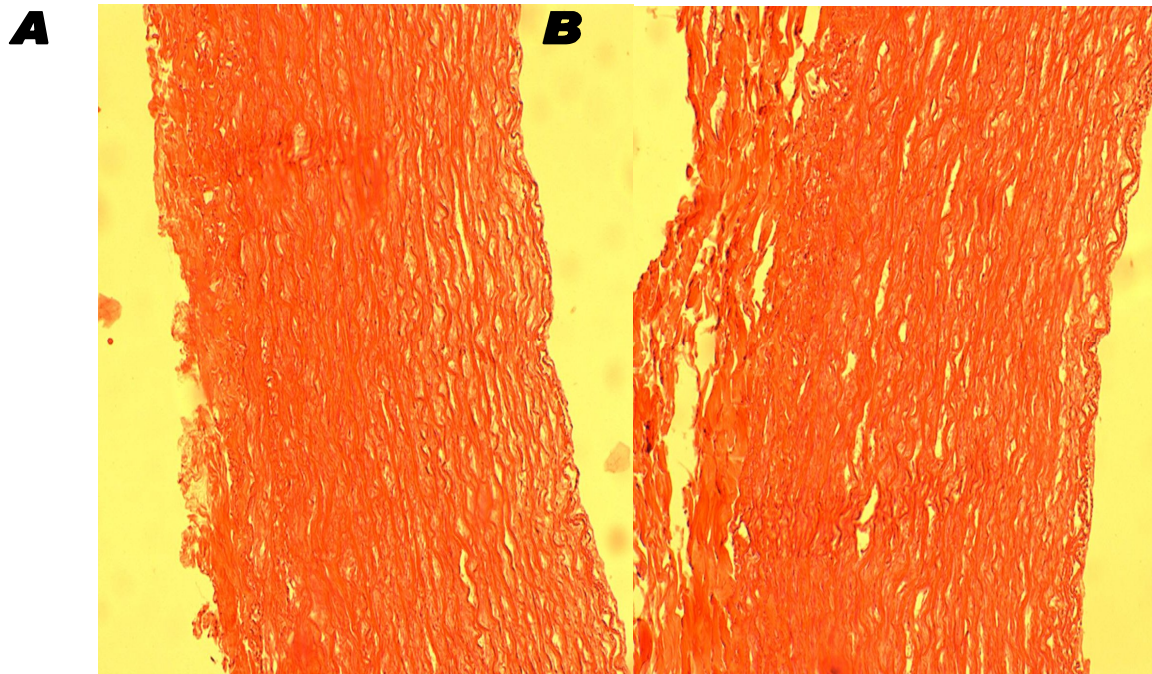


Figure 3.7. Scaffolds classified as 'Intact'. The wall of the vessel is continuously touching and each pink collagen line remains within close proximity to its neighboring fiber.

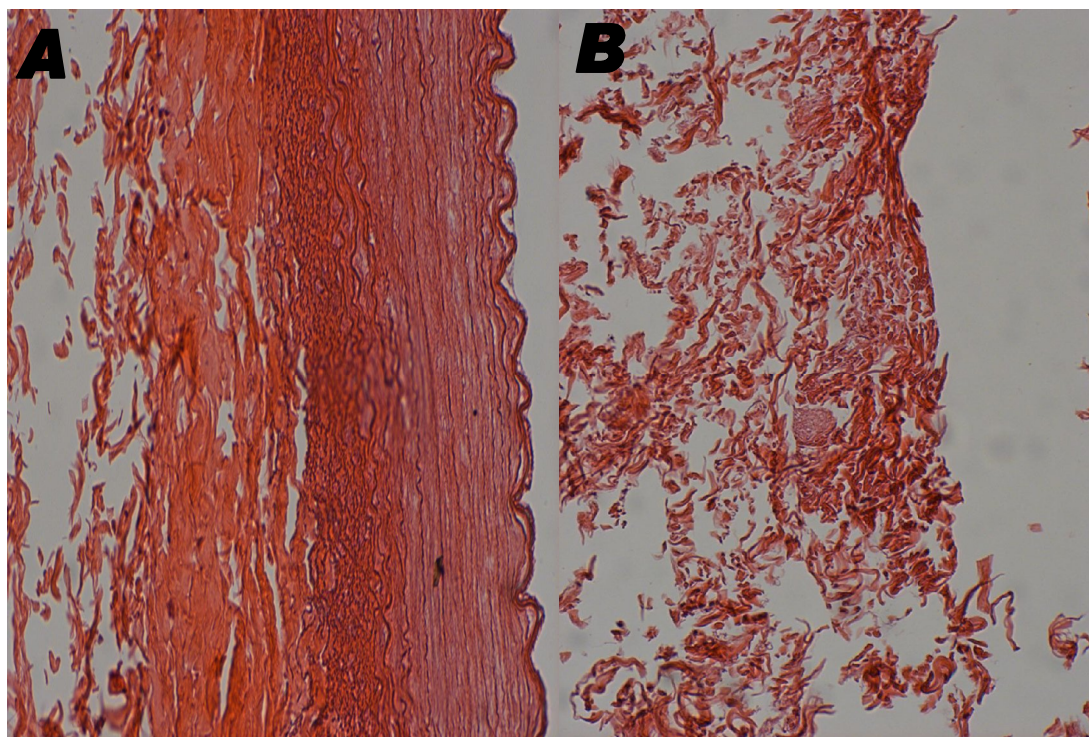


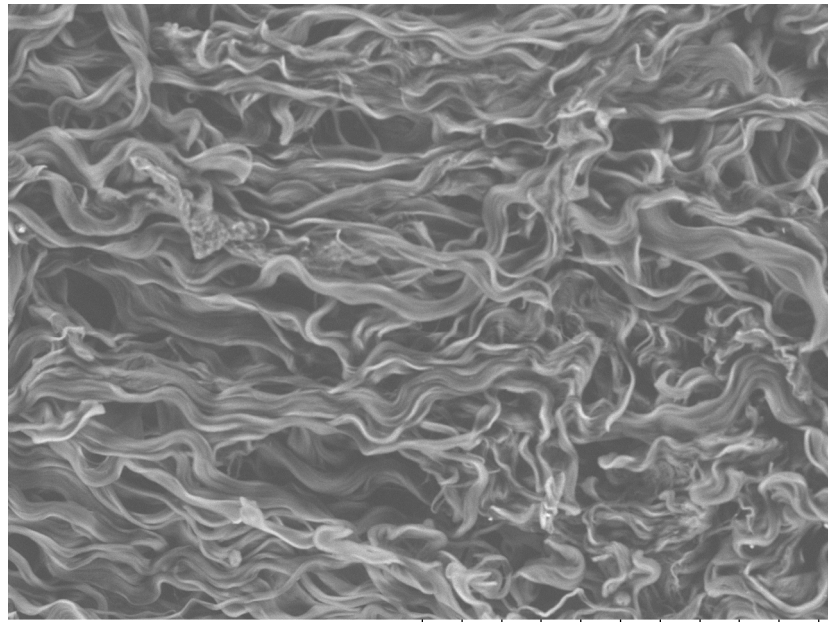
Figure 3.8. Scaffolds classified as 'Not Intact'. The pink collagen lines of the vessel do not retain their close proximity and continual interaction.

Table 3.1. Summary of Scaffold Classifications.

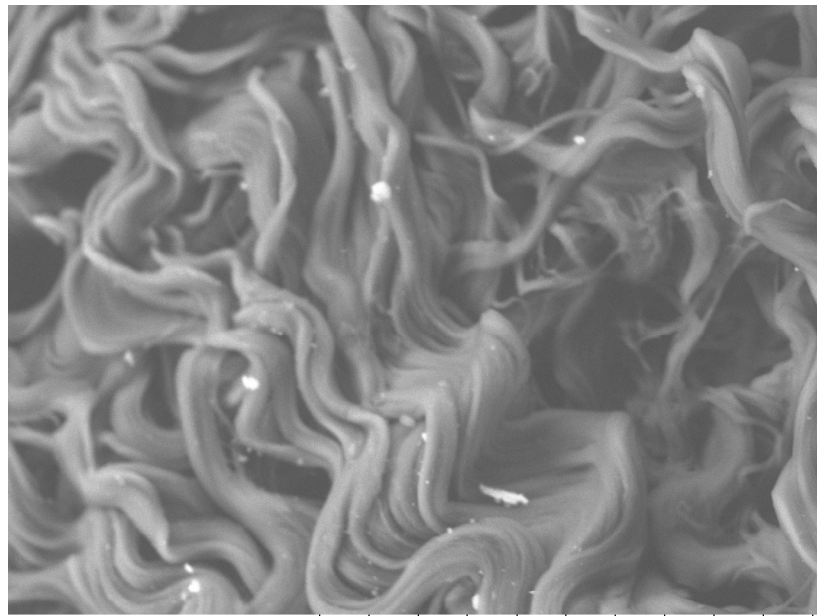
	Decellularized	Diameter (mm)
Intact	12	2 to 5
Not Intact	6	< 5

3.3.1.2 Scanning Electron Microscope Imaging

In Figure 3.9, the SEM images are the topographical images of the luminal surface of decellularized vessels at 400x and 1000x magnification. The wavy structure seen in histological images were two dimensional pictures of the collagen fibers, where are a topographical view (given by the shade of gray). There is some orientation, in that the fibers flow uniformly (horizontally in the 400x image on the top and vertically in the 1000x image on the bottom) in congruence with the orientation of normal blood flow through the vessel. Yet there is random orientation between the fibers, which is characteristic of a porous scaffold having the capacity to house cells and encourage cell proliferation and migration (41). These images are devoid of any cellular structure; where as in Figure 3.10, a native artery has a well defined endothelial cell lining.



CENG-2 2010/04/21 11:25 L x400 200 um



CENG-2 2010/04/21 11:27 L x1.0k 100 um

Figure 3.9. SEM images illustrate decellularized arteries. Top is at 400x magnification. Bottom is at 1000x magnification. *Note: this SEM image was acquired from a cell-sodded decellularized vessel, where no cells remained in the lumen (confirmed by H and E).

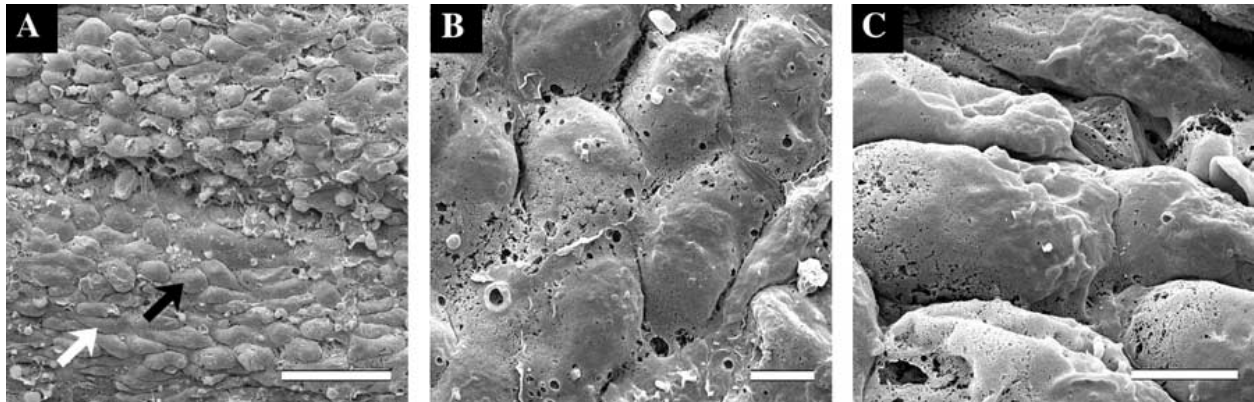


Figure 3.10. Images of intact native porcine arteries, with endothelial cell lining. Scale bars, 40 μm (A); 5 μm (B and C) (72).

3.3.2 Mechanical Evaluation

3.3.2.1 Tensile Testing

The tensile tests produced over 1000 raw data points for the force at each length extension. To summarize this data, a macro program in Excel was created and used (for full macro, see Appendix B: B.7). From this macro, raw data was used to calculate the stress and strain of each sample based on equations 3.1-3.4. The stress versus strain was graphed (Figure 3.11, top), to examine total behavior of the sample. The linear portion of the stress strain graph was re-graphed to show the elastic modulus and is determined by the slope of the equation of the line (Figure 3.11, bottom). The yield strength was considered to be the highest point of the elastic modulus, or the last point before plastic deformation. The original parameters for the example in Figure 3.11 were: original length (L_0) 13.42mm, original width (W) 11.43mm, and thickness of the sample (T) 0.79mm.

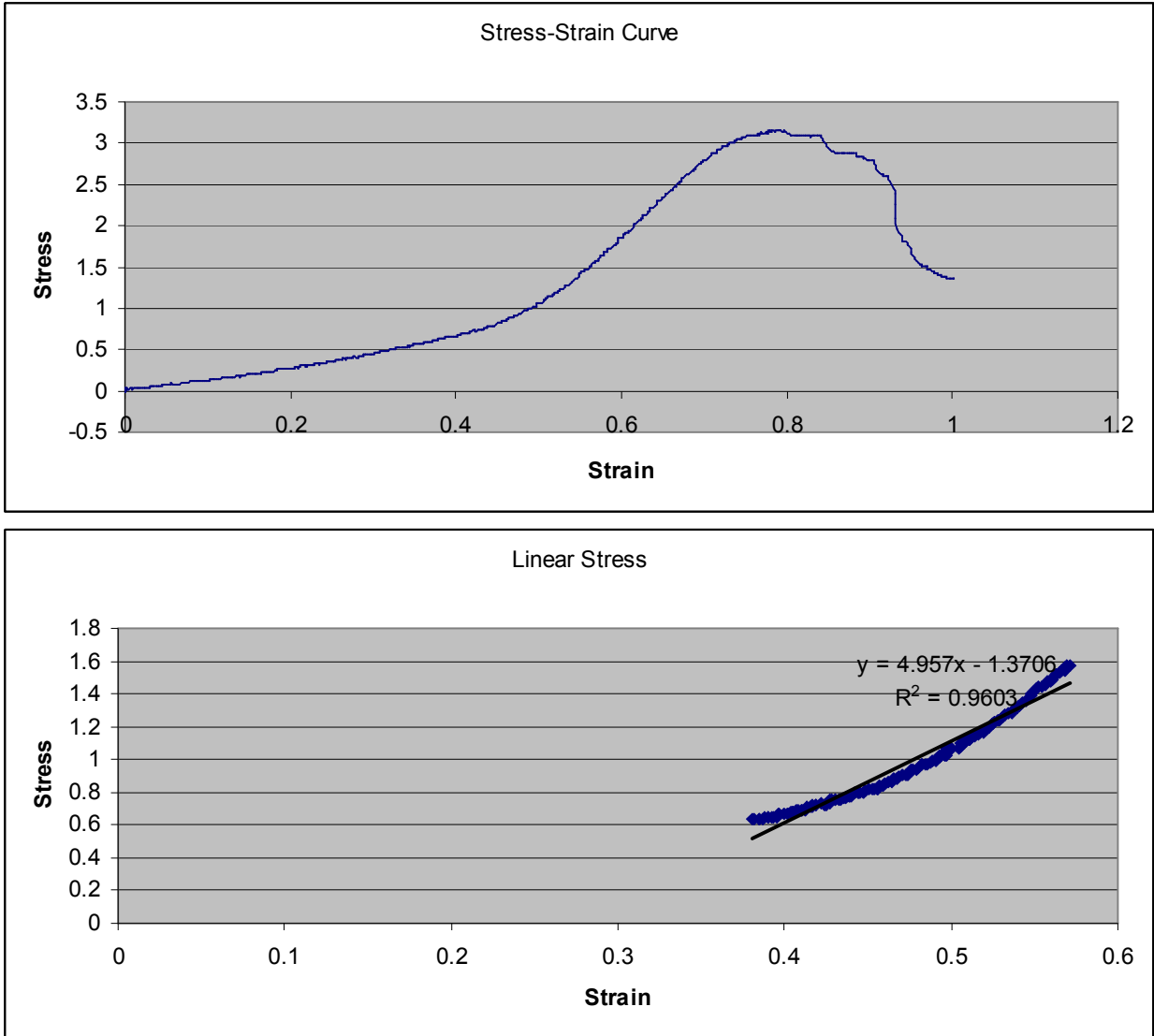


Figure 3.11. Sample stress versus strain graph (top) and linear component graph (bottom).

Additional data is in Appendix C.2.

Once the raw data for all samples was tabulated using the macro program, the Young’s Modulus and yield strength was identified for each sample (a summary table of the raw data is present in Appendix C: C.3). The raw data was summarized to show the average and standard deviation for each sample group (Table 3.2). A total of 12 scaffolds were tensile tested, 6 decellularized and 6 native. The average Young’s Modulus for the decellularized scaffold was 4.84 ± 1.91 MPa, whereas the average native modulus was 6.15 ± 2.63 MPa. These two groups were found to be statistically similar, with a p-value of 0.173 (Figure 3.12). The decellularized

material's elastic modulus was smaller than that of ePTFE which on the scale of GPa. The yield strength for decellularized vessels was 1.79 ± 0.786 MPa, versus a native value of 2.69 ± 1.23 MPa. When compared, the yield strength was statistically different between the groups with a p-value of 0.015 (Figure 3.13).

Table 3.2. Summary of the Average and Standard Deviation of Young's Modulus and Yield Strength (n = 6).

Treatment	Avg Young's (MPa)	Stdev Young's (MPa)	Avg Yield Strength (MPa)	Stdev Yield Strength (MPa)
Native	6.1553	2.6327	2.6901	1.2301
Decellularized	4.8463	1.9158	1.7997	0.78699

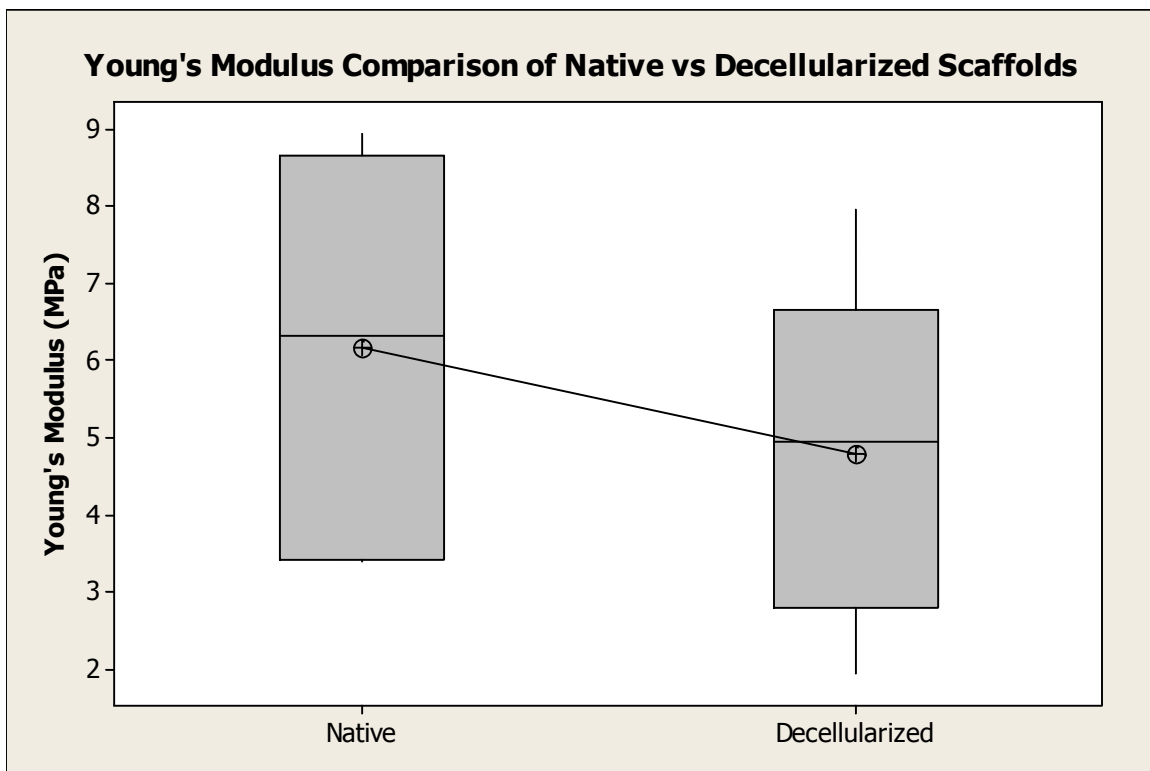


Figure 3.12. The Young's modulus of native and decellularized vessels. Not statistically different ($p = 0.173$, $n = 6$).

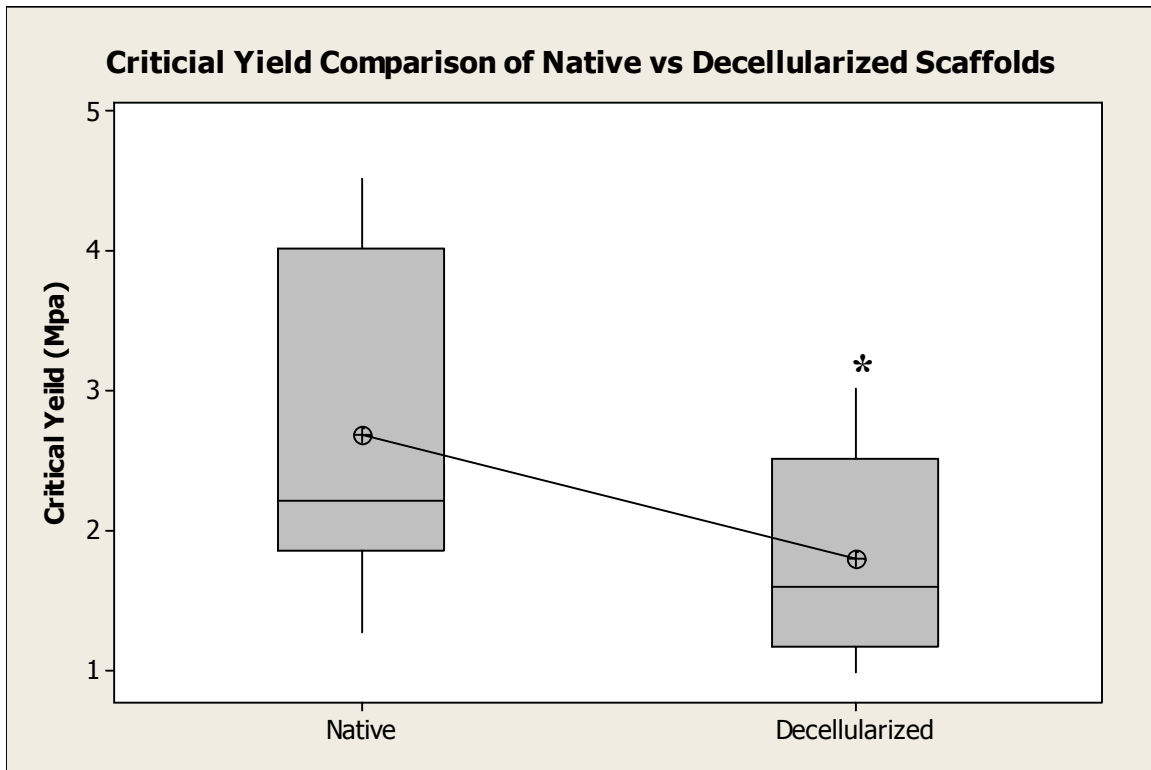


Figure 3.13. Comparison of the critical yield for native and decellularized scaffolds. Found to be statistically different (p -value = 0.015, n = 6).

3.3.2.2 Burst Pressure Evaluation

The burst pressure for native and decellularized arteries is summarized in Table 3.3. A total of 2 scaffolds were evaluated, one decellularized and one native. Literature regarding the burst pressure for native arteries have reported the burst pressure to average 3124 mmHg and the burst pressure for decellularized vessels at 2338 mmHg (71). Several scaffolds failed to reach higher pressures because of holes in the graft or poor suturing onto the barbs, and are not included in the reported data. When the scaffold broke, it appeared to tear longitudinally. The literature describes an acceptable burst pressure for a decellularized scaffold to be at least 2,000 mmHg (71).

Table 3.3. Summary of Experimental Burst Pressures.

Treatment	Burst Pressure
Control	2197.38 mmHg
Decellularized	1848.43 mmHg

3.3.3 Biological Evaluation

Figure 3.14, displays the bacterial content of the native and decellularized scaffolds after 12 hours of incubation. Images C and D from Figure 3.14 were the native samples, which have no bacterial colony growth. The decellularized samples in A and B had significant contamination, even in the presence of penstrep. Figure 3.15 shows samples that were placed in the LB broth, where a cloudy liquid indicates a contamination. Tubes 1 and 2 were decellularized samples and 3 and 4 are native samples; tubes 2 and 4 contained penstrep. The first 3 tubes were cloudy and contaminated, only the 4th tube was clear (the native with penstrep). These results indicate harvesting had some contamination, but the penstrep was potent enough to reduce the spread of bacteria. The contamination in both of the decellularized samples indicated the decellularization process was not performed sterilely.

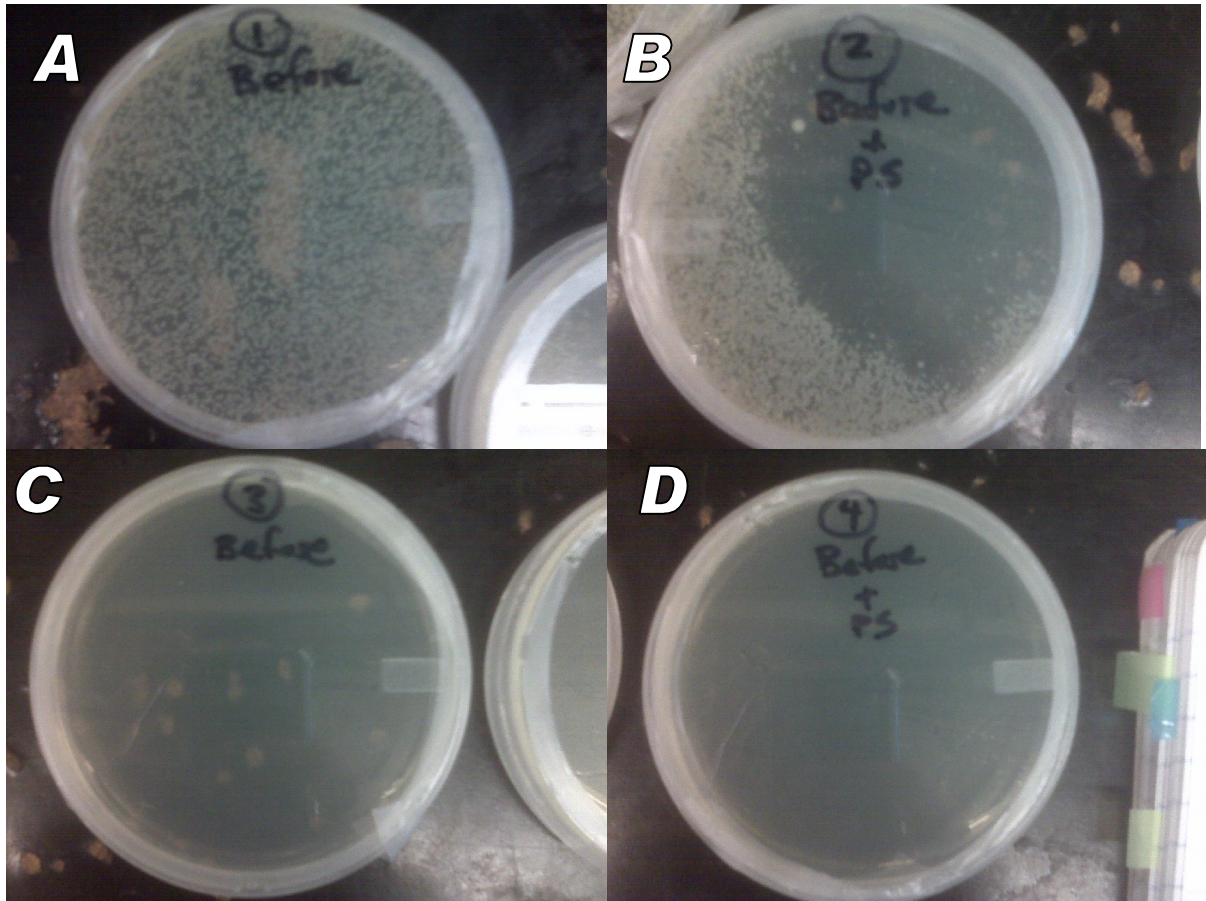


Figure 3.14. The TSA plate bacterial culture. A and B are decellularized tissues, C and D are native tissues. B and D received penstrep. Dots indicated bacterial colony formation.



Figure 3.15. Broth culture, from left to right 1 to 3 are contaminated and 4 is not. Tubes 1 and 2 were decellularized samples. Tubes 3 and 4 were native samples. Tube 4 was treated with penstrep. Cloudiness indicates the presence of bacterial contamination.

3.4 Discussion

3.4.1 Structural Evaluation

As seen in Chapter 2, the SDS treatment for decellularization was successful and did not have extreme effects on the structure of the scaffold. After H and E evaluation, the decellularization treatment did not extensively degrade the scaffold. Specifically, the collagen fibers appeared to remain intact, while the detergent successfully removed all cellular material; these results coincide with results found in literature (63, 64, 71, 73). The literature indicates that a change in the thickness of the scaffold is indicative of the decellularization process, identified by a decrease in the wall thickness of the scaffold after being decellularized (71).

However, in the decellularization process presented, the wall thickness appeared to increase rather than decrease. Although the wall thickness was not measured in the data presented, visual comparisons indicate an increase in overall vessel width. The change in thickness may possibly occur from the lack of smooth muscle cells (SMCs) in the media of the vessel wall, causing the structure to be more porous because there are fewer cellular bonds holding it together (73). The media and adventitia have some separation, having the appearance of slight degradation, but is considered superficial and caused by the release of fibroblasts from the connective tissue (64). From the experiments presented, the scaffold remains wavy indicating that collagen fibers remain in the scaffold (71). Although the increase in the wall thickness shows slight geometry changes within the scaffold, the gaps are characteristic of SMCs leaving the scaffold and do not seem to profoundly break-down the scaffold beyond recognition. Thus, the removal of cellular components from a native scaffold using the protocol presented in Chapter 2, does not present any drastic morphological complications.

Using the SEM to image the lumen of the scaffold reiterates the lack of drastic changes to the scaffold wall. The decellularized scaffolds on a micro-scale were not degraded, and showed no gaps, cells, or odd shapes. These images translate the cross-sectional views of the H and E images into a longitudinal topographical image. Again the wavy lines indicate the collagen fibers remaining intact, while the absence of small round cells embedded in the structure supports the complete decellularization of the scaffold. From the SEM images, the scaffold also appears to have a porous interconnected structure, which could encourage cellular adhesion if the scaffold is to be re-cellularized. As a proof of concept, these images along with the visual classifications of 'Intact' were indications that the decellularization treatment did not significantly deteriorate the scaffold structure.

3.4.2 Mechanical Evaluation

3.4.2.1 Tensile Testing

The elastic modulus is useful for describing the elasticity of the scaffold. This experimentation represents the biomechanical properties of a decellularized scaffold, thus having implications about the physiological relevance post decellularization (71). Also, with the construction of any new scaffold it is important to stringently evaluate all the properties to better understand the scaffold and how it may potentially respond under various stresses (71). The elastic, or Young's Modulus, was found to have no statistical difference between the control vessel and the decellularized scaffolds. However, the modulus for decellularized scaffolds showed a trend of being lower than the control. A lower elastic modulus implies the scaffold is more elastic, most likely due to a lack of cellular bonds that promote a firm structure. This trend was supported in the literature and is summarized in Table 8 (65, 71, 73, 74). However, it is difficult to compare all tensile testing methods. There are several apparatuses for tensile testing and all of them have different clamping and pulling methods. Even the way the sample is cut and prepared for testing varies between the published literature. While the results do follow similar trends, direct comparisons should not be made. Also, pig arteries are found to be more than three times as elastic as human arteries, and as such are not clinically translatable (75).

The yield strength is the measurement of the stiffness of a material. This measurement occurs at the transition between elastic deformation and plastic deformation (70). The stiffness was statistically decreased for the decellularized treatments versus the control, indicating the decellularized sample is stiffer. A stiffer material post decellularization was also suggested throughout the literature (Table 3.4). Thus, the decellularization treatment has no effect on the elasticity of the scaffold, but is more likely to reach plastic deformation before a native artery.

3.4.2.2 Burst Pressure Evaluation

Burst pressure provides information about the radial stress on the scaffold. Radial stress is related to compliance, which is described by the pressure per cross-sectional area (71). If the compliance is low in the scaffold, as in ePTFE, the stresses will be harsher because the scaffold does not have the capacity to dynamically react to the fluid flow (which is very dynamic in a physiological setting). There was some difficulty testing for burst pressure on decellularized arteries because during the harvesting and clean up processes, some of the scaffolds were compromised. Small nicks occurred from the razor blades or scissors when attempting to remove the sample or connective tissue. These small nicks were exposed when the luminal pressure was increased and thus the maximum stress was not able to be determined. Once an uncompromised vessel was tested, the burst pressure was found to be similar to that found in literature (Table 3.4).

Table 3.4. Summarized Averages Found in Literature (65, 71, 73, 74).

Average	Young's Modulus (MPa)	Yield Strength (MPa)	Burst (mmHg)
Contol	0.271	9.16	2338
Decellularization	0.812	7.19	3124

3.4.3 Biological Evaluation

Understanding the bacterial content in a scaffold that is difficult to sterilize is important for understanding its potential use in cell culture assays or as a tissue engineered construct. The decellularization process was not done in a sterile environment, and as such resulted in contamination that could not be ameliorated with simple antibiotics. However, the harvesting process was considered to be an aseptic procedure; contamination was minimal and a small dose of penstrep sufficiently decreased the potential for contamination. Thus, by decellularizing the

scaffold in sterile conditions and using a small dose of penstrep, an aseptic scaffold results for use in the BVM. Although simple, this biological evaluation provides important information regarding the scaffold and its potential use in the BVM; the scaffold in combination with a small dose of penstrep should support cell viability.

In conclusion, the experiments presented in this Chapter examined the structural integrity, mechanical, and biologic properties of the scaffold post decellularization. The structural, mechanical, and biological examinations helped to better characterize the scaffold and examined its physiological potential. All of these experiments suggest that the decellularization treatment does not negatively harm the scaffold. Images provided visual conformation of the lack of degradation within the scaffold, specifically compared to the native arteries. Mechanical tests confirmed that the elasticity and stiffness of the decellularized scaffold were similar to a native artery, which is important for its physical use. The biological evaluation illustrated the amount of contamination sustained throughout the harvesting and decellularization process, and suggested that using aseptic conditions for the decellularization process and a small dose of penstrep the scaffold will produce an aseptic scaffold. Since the scaffold is not affected by the decellularization treatment, the scaffold remains relatively similar to a native artery; thus, the use of a decellularized artery in the BVM model presents a relatively physiologic and appropriate scaffold.

Chapter 4 - Use of Decellularized Vessels in the Blood Vessel Mimic

4.1 Introduction

Chapters 2 and 3 of this thesis evaluated the potential to decellularize a porcine artery and the resulting mechanical properties to understand if the scaffold could be implemented in the BVM system. These experiments characterized several aspects of the scaffold to support the potential for recellularization. A successful protocol for complete decellularization was developed, ensuring that the native porcine cellular components were removed from the scaffold. After decellularization, there was little damage sustained to the structural integrity of the scaffold wall, where most of the components from the ECM were visually maintained. Furthermore, the mechanical properties were evaluated to further characterize the remaining ECM components. Mechanical testing revealed that the decellularization treatment did not change the elastic modulus or burst pressure of the scaffold. The scaffold was also evaluated for potential contamination risks; some contaminations were identified, but the addition of 0.1% penstrep was sufficient to alleviate potential contaminants. The results from these experiments provided conclusive background to support the use of a decellularized porcine artery as a scaffold in the BVM. The scaffold was considered similar to a native scaffold with the potential to house cells, thus supporting the basic requirements needed to fulfill the goals of the BVM system. The next step of characterization was to recellularize the scaffold and evaluate its ability to have a monolayer of cells.

The recellularization process entailed the incorporation of cells into a decellularized graft, thus completing the tissue engineering paradigm. The paradigm describes the combination of a scaffold with cells to produce a ‘functional’ tissue (76). In this case, the decellularized artery represented the scaffold by providing the support and essential structure of the tissue, while the addition of cells provides natural biological cues, creating a ‘functional’ vessel. Cells have the

capacity to communicate by the exchange of growth factors or through proteins, either expressed or received, which results in various dynamic responses (77-79). Thus, with the addition of cells to the scaffold, aids in integration with the body (or simulate a physiologic response in the *in-vitro* testing system). The decellularization process stripped the porcine of their native cells; therefore the addition of new cells was considered a recellularization procedure. There are two ways to recellularized, either by sodding or seeding. To seed a scaffold a small amount of cells are placed in the graft and expected to proliferate to cover the scaffold (80). Seeding a scaffold is typically a static procedure, encourages maximum cell retention within the scaffold. Sodding is done by introducing an excessive number of cells on the scaffold and expecting a high percentage to adhere, lowering the amount of proliferation needed (80). With a perfusion system the stress on the cells can be severe and not conducive for cell adhesion or drastic cell proliferation. Thus a sodding protocol was ideal for recellularization because the over compensations of cells necessary to fill the scaffold. Sodding cells within a tubular scaffold was accomplished by injecting cells into the lumen via pressure sodding.

The creation of an effective sodding protocol was one of the final stages in the development, characterization, and implementation of a biological scaffold for the BVM. The sodding protocols followed the work previously investigated by Dr. Kristen Cardinal utilizing human vascular endothelial cells sodded into the lumen of an ePTFE scaffold to create an endothelium (4). Once a sodding density was deemed reasonable for short term cultivation, the scaffold was cultured for longer time points. Equally important to the recellularization process was the use of a bioreactor, which housed the scaffold and allowed tissue cultivation. A bioreactor served as a sterile containment device to culture the scaffold; it supplied the external environment to the scaffold by accounting for the physiologic flow, gaseous exchange, and culture for the scaffold and cells. For the BVM, the bioreactor consisted of a peristaltic pump, a

media reservoir, a 'glad ware' type vessel chamber, and surgical grade tubing (Figure 4.1). The bioreactor, which has been developed through previous student projects, was imperative to recreating a physiologic environment (81).

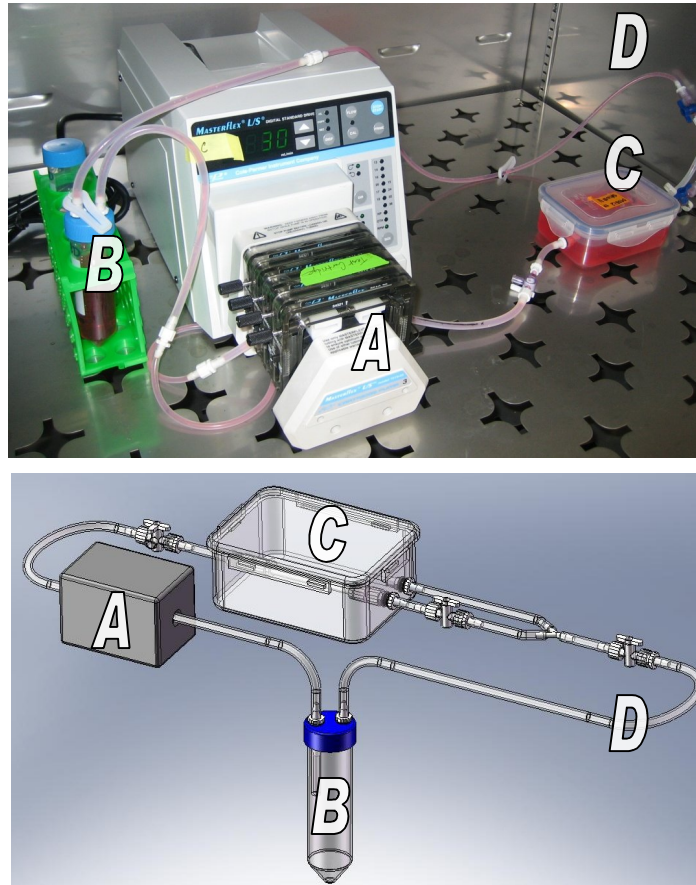


Figure 4.1. Model of the bioreactor setup for the BVM system. Closed loop containing: Peristaltic pump (A), media reservoir (B), housing(C), and tubing(D). Top depicts the actual set-up. Bottom is a solidworks generated image.

A variety of cell types were used to develop the recellularization process for a decellularized scaffold. Preliminary work utilized 3T3 fibroblasts for information regarding the ideal seeding density, the toxicity of the scaffold, the protocol for seeding, and the cell density and distribution throughout the length of the scaffold. The 3T3 fibroblasts were ideal for this

work because they are an immortalized cell type, making them relatively inexpensive for preliminary work. For physiologically relevant work, human umbilical vein smooth muscle cells (hUVSMCs) and human umbilical vein endothelial cells (hUVECs) were utilized. The hUVSMCs comprise the main natural cell type in the media of an artery, while hUVECs make up the endothelium. This chapter will describe the results of sodding the different cell types onto the decellularized scaffold to effectively mimic a native artery.

4.2 Methods

4.2.1 Short-Term Cultivation – *Trial 1*

Initial work for recellularizing the scaffold began with determination of the optimal cellular sodding density in order to create a continuous monolayer on the lumen of the scaffold. The short term experiments, lasting 1-12 hours, examined the optimal sodding density for a decellularized scaffold and subsequently the potential toxicity of the scaffold from the SDS solution. The optimal sodding density will coat the lumen with a single layer of cells consistently throughout the length of the vessel as well as around the circumference of the lumen. Cells should be dispersed thinly and evenly throughout the scaffold limiting cell clumps while promoting cell integration and adhesion. The preliminary work for a sodding density and protocol was based on previous work done by Dr. Cardinal, where a similar sized scaffold and BVM configuration was utilized (4).

Dr. Cardinal's original protocol for sodding the scaffold in Appendix B: B.10, used a scaffold approximately 3 to 4 mm inner diameter, 4.5cm in length, and sodded at a density of 5×10^5 cells per cm^2 . The previous work was modified for sodding the decellularized scaffold, mainly regarding scaffold preparation and media used. Additional steps were also added to account for the decellularization of the scaffold. These modifications are described in Appendix

AB: B.11; note the scaffold dimensions as well as the seeding density did not change from the previous work.

For initial experiments, 3T3 fibroblasts were expanded to obtain approximately 10 million cells per scaffold. The native porcine artery was decellularized following the methods from Appendix B: B.3. The decellularized scaffold was cut to approximately 3 cm in length with an inner diameter of 3 to 4 mm. The scaffold was sutured to the male barbs and luer locked into the bioreactor. The scaffold was perfused, using a syringe, with culture media to remove all bubbles from the scaffold. The 3T3 cells were trypsinized to a cells into suspension, and the cell solution, approximately 10 million cells, was perfused using transmural flow into the proximal portion of the scaffold. Transmural pressure seeding ensures the cells are pushed into the pores of the scaffold. An additional bolus of media was transmurally perfused through the scaffold to push all cells remaining in the lumen into the scaffold wall. Transmural flow was continued using an 8 roller (model 7519-25 Cole Parmer) peristaltic pump (Model 7523-60 Cole Parmer Master Flex L/S) at a slow, steady rate of 10 rpm (0.5 ml/min) providing continuous pressure on the scaffold wall. The transmural pressure pushes the cells into the scaffold encouraging cell adhesion and a high yield of cellular attachment.

After 1 hour, the scaffold was carefully cut from the barbs in the bioreactor using a razor blade. Extreme care was taken to not compress or jar the scaffold as to prevent accidental removal of cells. Once removed, the scaffold was placed in histochoice for approximately 30 minutes to cross-link the structure. Scissors were then used to cut the scaffold longitudinally creating 2 hemispheres and exposing the lumen for examination, again extreme care was taken to keep the seeded cells intact (Figure 4.2). The scaffold was stained with bisbenzimidazole (BBI, a Hoechst Stain Kit, St Louis, MO), which fluorescently labels the DNA in each cell to visualize individual cells on the surface of the lumen (protocol Appendix B: B.12). Images were taken

from the proximal side (where flow originates from) to the distal side on both the top and bottom of the scaffold. Cell density and consistency was evaluated for each of the images by counting the number of cells on the scaffold. The counting method used five 1 mm² squares were drawn on each image and then the cells within each square were counted. The average number of cells on each image was used to determine if the seeding protocol and cell density effectively created a monolayer of cells. All scaffolds were imaged at 10x on an Olympus BX41 Fluorescence Microscope.

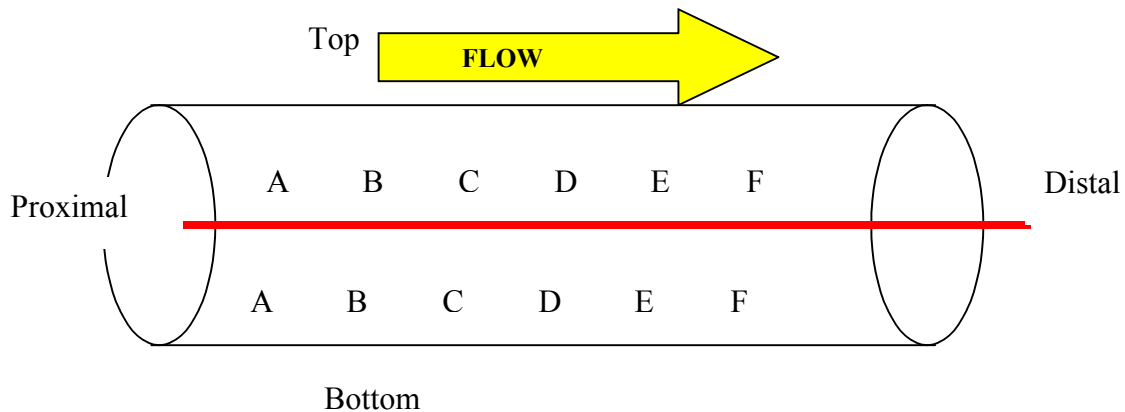


Figure 4.2. Longitudinal cut of the recellularized scaffold. Images were taken from proximal to distal edges to visualize cell consistency.

4.2.2 Long-Term Cultivation – Trial 2

The BVM is intended to evaluate intravascular devices which require extended culture duration. Thus, the scaffold must be tested for its ability to remain in culture for longer than 12 hours. Ideally, long term culture of the cells on a tubular scaffold should result in the production of a nearly continuous cellular monolayer and mimic a native artery. Therefore, in addition to a long term culture, a more physiologic cell type was utilized to recreate the cellular layers of a

native artery. hUVSMCs may be used to populate the media of the vessel, while HUVECs would be better suited to create the endothelium.

Trial 2, Experiment A - Human Umbilical Vein Smooth Muscle Cell Sodding A

HUVSMCs were the first physiologically relevant cell type to be sodded into the scaffold. In addition to the new cell type it was also the first time performing a long-term cultivation. Although hUVSMCs are not the prime cell type for effectively mimicking the endothelium, however they contribute to the vascular wall and would be acceptable for preliminary testing. The set up for long term cultivation followed similar procedures as short term; only the cell culture media was HUVSMC specific, and the flow rate was slowly increased over time to ultimately reach a near-physiologic flow rate (Appendix B: B.14). Three individual scaffolds/systems were set up. Once each scaffold was sutured into the BVM and the systems were connected to the 8 roller peristaltic pump, scaffolds were pressure sodded with approximately 3.4 million cells per cm² each (estimated 10 million cells per scaffold) with transmural flow at 7 rpm for 1 hour (Figure 4.3).

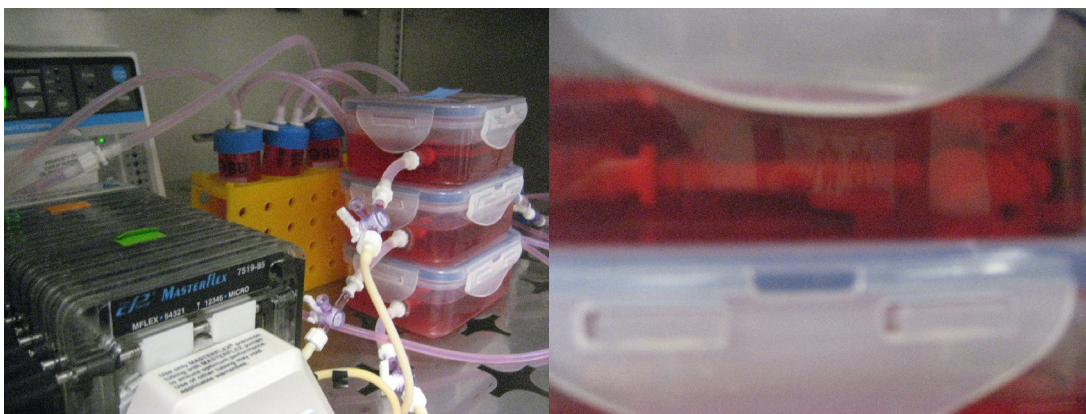


Figure 4.3. A setup of decellularized scaffold with the peristaltic pump and BVM.

After the 1 hour of transmural flow, the tubing was unclamped and flow was continued lumenally at 10 rpm for one additional hour, after which flow was increased to 15 rpm over night

(approximately 12 hours). The next day, the flow rate was increased by 10 rpm every 30 minutes until reaching 90 rpm. Once the flow rate reached 90 rpm (approximately 5 mL/min), the BVM was monitored daily. Two of the scaffolds were cultured for 1 day, about 24 hours, and the third scaffold was cultured for 5 days. The culture media was kept fresh by exchanging old media for fresh media via the reservoir every 3 days. As previously described, extra care was taken when detaching the scaffold to prevent accidental removal of cells. Once excised from the BVM, the scaffold was placed into histochoice for approximately 30 min. Then the scaffold was cut longitudinally (Figure 4.2) and stained with BBI. Images were taken from proximal to distal sides of the scaffold following the direction of flow. BBI images were evaluated for cell density and consistency along the length of the scaffold by counting five 1 mm² areas. Comparing these counts across the length of the scaffold determined if the seeded cell density successfully created a cellular monolayer along the lumen of the scaffold. All scaffolds were imaged on an Olympus BX41 Fluorescence Microscope.

To learn more about the scaffold and the seeding procedure on a decellularized scaffold it was deemed prudent to analyze all 3 of the scaffolds via sectioning and staining. The experiment was repeated exactly as before with hUVECs seeded onto a decellularized scaffold at 3.4 million cells per cm². The scaffold was again removed from the BVM and preserved in histochoice for embedding in paraffin wax for histological analysis via H and E staining. Sections of the scaffold were imaged on an Olympus BX41 Microscope. Images of the sections were only analyzed for the presence and location of the cells throughout the scaffold.

Trial 2, Experiment B – Human Umbilical Vein Endothelial Cell Seeding

To produce the most ideal scaffold, it must contain the endothelial cell monolayer naturally found on the lumen of an artery. HUVECs have been utilized in previous work to effectively mimic the endothelium on ePTFE scaffolds and should provide similar results on a

decellularized scaffold (4). The successful culture of hUVECs on a decellularized scaffold provided the final proof of concept that this scaffold can house cells on the lumen of the scaffold, thus providing the necessary results to implement a decellularized scaffold as part of the BVM model.

The decellularized scaffold was sodded and cultured similarly to the hUVSMCs in Appendix B: B.14, but again different cell types and medias were used (Appendix B: B.15). First, two porcine arteries were decellularized following the protocol from Appendix B: B.3. The hUVECs were labeled prior to sodding with Cell Tracker Green. The hUVECs were cultured to 90% confluency. Cells were stained with a 15 μ M concentration of Cell Tracker Green following the manufacturer's protocol, this protocol and optimization is further explained below in section: *4.2.3 Dual sodding Proof of Principle – Trial 3* (see Appendix B: B.16 for exact staining protocol). The cells were trypsinized and pressure sodded onto two grafts, at approximately 1.5 million cells per cm^2 . The sodding density was less than previously used because an unanticipated increase of vessel length. After sodding, vessels were placed on a peristaltic pump with transmural flow at 10 rpm for 1 hour. Then, flow was averted lumenally at 10 rpm for 24 hours, no increase in flow rate over time occurred to reduce shear stress on the cells. The vessels were taken down by cutting them from the barbs using a blade. To image the vessels a longitudinal cut was made creating 2 semi circular halves. The endothelium was exposed for imaging from proximal to distal, as seen in Figure 4.2.

4.2.3 Dual Sodding Proof of Principle – Trial 3

The overarching purpose of this experiment was to develop a method to pressure sod two different cell types onto a scaffold for the BVM using two different fluorescent cell trackers. The concept of the cell tracker is to visually monitor a cell type as it migrates, divides or interacts with other cells types using a wide field fluorescent microscope. This protocol aims to

provide successful dual sodding (i.e. pressure sodding two different cell types onto the vessel). Ultimately, it would be desirable to use both hUVSMCs and hUVECs to dual-sod BVMs, therefore the goal of these experiments was to develop and test two cell tracker dyes for concurrent use to assess a dual-stained BVM

Staining Protocol

The cell tracker dye was made following the manufacturers instructions. Two cell trackers were utilized in this methodology: Cell Tracker Green CMFDA (5- Chloromethyl Fluorescein Diacetate; Invitrogen; Carlsbad, CA) catalog number C 7025 and Cell Tracker Red CMPX (Invitrogen; Carlsbad, CA) catalog number C34522. The stock solution was created by adding high-quality DMSO (D8418, St Luis, MO) to the lyophilized dye product. 10.8 μ L of DMSO was added to the 50 μ g vial of cell tracker to produce a 10mM concentration of **stock solution**. The stock solution was then diluted with serum free media to a concentration ranging from 0.5 to 20 μ M (this work shows a 5 μ M concentration, but other concentrations are characterized below in the graph), this was the **working solution**. Differences in concentration depend upon the specific cell type and application of the cells. Higher concentrations are used for cells which will go through several population doublings or for longer durations prior to imaging. Lower concentrations of the working solutions can be utilized for less proliferative cells or for short term experiments. Once the working solutions were made, the general dying process was preformed as described below.

The cell culture media in a flask of cells was removed and the cell tracker working solution was added in a volume to cover the total surface area of the cell culture flask. The Cell Tracker Green working solution incubated for 30 minutes, while the Cell Tracker Red working solution was incubated for 15 minutes, timing differences based on the lower range suggested by the manufacturers protocol. Then the cell tracker working solution was aspirated from each of

the culture flasks and replaced with the normal cell media for that culture. The cell culture media was incubated on the dyed cells for at least 30 minutes cells prior to use. The cell culture was then imaged on an Olympus BX41 microscope; the green dyed cells were excited at 488 nm and with an emission at 520 nm (turret 4, S1, filter wheel one on 3, and filter wheel two on 2), where red cells were excited at 587 nm and had an emission at 615 nm (turret 4, S1, filter wheel one on 4, and filter wheel two on 3). The protocol for using cell tracker dyes to stain cells is summarized in Appendix B: B.16.

Trial 3, Experiment 1 – Optimization of Cell Tracker Green Concentration

The purpose of experiment 1 was to determine the ideal concentration for the working solution, with the goal of using moderately proliferative cells for one-week duration. The cell type used in this experiment was 3T3 fibroblasts in order to gain a sufficient amount of knowledge about the dye, while minimizing costs. The fibroblasts were cultured to 90% confluency in a 6-well plate. Each well had a different concentration of the working solution of Cell Tracker Green added; the concentrations were 0.5, 1.0, 5.0, 10.0, 15.0, and 20.0 μ M. The previously mentioned staining methods were followed to dye the cells. These cells were examined and imaged every other day for one week, assessing the changes in intensity.

Trial 3, Experiment 2 – Cell Tracker Green with Trypsin

The purpose of experiment 2 was to examine the effects of trypsin on the cell tracker dye. Trypsin is a harsh enzyme that is necessary for cellular disassociation and the sodding process, therefore it may affect the properties or intensity of the dye and needed to be evaluated prior to use in a sodding experiment. 3T3 fibroblast cells were cultured to 90% confluency and stained with a 5.0 μ M concentration of Cell Tracker Green in a T75 culture flask following the previously mentioned staining methods. Once stained, the cells were trypsinized to make a cell solution. Then approximately 0.5 million cells were placed in each well of a six-well plate.

Cells were left in the six-well plate overnight (14 hours) to allow for cell adhesion. Cells were then imaged and the intensity of the Cell Tracker Green was assessed.

Trial 3, Experiment 3 – Cell Tracker Green and Red in Co-Culture

The purpose of experiment 3 was to evaluate the ability of two different cell trackers to be used together. This was a proof of concept for the potential use of two cell trackers for analysis of a dual sodded vessel. Two T75 flasks of 3T3 fibroblasts were cultured to 90% confluency. One T75 was dyed with Cell Tracker Red, and the other T75 was dyed with Cell Tracker Green both at a concentration of 5 μ M, following the previously described staining methods. Once dyed, the cell cultures were trypsinized and placed into a six-well plate. The six-well plate contained two wells of Cell Tracker Green alone, two wells of Cell Tracker Red alone, and two wells containing a combination of cells with both cell trackers, as seen in Figure 4.4. There was approximately 0.5 million cells per well, and the cells were left for 14 hours to adhere for better imaging. Cells were imaged to analyze their interaction. The trials done throughout this Chapter are summarized below in Table 4.1.

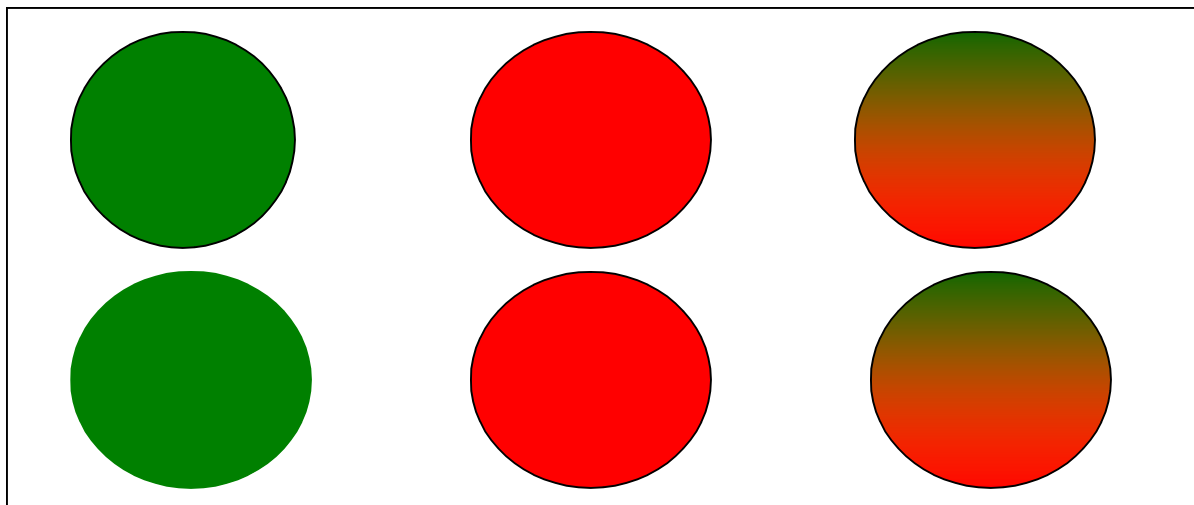


Figure 4.4. This image represents the six-well plates used in experiment 3. The dyes are represented by the colors, left is Cell Tracker Green, center is Cell Tracker Red, and right is the combination of Cell Tracker Green and Red.

Table 4.1. Summary of Experiments From This Chapter.

	Cell Type	Duration	Analysis	Sub Experiments
Trial 1	3T3	1 hour	BBI	None
Trial 2	HUVSMC and HUVEC	1-3 Days	BBI and H/E	Experiments A and B
Trial 3	3T3	1 Day	Cell Tracker Green	Experiments 1,2, and 3
Experiment A	HUVSMC	1-5 Days	BBI and H/E	
Experiment B	HUVEC	1 Day	Cell Tracker Green	
Experiment 1	3T3	1 week	Optimization of Cell Tracker Green Concentration	
Experiment 2	3T3	1 hour	Cell Tracker Green with Trypsin	
Experiment 3	3T3	1 day	Cell Tracker Red and Green Co-Culture	

4.2.4 Analyzing Images

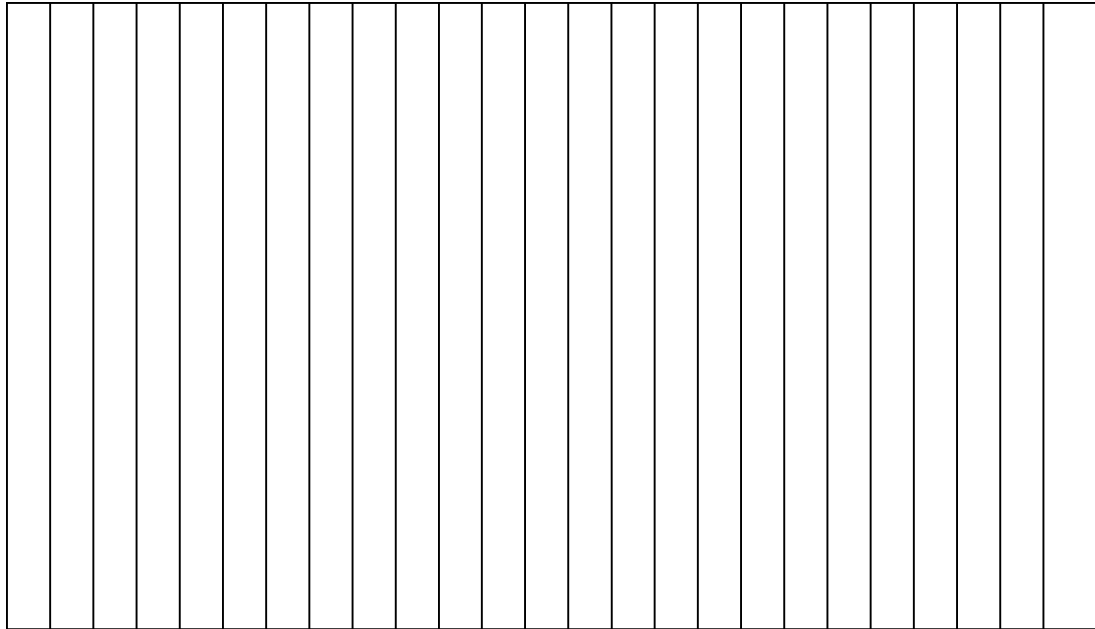
Counting the cells

To quickly count cell numbers, an imaging program was utilized (full detailed instructions are in Appendix B: B.17). Images were opened and analyzed in the ‘Image J’ program. The image was made binary by going to Image, Color, split channels. This created three images in grey scale labeled red, green, and blue. The green labeled images in grey scale were selected. Next, by selecting Image, Adjust, and Threshold the image was changed to black and white where black represents the most intense parts of the image (press dark background making the highlighted cells black). To tabulate the average area of each cell and the number of cells in the image select Analyze, Analyze Particles. A screen emerges asking for specificity of the Size, Circularity. The size describes the range of pixels that must be found together to be counted as a ‘cell’. The formula for circularity is given by equation 4.1.

$$\text{circularity} = 4\pi \left(\frac{\text{Area}}{\text{Perimeter}^2} \right) \quad \text{Equation 4.1}$$

A value of 1.0 indicates a perfect circle. For green images the size should be “20-Infinity” and circularity should be “0.00-1.00”. For red images the size should be “300-Infinity” and circularity should be “0.50-1.00”. This effectively counts all the cells within the image. It is important to note that the Cell Tracker Red dye was not optimized for the ideal concentration, therefore the concentration used was saturated and the stains appeared spotted throughout the cytoplasm of the cell. The lack of optimization for Cell Tracker Red explanations the change required in analysis settings. In future experiments, Trial 3 - Experiment 1 should be repeated for the Cell Tracker Red dye to determine the ideal concentration of dye that produces similar visual results within the cell as the Cell Tracker Green Dye.

To determine the cells per cm^2 a Ronchi ruling was used to calibrate the pixels of the image. An image of the calibration slide was taken at the same magnification where vertical lines were the focal point of the image. By counting how many lines (through the use of cell counter processing tool in Image J) span the width of the image, a ratio can be found to determine the total surface area of the image. To calculate the size of one edge of an image is as follows (Figure 4.5 for visual descriptions). In this case the numbers of pixels are seen in the top left corner. The first number represents the number of pixels on the x-axis, which is 1392. 135 vertical lines were counted (Figure 4.5) and using equation 4.2, the x-length was calculated using. Then equation 4.3 was used to calculate the y-length. These two numbers were then multiplied together to calculate the area of the images.



calibration_40x.jpg (50%)
1392x1040 pixels; RGB; 5.5MB



Figure 4.5. Top is a representative image of a Ronchi ruling. Bottom is the actual image of a Ronchi ruling, although faint, the vertical lines are the incremental measurements.

$$\frac{\text{Number of Vertical Lines}}{\text{Number of Pixels in the x direction}} = \text{the length of that side} \quad \text{Equation 4.2}$$

Example 1: 135 vertical lines at 1392 pixles.

$$\frac{135}{1392} = 0.9mm$$

The ratio calculation can be seen as follows, where x is the length the other side:

$$\frac{\text{Length of side 1}}{\text{Pixels on side 1}} = \frac{x}{\text{Pixels on side 2}} \quad \text{Equation 4.3}$$

Example 2: Known side is 0.9mm on 1392, the other side has 1040 pixels.

$$\frac{.9mm}{1392 \text{ pixels}} = \frac{x}{1040 \text{ pixels}} \rightarrow x = 0.67mm$$

Once each side of the image has a calculated length, the sides can be multiplied together to find the surface area of the image (detailed protocol for counting is in Appendix B: B.17). By calculating the surface area of the image and count the number of cells within that image, the cells per cm² in the scaffold was determined.

Calculating the Intensity of the Image

The intensity of the image was calculated in order to compare the effectiveness of the dye to remain in the cell through time and proliferation. The dye will photobleach and fade with time and excess exposure to light, thus measuring the intensity describes any changes within the dyed cells. Images were opened and analyzed in the 'Image J' program. The images were made binary by selecting Image, Color, split channels. This created three images in grey scale labeled red, green, and blue select and the color of the image was selected. Then, the circular button, on the tool bar was clicked. This tool was used to circle a single cell on the image, allowing analysis of the intensity for that part of a given cell. Once one cell was highlighted Analyze, Histogram was selected. The histogram provided a mean number, which represented the mean intensity of the area circled. This process was repeated for five cells in the image and the numbers were averaged to get the relative intensity of all the cells (Appendix B: B.17). By

determining the relative intensity, combined with the surface area, it was possible to count the cells and examine the ability to retain the Cell Tracker Dye within the cells.

4.3 Results

4.3.1 Short-Term Cultivation – Trial 1

Short term cultivation provided a proof of concept regarding the sodding procedures, specifically investigating the cellular density and consistency along the length of the scaffold. Short term cultivation from Trial 1 included pressure sodding 3T3 fibroblasts followed by transmural flow for 1 hour. Cell density and consistency were determined based on a square counting method (Figure 4.6). The average number of cells from the 1 cm² squares for each image was used to compare the cell density throughout the length of the scaffold (Table 4.2 The Quantitative Characterization of the 3T3 Fibroblasts on the Scaffold – Trial 1). After 1 hour of cultivation about 1.6x10⁵ cells/cm² of the original 3.5 million cells/cm². This remaining density was consistent on top and bottom from proximal to distal and was assumed to be a monolayer of cells on the scaffold as compared to densities found throughout literature, 2 x10⁵ to 6 x 10⁶ cells/cm² was found to effectively create a monolayer of cells on several surface types (with hUVECs) (82-86).

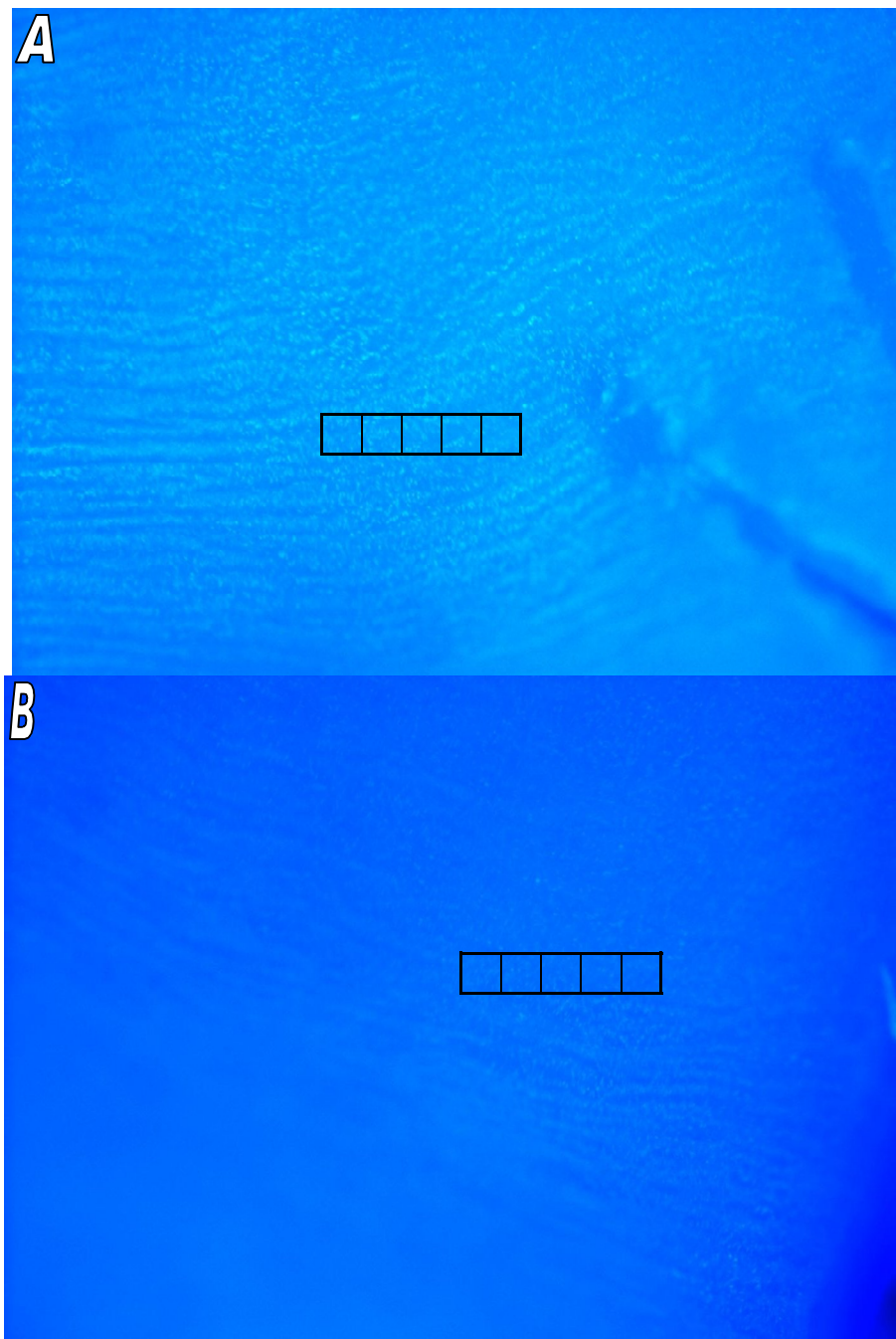


Figure 4.6. Trial 1 with 3T3 fibroblasts sodded. The top of a sodded scaffold (A) and is the bottom of the sodded scaffold (B). The boxes represent the 1 mm² section of cells that were counted.

Table 4.2. The Quantitative Characterization of the 3T3 Fibroblasts on the Scaffold – Trial 1

Position on the length of the scaffold	Bottom Box 1	Bottom Box 2	Bottom Box 3	Bottom Box 4	Bottom Box 5	Top Box 1	Top Box 2	Top Box 3	Top Box 4	Top Box 5	Avg Per square	Avg Per cm²
A	25	16	26	8	19	25	21	20	24	21	20.5	2.05x10 ⁵
B	19	9	23	16	24	14	16	18	25	12	17.6	1.76x10 ⁵
C	18	16	12	20	14	14	12	16	15	11	14.8	1.48x10 ⁵
D	7	11	10	11	12	18	25	23	19	18	15.4	1.54x10 ⁵
E	14	14	12	20	12	13	16	9	13	10	13.3	1.33x10 ⁵
F	14	16	17	17	18	20	20	17	24	29	19.2	1.92x10 ⁵
G	14	15	21	16	13	18	16	11	17	15	15.6	1.56x10 ⁵
H	18	17	15	10	6	16	13	18	17	17	14.7	1.47x10 ⁵
I	12	18	16	13	11	3	9	8	6	5	10.1	1.01x10 ⁵
J	24	17	27	20	13	19	25	22	20	17	20.4	2.04x10 ⁵
K	12	12	13	12	12	17	13	22	18	21	15.2	1.52x10 ⁵
											Average	1.60x10 ⁵

4.3.2 Long-Term Cultivation – Trial 2

Trial 2, Experiment A - Human Umbilical Vein Smooth Muscle Cell Sodding

The scaffold sodded with hUVSMCs was taken down and stained with BBI following the protocol from Appendix B: B11. No cells were visualized on the lumen of the scaffold, hence no counting was performed (Figure 4.7).

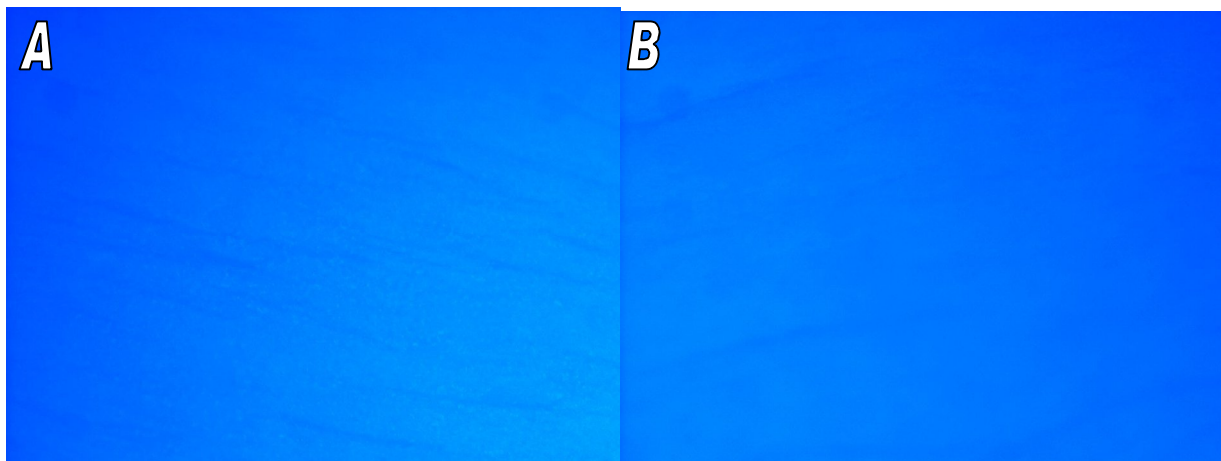


Figure 4.7. Trail 2, Experiment 1 with hUVSMC sodding. Top (A) and bottom (B).

After not visualizing any hUVSMCs using BBI staining, the experiment was redone and the scaffold was embedded in paraffin wax for H and E staining. This basic staining enabled easy visualization of the cell's location post sodding. These images revealed that the hUVSMCs migrated through the wall of the vessel and appeared to reside in the adventitia (Figure 4.8).

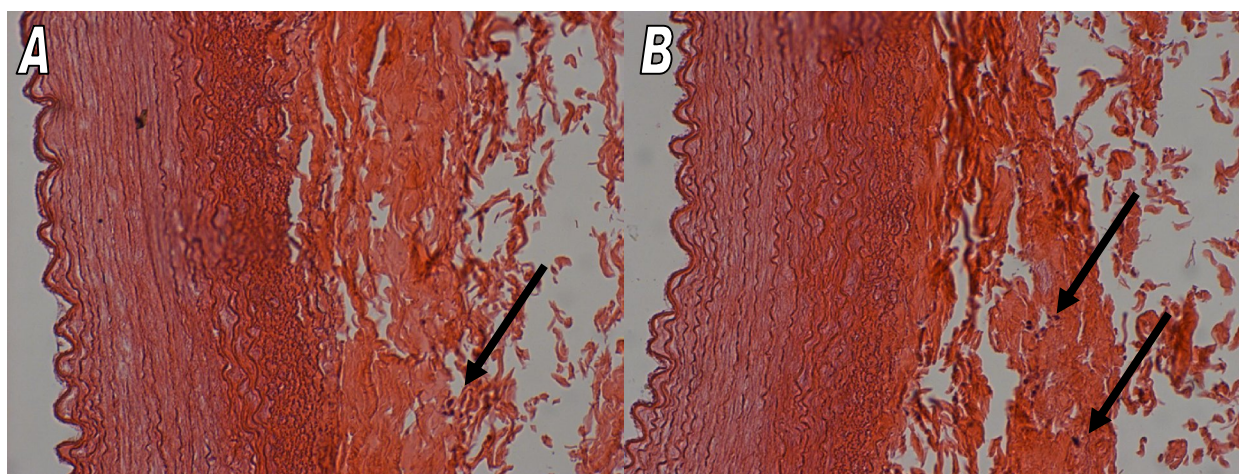


Figure 4.8. Trial 2, Experiment A - H and E staining. Top (A) and bottom (B), the cells are indicated by the arrows.

Trial 2, Experiment B – Human Umbilical Vein Endothelial Cell Sodding

Experiment B assessed the ability of the Cell Tracker Green dye to remain within hUVECs following pressure sodding onto a decellularized porcine artery. Fluorescent cells were observed on each of the two vessels when viewed using the Olympus BX41 wide field fluorescent microscope. However, vessel A (Figure 4.9 A) displayed more even distribution of cells throughout the length of the scaffold than vessel B (Figure 4.9 B). Figure 4.9 was imaged following a 24-hour incubation period with initial transmural flow for 1-hour at 10 rpm followed by luminal flow for 24-hours at 10 rpm. The decellularized porcine vessel A had a strong disbursement of cells throughout the length, each retaining some degree of fluorescence, while vessel B had a sparse distribution of cells throughout the vessel. The number of cells on each vessel was determined and the results are displayed in Table 4.3. The information in Table 4.3 shows a greater average number of cells per cm^2 on vessel A compared to vessel B. Averages of the cell counts from at the proximal and distal ends of the vessel were taken to obtain an overall average across the entire vessel. Despite the difference in distribution, the presence of cells on each vessel suggesting the cell tracker remains within the cells during the pressure sodding process. The difference in distribution is likely due to external set-up factors, rather than the ability of the cell tracker; i.e. transmural pressure sodding did not occur properly.

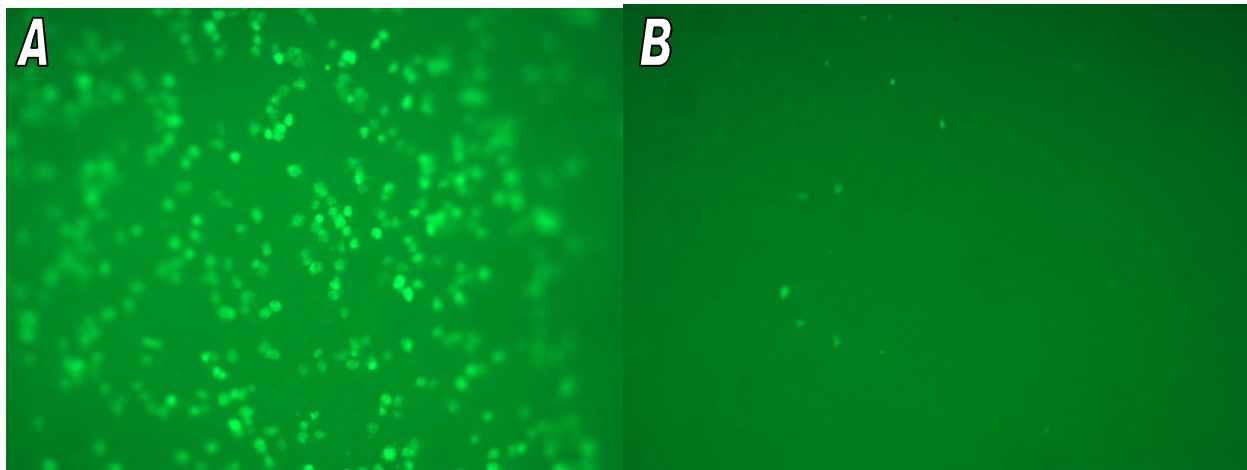


Figure 4.9. Trial 2, Experiment B sodded with hUVECs. Vessel A (A) and vessel B (B).

Table 4.3. Average Number of hUVECs on Each Vessel per cm².

	Cells/cm ²
Avg Vessel A top	1,785.12
Avg Vessel A bottom	21,652.89
Avg Vessel B top	1,421.49
Avg Vessel B bottom	2,876.03
TOTAL	
Avg Vessel A	11,719.01
Avg Vessel B	2,148.76

4.3.3 Dual Soodding Proof of Principle – Trial 3

To evaluate the potential to dual sod a scaffold, two cell trackers were utilized to identify each cell type. The cell tracker dye incorporates into the cytoplasm of the cell and will remain with it for a short duration as the cell proliferates and migrates. Thus, multiple cell types may be dyed during the separate culturing process and the dye will remaining in the respective cells once they have been combined in a given application.

Trial 3, Experiment 1 - Optimization of Cell Tracker Green Concentration

Experiment 1 demonstrated the optimal dilution of Cell Tracker Green for a consistent and bright stain on the cells. Over the duration of seven days, the intensity of Cell Tracker Green changed substantially at each concentration until the seventh day when each of the dilutions reached an intensity lower than that at the start of the experiment (Figure 4.11). Note these times and respective concentrations are based on the moderately proliferating 3T3 fibroblasts, and the intensity may vary when the dye is applied to other cell types. The intensity of the cell tracker was assessed by averaging the intensity of five different cells from each image using ImageJ analysis software. Table 4.4 summarizes most intense, or brightest, concentration of dye at each time point; 15 μ M retained the greatest intensity both at time zero and day 7; 20 μ M fluoresced most intensely following 24 hours; 10 μ M remained the most intense concentration following a five day period. These numbers suggest smaller dilutions of the original working solution result in longer retention of fluorescence intensity. 15 μ M retained the average greatest intensity over a seven day duration.

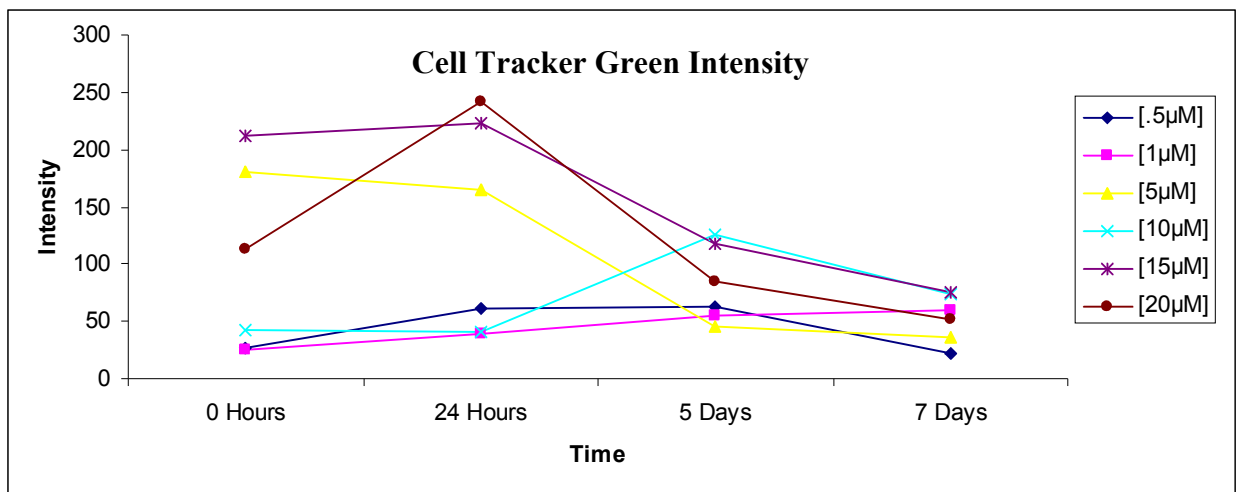


Figure 4.11. Cell Tracker Green intensity at various concentrations over a 7-day duration.

Table 4.4. Concentration for the Brightest Fluorescent Intensity.

	Concentration
0 Hours	15 μ M
24 Hours	20 μ M
5 Days	10 μ M
7 Days	15 μ M

Trial 3, Experiment 2 - Cell Tracker Green with Trypsin

Experiment 2 demonstrated the effects of trypsinization on the cells stained with Cell Tracker Green, to show the treatments to the cells would not affect the dye properties. The number of cells that remained dyed in culture were post trypsinization counted using Image J. If trypsin affects the capacity for a cell to retain the Cell Tracker Green dye, the number of cells visualized will change. The two treatments were sodded with the same number of cells and imaged, then the number of cells present were counted using Image J (see Table 4.5). Using a two-sample t-test, the number of cells for each treatment were compared and the p-value was determined to be $p = 0.418$, which is not statistically different (Figure 4.12). Thus, Cell Tracker Green is not affected by the trypsinization process of cell culture and the dyed cells should not be altered as they are prepared for sodding.

Table 4.5. 3T3s Visualized Pre and Post Trypsinization.

With Trypsin	Cells/cm²		Without Trypsin	Cells/cm²
A	17355.37		A	127777.78
B	33223.14		B	50000.00
C	47438.02			
D	38181.82			
E	30743.80			

F	60330.58		
---	----------	--	--

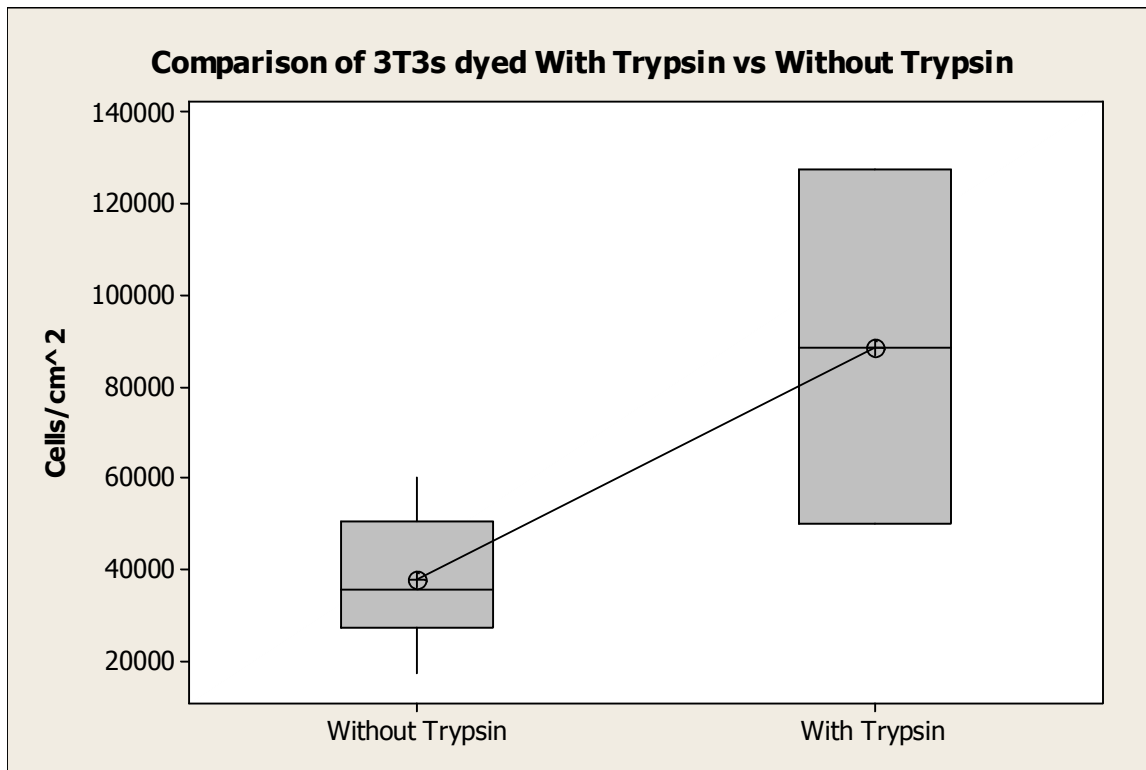


Figure 4.12. Dyed 3T3 cells with and without trypsinization, p-value = 0.418.

Trial 3, Experiment 3 - Cell Tracker Green and Red in Co-Culture

Experiment 3, looked at the use of two different cell trackers in conjunction with one another. Cell Tracker Green and Red were used to stain two separate cultures, then dyed cells were combined to observe their interaction. Following combination of the dyed 3T3 cells, the cultures were examined using the Olympus BX41 wide field fluorescent microscope and the results are displayed in Figure 4.13. Each cell tracker fluoresced at its respective excitation/emission energy (Figure 4.13a, 4.13b) and using ImageJ the images were overlaid such that the entire picture was shown (Figure 4.13c). The overlaid image exhibits the potential of using two separate cell trackers to track the final location of the stained cells. The Cell Tracker Red dye looks spotty because it was oversaturated and began to particulate within

the cytoplasm of the cell, as confirmed by the manufacturer. The red dye worked to identify the cell, but was not as well incorporated into the cytoplasm.

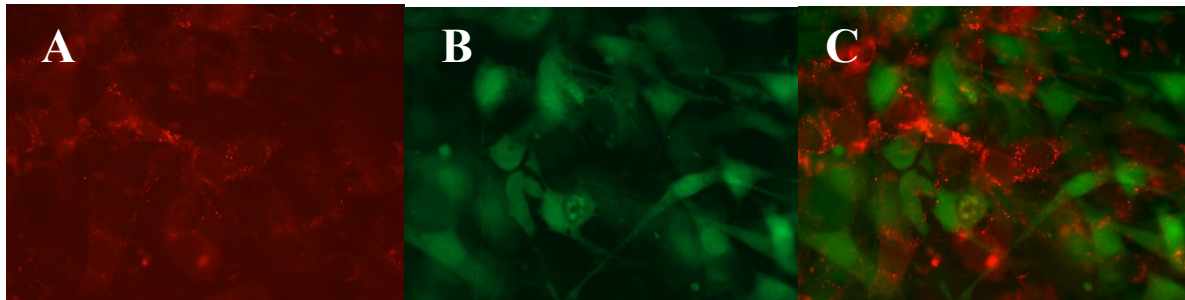


Figure 4.13. Staining using Cell Tracker Green and Red. Cell Tracker Red (A), Cell Tracker Green (B), and merged (C).

4.4 Discussion

The work summarized in this chapter examined the decellularized scaffold's ability house cells on its lumen. This was shown through the development of a sodding protocol with various cells types, and progressively showed the feasibility of sodding physiological cell types into a scaffold. These experiments created a monolayer of cells on the lumen of the scaffold and fulfilled the goal of the BVM.

4.4.1 Short-Term Cultivation – Trial 1

Work began with the 3T3 fibroblasts in Trial 1, 'Short-Term Cultivation', to develop sodding techniques and optimize cell density for the recellularization of a decellularized scaffold. Utilizing this particular cell type was advantageous because of its availability and low cost. Through these experiments imaging techniques, transmural sodding procedures, and BVM setup techniques were developed and established for future experiments. Trial 1 provided further characterization of the decellularized scaffold. A successful culture indicated cell adhesion was possible post decellularization.

Prior to developing an appropriate sodding process, as described in Trial 1, several preliminary trials (described below) were performed to optimize the final sodding protocol used throughout all experimentation. Skills such as sodding procedures, bioreactor set up, and analysis techniques were integral to the development and implementation of a scaffold into the BVM. These trials provided the ideal opportunity to practice and improve the techniques needed to successfully sod a scaffold in the BVM. These early trials were not discussed earlier in the methods or results, but were imperative to the development of the sodding procedures and worth mentioning. Attempts 1, 2, and 3 were performed prior to any experiments described previously as a way to learn about the BVM set-up, several lessons were learned and are summarized below. All of the set up and analysis procedures were performed as previously described in Appendix B: B.11, but as the techniques improved so did the results.

Early Fibroblast Trials – Initial Lessons Learned

Attempt 1 was the first bioreactor set up done with a decellularized scaffold, as well as my first experience with the BVM. Although several mistakes were made, the lessons learned were by far the most helpful. Attempt 1 intended to have transmural flow, but due to unsuccessful clamping of the tubing, luminal flow occurred, causing a reduced potential for any cellular adhesion from occurring. The analysis techniques in this experiment were also very poor, in that the scaffold was not properly handled. The BBI stain is normally diluted and mixed vigorously prior to staining. In Attempt 1, the scaffold was vigorously shaken while attempting to mix the BBI dye; this excess force potentially dislodged cells from the scaffold. Ultimately, when the scaffold was imaged there were very few cells on the lumen.

Attempt 2 had a better set up after adapting to techniques learned from Attempt 1; although in this experiment, more unexpected problems arose. The shake table, which is an essential part of the decellularization process, broke at some point during the 20 hour procedure.

This equipment is imperative to successful decellularization and unfortunately there was no method to quickly assess if the scaffold had been properly decellularized. Attempt 2 went forward as planned in order to continue to develop techniques and to utilize all prepared materials. It would have been prudent to isolate a portion of the scaffold to embed for hematoxylin and eosin staining as confirmation of decellularization prior to recellularization. However, no section was isolated, because the scaffold was specifically measured to fit into the BVM. The analysis of the scaffold still proved to be difficult as the set up of the Olympus BX41 Fluorescence Microscope was not mastered and the inappropriate color filter was used, resulting in a green images. From this, a protocol was developed to ensure the proper set up and usage of the scope (Appendix B: B.13). Attempt 2 resulted in images with cells sodded on the lumen, but could not be trusted because of the unclear decellularization.

Finally, Attempt 3, referred to in this chapter as ‘Trial 1’, went according to plan and followed the methodology that was described in detail earlier in the methods section. The techniques learned previously from Attempts 1 and 2 helped to successfully perform acute sodding with about 3.5 million cells per cm² of 3T3 fibroblasts onto 2 scaffolds, following the protocol from Appendix B: B.13. Table 4.6 summarizes many of the lessons learned through these initial experiments.

Table 4.6 Skills Developed Through Experimentation with 3T3 Fibroblasts.

Attempt	Cell Type	Duration	Lessons Learned
1	Fibroblasts	1 hour	Ensure transmural flow by clamping
			Make the BBI solution prior to staining the scaffold
2	Fibroblasts	1 hour	Proper Decellularization
			Understanding the Fluorescent Scope
3	Fibroblasts	1 hour	Successful Trial!

An additional limitation of this work was the cell count methodology. As described, the method involved using 5 side-by-side boxes to count cells. The five side-by-side 1mm² boxes caused the counts to occur in only one populated area. To better define the cell density throughout the length. Where as the boxes should have been randomly distributed throughout the image and remain in consistent positions for every image. This may reduce any biased that may occur during the counting process.

4.4.2 Long-Term Cultivation – Trial 2

Once the decellularized scaffold was utilized in the BVM and a successful sodding procedure was established, the cell type was then changed to a physiologically relevant cell. Work started with the hUVSMCs because they were slightly less expensive and would still provide a vascularly relevant cell type for recellularization. All sodding procedures were performed as done with Trial 1, ensuring transmural pressure sodding for maximum cell adhesion. Each of these trials will be discussed below.

Trial 2, Experiment A – Human Umbilical Vein Smooth Muscle Cells

The culture of hUVSMCs in Experiment A was extended to a longer duration and as such required modifications to the flow rate. Flow was moved from a transmural direction to a luminal direction and the flow rate was slowly ramped up. The changes in flow rate, although novel for a decellularized scaffold, had been successfully done with hUVECs on ePTFE scaffolds (4). The result of trial 2 was not as expected, as the BBI analysis showed little to no cells on the lumen of the scaffold. Before assumptions were made about problems the sodding process, the trial was repeated and scaffolds were embedded in paraffin for histological analysis. Once stained with H and E, a few of the hUVSMCs were visible in the adventia of the scaffold. The cells seen were most likely components of cells that were not fully removed during the decellularization process. The decellularized scaffold is highly water proof and the hUVSMCs

would not have migrated through the entire scaffold. While this result was not ideal, it also proposed many questions about the sodding process and if this scaffold could still be utilized in the BVM.

After looking into the literature regarding sodding hUVSMCs into a scaffold, it was concluded that these cells are difficult to pressure sod (87, 88). Some successful sodding procedures for SMCs incorporated have been performed by seeding cells on the exterior of the scaffold and allowing them to migrate in towards the endothelium (87, 88). SMCs are attracted to the highly collagenous media of the decellularized scaffold and are not able to adhere to the lumen (87). This migration process occurs because of the great force used during pressure sodding, resulting in cells residing in the adventia of the scaffold or beyond the wall rather than the media. Successful pressure sodding of hUVSMCs has been done, but on a fibronectin scaffold with no porosity and thus cells were did not migrate through the vessel wall (89). Other successful SMC incorporation was done by creating a sheet out of the SMCs, then the sheet is formed into a tube and used as a scaffold (28). Thus, other successful methodologies exist to introduce SMCs into a scaffold, but pressure sodding is not ideal. Future SMC sodding should investigate a external seeding methods as done by Williams et al (88). Externally seeding will allow the SMCs to slowly migrate into the media of the scaffold.

Trial 2, Experiment B – Human Umbilical Vein Endothelial Cells

To further evaluate the potential for the decellularized scaffold to be used in the BVM and to continue to use a pressure sodding method, hUVECs were introduced to mimic the native cellular monolayer on the lumen of an artery. Dr. Cardinal had previously established a protocol for pressure sodding hUVECs into an ePTFE scaffold to create a consistent monolayer of cells on the lumen. The combination of Dr. Cardinal's established methods and the skills learned in this Chapter resulted in the successful sodding of a decellularized scaffold with hUVECs. This

cell type remained in the endothelium as a consistent monolayer of cells throughout the length and inner circumference of the scaffold. Utilizing hUVECs to create an endothelium effectively mimics a native artery, fulfilling the goal of the BVM.

The longer durations cultures were somewhat unsuccessful because a contamination would generally occur approximately 12 hours post sodding. Contaminations were identified by a change in the culture media, from pink to orange. The media was also slightly cloudy and had a distinct smell; indicating a change in pH or a bacterial contamination. There were several instances when the setup could have been contaminated. Although the setup process uses all sterile equipment and instruments, a contamination from poor sterile technique is still always possible. However, the scaffold never underwent a sterilization process and could retain some bacteria that could not be controlled by the 1% penstrep in the media. These results suggest that hUVECs can be sodded into the scaffold to create a monolayer of cells on the lumen of the scaffold to effectively mimic the endothelium. Also, assuming that decellularizing with penstrep will lower the occurrence of a contamination, meaning longer culture duration and greater potential to fulfill the goals of the BVM.

4.4.3 Dual Sodding Proof of Principle

All of the dual staining experiments led to a proof of concept for the use of cell tracker dyes in dual sodding of decellularized porcine vessel to create a physiologically relevant scaffold. Use of this dye will lead to a promising analysis tool for dual sodded scaffolds. Not only was this powerful analysis tool identify multiple cell types, but it could also be utilized in real time imaging because the dying process was complete prior to sodding. Samples can be imaged while they grow because the dye has integrated with the cell, for a limited duration. Future work will further optimize the Cell Tracker Red concentrations as well as use both cell trackers on a dual sodded scaffold.

Overall, the work in this chapter provided important results relevant to the use of decellularized vessels as scaffolds in the BVM. Table 4.7 summarizes the progression of the recellularization experiments and reasons for support of the decellularized scaffold's use. In conclusion, the decellularized scaffold was successfully sodded and cultured with both 3T3 fibroblasts and HUVECs. With improved sterile decellularization and analysis techniques, the decellularized scaffold has the potential to become a unique scaffold type for the BVM.

Table 4.7. Summary of the Results from Recellularization the Decellularized Scaffold.

	Cell Type	Duration	Analysis	Sub Experiments	Results
Trial 1	3T3	1 hour	BBI	None	Successful Monolayer
Trial 2	HUVSMC and HUVEC	1-5 days	BBI, H/E, Cell Tracker Green	Experiments A and B	See experiments A and B
Trial 3	3T3	1 Day	Cell Tracker Green	Experiments 1,2, and 3	Successful
Exp. A	HUSMC	1-5 Days	BBI and H/E	None	Unsuccessful
Exp. B	HUVEC	1 Day	Cell Tracker Green	none	Successful
Exp. 1	3T3	1 week	Optimization of Cell Tracker Green Concentration	None	Successful
Exp. 2	3T3	1 hour	Cell Tracker Green with Trypsin	None	Successful
Exp. 3	3T3	1 day	Cell Tracker Red and Green Co-Culture	None	Successful and Plausible for dual sodding

Chapter 5 - Discussion and Conclusions

5.1 Overview and Summary

Cardiovascular disease affects one in three Americans and in 2006 claimed the lives of an estimated 17.1 million individuals around the world (90, 91). These statistics demonstrate the growing need for the use and development of effective therapies to treat cardiovascular disease. The evaluation of a stent and its function requires both *in-vitro* as well as *in vivo* testing. Bench testing provides a controlled environment to test specific aspects such as device fatigue, proper expansion, or mechanical strength of the stent (29). *In-vitro* testing also provides initial screening of biocompatibility and cell interaction. *In-vivo* testing examines the effectiveness, biodegradation, inflammatory response, or elution profiles in a living organism (29). The combination of these testing modalities affords a more complete analysis of the stent and its physiological interactions within the body. This research seeks to bridge the gap between *in-vitro* and *in-vivo* testing through the development of an *in-vitro* BVM to test intravascular devices such as stents. This system provides an *in-vitro* model that represents a physiologic system, while permitting high-throughput and cost-effective testing. This allows for multi-dimensional analysis of stents and other intravascular devices because the mimic reproduces a simplistic living vessel in an *in-vitro* environment.

Currently, the BVM utilizes an ePTFE scaffold, which has been shown to support a monolayer of endothelial cells, therefore demonstrating the ability to mimic the intima of a native artery (4). The model provides a quick and repeatable testing modality for new intravascular devices. As a material, ePTFE is biocompatible and dependable, but has several

physiologic limitations. The polymer scaffold has little compliance and is devoid of any biological components, which will alter the interactions between the device and scaffold wall when compared to responses *in vivo*. To address the physiological limitations of the current BVM scaffold, the development and implementation of a completely biological scaffold was evaluated.

One option for creating a biologic scaffold is to decellularize an existing vessel. Decellularization is a promising technique that can be utilized to remove cells from a tissue. Several groups have found a multitude of uses for the ECM from a decellularized tissue. Some have focused on using the decellularized scaffold for use *in-vivo*, due to the lack of donors and/or viable tissues. Ott et al. applied decellularization to remove the cells from an entire rat heart and were able to recellularize the heart to regain function by stimulated electronic pulse (48). Schaner et al. decellularized whole arteries to investigate their potential for use in bypass surgery (49). Other groups such as Singelyn et al. have utilized decellularized tissues to isolate the complex combination of proteins that comprise the native ECM (51). New decellularization techniques will continue to develop to become a unique source of biologic materials for specific applications.

To improve the capabilities of the BVM, this thesis examined the potential use of a decellularized artery as a more physiologically relevant scaffold type, when compared to current synthetic polymers. Utilizing a decellularized scaffold provides several potential advantages including maintenance of structural integrity (mechanical strength and compliance) and incorporation of natural binding sites for cells (40, 44). This type of scaffold would create a more physiologic *in vitro* testing modality and further bridge the gap between bench tests and *in vivo* studies. The following summarizes the work performed in this thesis to develop and implement the decellularized scaffold into the BVM.

The work from Schaner et al. supported the use of a decellularized porcine artery as a vascular scaffold and provided the basic methods for the decellularization protocol (49). The first step of this thesis developed a decellularization protocol, utilizing SDS as a detergent to remove all cellular bonds from porcine arteries in order to produce an acellular scaffold. After numerous trials, the final decellularization protocol included a 0.075% SDS solution perfused through the lumen of the vessel, while concurrently being shaken at 30 rpm for 20 hours. Decellularization was evaluated by staining with H and E dyes, to visualize the nuclei and cellular material within the vessel. The complete decellularization of an artery, as determined by a lack of hemotoxylin-stained nuclei, produced a biological-acellular scaffold type. Furthermore, the structure of the scaffold remained intact through the harsh SDS washing. The perfusion of the SDS solution during decellularization (as opposed to shaking alone) was vital to ensure the lumen of the scaffold was kept open for use in future experiments, such as tensile testing or burst pressure testing. Before implementation into the BVM, the scaffold was examined for the maintenance of structural integrity and mechanical properties.

To ensure the scaffold maintained its native characteristics post-processing, the structural and mechanical properties were evaluated. These experiments conducted as a side by side comparison between the decellularized scaffold and a native artery. Visual inspections of the wall thickness for decellularized scaffolds were similar to that of native controls, indicating no drastic changes to the structure. Tensile testing and burst pressure tests were also performed on the scaffold post-decellularization. The scaffold was stretched longitudinally until broken to evaluate its elastic modulus and yield strength via tensile testing. The resulting elastic modulus was not statistically different from that of a native artery at about 4 MPa; whereas the yield strength of the scaffold (1.7MPa) was significantly lower than the native artery (2.6 MPa). Radial strength was tested via burst pressure analysis, where the scaffold was filled with water

until it burst. The burst pressure was determined to be similar to a native artery found in literature at 1600 mmHg (71). Mechanical properties indicated that the decellularized scaffold is not significantly different than a native artery, thus providing a physiologically relevant scaffold for use in the BVM. This scaffold can be used in several ways; for its ideal compliance when evaluating stents, investigating drug eluting stents effects on the vasculature, to explore new imagine modalities and their ability to visualize several layers of an artery, and potentially to model disease pathways such as restenosis.

Once the physical properties of the scaffold were evaluated, the scaffold's capacity to house cells was evaluated by pressure sodding cells into the lumen of the scaffold. Sodding 3T3 fibroblasts was a proof-of-concept to asses if cells could be distributed throughout the length of the scaffold and were not harmed by the scaffold. Based on this success, more relevant cell types were sodded to better mimic a native artery. Pressure sodding was not effective for hUVSMC, as they prefer to adhere in a static environment where they slowly migrate into the scaffold (87, 88). Whereas the hUVECs were pressure sodded and able to remain of the scaffold. BBI and Cell Tracker Green staining were used to visualize the nuclei of the hUVECs on the lumen of the scaffold post sodding. These results indicated that hUVECs were able to be sodded to produce a monolayer of cells on the lumen of the scaffold, effectively mimicking a native artery. In conclusion, the development of a decellularized scaffold created a biomentic material with the capacity to model and artery.

5.2 Challenges and Limitations

There are some key limitations to using a decellularized scaffold to model an artery. Limitations include extensive contaminations, non-ideal mechanical testing methods, and poor staining optimization. When the decellularized scaffold was used in the BVM for longer than 12 hours contaminations occurred. For example, in the first long term study with hUVSMCs, three

time points were to be examined (1, 3, and 5 days). After 12 hours of culture, two of the three setups had to be stopped due to contaminations. After 36 hours of experimentation, the third set up was taken down due to contamination once again. These losses severely altered the goal of the experiment and resulted in a shorter evaluation time. Assuming this setup was performed sterilely, the decellularized scaffolds were the only components that were not sterilized and would be the source of contamination. If the BVM for the duration of the experiment, all long-term tests will be compromised, skewing the subsequent results.

The mechanical tests performed in this thesis did not evaluate the most relevant aspects of the scaffold. Traditional tensile tests effectively examine elastic modulus and critical yield of the material's longitudinal strength; however this is not critical data. Although this test provided useful background information, the decellularized scaffold is measured to fit within the BVM, thus was not required to stretch longitudinally. In addition, the traditional methods require a relatively flat material, two dimensional with only a small thickness. The scaffold is a tube and needed to be cut longitudinally to fit the desired form. Altering the geometry, produces data that doesn't effectively mimic what occurs in the BVM. Ideally, more information about the radial strength would provide more appropriate data. The radial strength is important during the pressure sodding process as well as any interactions the scaffold will have with intravascular devices.

Finally, to properly analyze a recellularized scaffold all dyes and analysis tools must be optimized for proper identification of the structures within the culture. Specifically, the Cell Tracker dyes utilized for the dual sodding proof of concept had to be optimized for the best use. Cell Tracker Green was the main dye used and was properly optimized for the ideal concentration. Once Cell Tracker Red was introduced, it was assumed it would function similarly to the Green. However, the Cell Tracker Red dye resulted in spotty and inconsistent

cell dying; although it had penetrated the cellular membrane, it was not evenly dispersed throughout the cytoplasm. The dye was too concentrated, causing it to conglomerate; resulting in a technically false representation of the cells. With further optimization of the Cell Tracker Red, this crucial issue can be addressed and the stains will be consistent between the colors.

5.3 Future Work

Addition of Antibiotics: The primary isolation of the porcine arteries is not a sterile process and the vessel was exposed to bacterial contaminants. Chapter 3 investigated the use of antibiotics, penstrep, as a way to limit contamination. It was determined that one percent of penstrep was sufficient to stop bacterial colonies from forming. This thesis utilized the antibiotic only in culture media, during the final stages of the experiment. Theoretically if the scaffold is exposed to antibiotics during multiple phases of experimentation, the exponential growth of bacteria could be reduced. As seen in other work, the incorporation of 1% penstrep with 1% SDS in the decellularization process may prevent contamination from occurring.(51). Additionally, arteries are available for commercial purchase, and thus have a much smaller amount of contamination with an increase in consistency (due to the high throughput more sterile harvesting process).

Balloon Catheter for Burst Pressure: The burst pressure testing done in this thesis was sufficient to provide a comparison between decellularized and native scaffolds. The burst pressure was recorded at the moment before bursting at one point on the scaffold. This method does not represent the overall radial compliance, but rather the critical strength of the scaffold. To better investigate the radial compliance of the scaffold a balloon catheter can be inserted inside the scaffold and filled to determine the pressure on the surface area of the lumen. The resulting data will better represent the radial compliance throughout the scaffold. Evaluating the

scaffold in this manner will not only improve the quality of the data, but also further demonstrate the capacity of the BVM to test intravascular devices.

Radial Tensile Testing: The current tensile testing methods utilized in this thesis were accurate to test the longitudinal strength of the scaffold, but were not relevant to the uses of the scaffold in the BVM. The longitudinal strength is not imperative knowledge for use in the BVM system, as the length of the scaffold was measured to fit rather than stretch. Modifying the tensile testing apparatus could provide the elastic modulus and the critical yield in a radial direction. Changing the ‘clamping’ mechanisms from a vice style to two rods, would allow the scaffold to remain intact while still evaluating the elastic modulus and yield strength. The two rods would be inserted into the lumen of the scaffold and pulled while remaining parallel to each other. A modified tensile testing apparatus was suggested by Colby James, who also found longitudinal elastic modulus relatively unhelpful. His thesis suggests the described modifications to the tensile testing apparatus (92) – page 140, Figure 56. With a simple modification of the current testing apparatus, more relevant data might be produced.

Optimize Cell Tracker Red: The optimal concentration of dye was determined for Cell Tracker Green but not for Cell Tracker Red. Cell Tracker Red was too concentrated in the cell, causing the dye to conglomerate and form spots within the cytoplasm rather than disperse evenly throughout the cell. By investigating lower concentrations of Cell Tracker Red within the cells, a concentration can be determined that will last during cell proliferation, while consistently dyeing the cytoplasm of the cell. Investigating various concentrations of Cell Tracker Red can easily be optimized to produce an accurate and consistent stain.

Dual Sodding the Scaffold: To develop the most physiologically relevant scaffold, recellularizing the scaffold with two native cell types would better mimic the native artery. This thesis sodded two cell types independently, but sodding two cell types together is plausible. The

hUVSMCs should be externally sodded and given a chance to migrate into the media of the scaffold, while hUVECs are luminaly pressure sodded. External sodding was used for recellularization hUVSMCs and a potential method could be performed following the protocol from Williams et al (88). Once the media of the scaffold has been recellularized with hUVSMCs, the intima of the scaffold can be pressure sodded with hUVECs.

Translational Investigations: Although decellularizing an intact artery can produce a scaffold to model an *in vivo* artery, the basic materials, or extracellular matrix, of the tissue can be used to improve other scaffold models. Singelyn et al. decellularized tissues, then digested it with pepsin and solubilized it to resulting in a temperature-responsive hydrogel (51). From this research, it was found that collagens, laminin, and proteoglycans naturally found within a tissue were retained throughout processing. Therefore, the solubilized decellularized material can be used to coat a different scaffold type to improve the cellular adhesion properties and overall culture. This theory was tested in Appendix D: Decellularized Coatings, where ePTFE scaffolds were coated with solubilized decellularized porcine aorta ECM. The ability to use a decellularized artery as a scaffold or as a coating to improve upon other scaffold types would provide several potential uses for the decellularized material.

5.4 Conclusion

The *in vitro* BVM was developed to test intravascular devices and as such has a great potential to be utilized for pre-clinical evaluations. Before this model is created, further optimization of the current BVM system must be addressed. The current gold standard for the BVM supports a polymer scaffold that is not physiologically representative of a native artery. The development of a physiologically relevant tissue engineered blood vessel scaffold is critical to the improvement of the BVM. A decellularized artery has the biomemtic properties necessary to improve the physiological relevance of the BVM. In conclusion, this research provided the

documentation to support the potential for a decellularized porcine scaffold to be utilized as a unique scaffold in the BVM.

LIST OF REFERENCES:

1. Lloyd-Jones D, Adams RJ, Brown TM, Carnethon M, Dai S, De Simone G, et al. Heart disease and stroke statistics--2010 update: a report from the American Heart Association. *Circulation*.121:e46-e215.
2. Waksman R. Drug-eluting stents: from bench to bed. *Cardiovasc Radiat Med*.3:226-41. 2002.
3. Cantor WJ, Peterson ED, Popma JJ, Zidar JP, Sketch MH, Jr., Tcheng JE, et al. Provisional stenting strategies: systematic overview and implications for clinical decision-making. *J Am Coll Cardiol*.36:1142-51. 2000.
4. Cardinal KO, Bonnema GT, Hofer H, Barton JK, Williams SK. Tissue-engineered vascular grafts as in vitro blood vessel mimics for the evaluation of endothelialization of intravascular devices. *Tissue Eng*.12:3431-8. 2006.
5. Cardinal KO, Williams SK. Assessment of the intimal response to a protein-modified stent in a tissue-engineered blood vessel mimic. *Tissue Eng Part A*.15:3869-76. 2009.
6. Naghavi M, Libby P, Falk E, Casscells SW, Litovsky S, Rumberger J, et al. From vulnerable plaque to vulnerable patient: a call for new definitions and risk assessment strategies: Part I. *Circulation*.108:1664-72. 2003.
7. Health NIo. Coronary Artery Disease. In: Services USDoHaH, ed.
8. Association AH. Prevention and Treatment of Heart Attack. *Heart Attack*2009.
9. Gottdiener JS, Reda DJ, Massie BM, Materson BJ, Williams DW, Anderson RJ. Effect of single-drug therapy on reduction of left ventricular mass in mild to moderate

- hypertension: comparison of six antihypertensive agents. The Department of Veterans Affairs Cooperative Study Group on Antihypertensive Agents. *Circulation*.95:2007-14. 1997.
10. Health NIo. Coronary Artery Bypass Grafting. In: Services USDoHaH, ed.
 11. Hoffman SN, TenBrook JA, Wolf MP, Pauker SG, Salem DN, Wong JB. A meta-analysis of randomized controlled trials comparing coronary artery bypass graft with percutaneous transluminal coronary angioplasty: one- to eight-year outcomes. *J Am Coll Cardiol*.41:1293-304. 2003.
 12. Braunwald E, Antman EM, Beasley JW, Califf RM, Cheitlin MD, Hochman JS, et al. ACC/AHA guidelines for the management of patients with unstable angina and non-ST-segment elevation myocardial infarction: executive summary and recommendations. A report of the American College of Cardiology/American Heart Association task force on practice guidelines (committee on the management of patients with unstable angina). *Circulation*.102:1193-209. 2000.
 13. Moneta GL, Porter JM. Arterial substitutes in peripheral vascular surgery: a review. *J Long Term Eff Med Implants*.5:47-67. 1995.
 14. Colvin RB. The renal allograft biopsy. *Kidney Int*.50:1069-82. 1996.
 15. Konakci KZ, Bohle B, Blumer R, Hoetzenecker W, Roth G, Moser B, et al. Alpha-Gal on bioprostheses: xenograft immune response in cardiac surgery. *Eur J Clin Invest*.35:17-23. 2005.
 16. Klymiuk N, Aigner B, Brem G, Wolf E. Genetic modification of pigs as organ donors for xenotransplantation. *Mol Reprod Dev*.77:209-21.
 17. Bach FH. Xenotransplantation: problems and prospects. *Annu Rev Med*.49:301-10. 1998.

18. Chlupac J, Filova E, Bacakova L. Blood vessel replacement: 50 years of development and tissue engineering paradigms in vascular surgery. *Physiol Res.*58 Suppl 2:S119-39. 2009.
19. L'Heureux N, McAllister TN, de la Fuente LM. Tissue-engineered blood vessel for adult arterial revascularization. *N Engl J Med.*357:1451-3. 2007.
20. Abbott WM, Megerman J, Hasson JE, L'Italien G, Warnock DF. Effect of compliance mismatch on vascular graft patency. *J Vasc Surg.*5:376-82. 1987.
21. Webb AR, Macrie BD, Ray AS, Russo JE, Siegel AM, Glucksberg MR, et al. In vitro characterization of a compliant biodegradable scaffold with a novel bioreactor system. *Ann Biomed Eng.*35:1357-67. 2007.
22. Ballyk PD, Walsh C, Butany J, Ojha M. Compliance mismatch may promote graft-artery intimal hyperplasia by altering suture-line stresses. *J Biomech.*31:229-37. 1998.
23. Pasic M, Muller-Glauser W, von Segesser L, Odermatt B, Lachat M, Turina M. Endothelial cell seeding improves patency of synthetic vascular grafts: manual versus automatized method. *Eur J Cardiothorac Surg.*10:372-9. 1996.
24. Begovac PC, Thomson RC, Fisher JL, Hughson A, Gallhagen A. Improvements in GORE-TEX vascular graft performance by Carmeda BioActive surface heparin immobilization. *Eur J Vasc Endovasc Surg.*25:432-7. 2003.
25. Walpoth BH, Rogulenko R, Tikhvinskaia E, Gogolewski S, Schaffner T, Hess OM, et al. Improvement of patency rate in heparin-coated small synthetic vascular grafts. *Circulation.*98:II319-23; discussion II24. 1998.
26. American Heart Association. Stent Procedure 2009.
27. Services DoHaH, Health NIO, Institute NHLaB. Coronary Angioplasty.

28. L'Heureux N, Paquet S, Labbe R, Germain L, Auger FA. A completely biological tissue-engineered human blood vessel. *FASEB J.*12:47-56. 1998.
29. Blitterswijk Cv. *Tissue Engineering*. 1 ed. San Diego: Elsevier; 2008.
30. Foxall TL, Auger KR, Callow AD, Libby P. Adult human endothelial cell coverage of small-caliber Dacron and polytetrafluoroethylene vascular prostheses in vitro. *J Surg Res.*41:158-72. 1986.
31. Weinberg CB, Bell E. A blood vessel model constructed from collagen and cultured vascular cells. *Science.*231:397-400. 1986.
32. Ravi S, Chaikof EL. Biomaterials for vascular tissue engineering. *Regen Med.*5:107-20.
33. Gong Z, Niklason LE. Blood vessels engineered from human cells. *Trends Cardiovasc Med.*16:153-6. 2006.
34. Kim BS, Mooney DJ. Development of biocompatible synthetic extracellular matrices for tissue engineering. *Trends Biotechnol.*16:224-30. 1998.
35. Zhao Y, Zhang S, Zhou J, Wang J, Zhen M, Liu Y, et al. The development of a tissue-engineered artery using decellularized scaffold and autologous ovine mesenchymal stem cells. *Biomaterials.*31:296-307. 2009.
36. Xu CY, Inai R, Kotaki M, Ramakrishna S. Aligned biodegradable nanofibrous structure: a potential scaffold for blood vessel engineering. *Biomaterials.*25:877-86. 2004.
37. Carpenter J, Khang D, Webster TJ. Nanometer polymer surface features: the influence on surface energy, protein adsorption and endothelial cell adhesion. *Nanotechnology.*19:505103. 2008.
38. Niklason LE, Gao J, Abbott WM, Hirschi KK, Houser S, Marini R, et al. Functional arteries grown in vitro. *Science.*284:489-93. 1999.

39. Li C, Hill A, Imran M. In vitro and in vivo studies of ePTFE vascular grafts treated with P15 peptide. *J Biomater Sci Polym Ed.*16:875-91. 2005.
40. Gui L, Muto A. Development of Decellularized Human Umbilical Arteries as Small-Diameter Vascular Grafts. *Tissue Engineering.*15:12. 2009.
41. Chung S, Moghe AK, Montero GA, Kim SH, King MW. Nanofibrous scaffolds electrospun from elastomeric biodegradable poly(L-lactide-co-epsilon-caprolactone) copolymer. *Biomed Mater.*4:015019. 2009.
42. Swartz DD, Russell JA, Andreadis ST. Engineering of fibrin-based functional and implantable small-diameter blood vessels. *Am J Physiol Heart Circ Physiol.*288:H1451-60. 2005.
43. Ogle BM, Mooradian DL. Manipulation of remodeling pathways to enhance the mechanical properties of a tissue engineered blood vessel. *J Biomech Eng.*124:724-33. 2002.
44. Schmidt CE, Baier JM. Acellular vascular tissues: natural biomaterials for tissue repair and tissue engineering. *Biomaterials.*21:2215-31. 2000.
45. Lalka SG, Oelker LM, Malone JM, Duhamel RC, Kevorkian MA, Raper BA, et al. Acellular vascular matrix: a natural endothelial cell substrate. *Ann Vasc Surg.*3:108-17. 1989.
46. Conklin BS, Wu H, Lin PH, Lumsden AB, Chen C. Basic fibroblast growth factor coating and endothelial cell seeding of a decellularized heparin-coated vascular graft. *Artif Organs.*28:668-75. 2004.
47. Glibert TW, Sellaro TL, Badylak SF. Decellularization of Tissues and Organs. *Biomaterials.*27:9. 2006.

48. Ott HC, Matthiesen TS, Goh SK, Black LD, Kren SM, Netoff TI, et al. Perfusion-decellularized matrix: using nature's platform to engineer a bioartificial heart. *Nat Med*.14:213-21. 2008.
49. Schaner PJ, Martin ND, Tulenko TN, Shapiro IM. Decellularized Vein as a Potential Scaffold for Vascular Tissue Engineering. *Vascular Surgery*.40:8. 2004.
50. Nagatomi J, Toosi KK, Chancellor MB, Sacks MS. Contribution of the extracellular matrix to the viscoelastic behavior of the urinary bladder wall. *Biomech Model Mechanobiol*.7:395-404. 2008.
51. Singelyn JM, DeQuach JA, Seif-Naraghi SB, Littlefield RB, Schup-Magoffin PJ, Christman KL. Naturally derived myocardial matrix as an injectable scaffold for cardiac tissue engineering. *Biomaterials*.30:5409-16. 2009.
52. Gutensohn K, Beythien C, Bau J, Fenner T, Grewe P, Koester R, et al. In vitro analyses of diamond-like carbon coated stents. Reduction of metal ion release, platelet activation, and thrombogenicity. *Thromb Res*.99:577-85. 2000.
53. Migliavacca F, Petrini L, Colombo M, Auricchio F, Pietrabissa R. Mechanical behavior of coronary stents investigated through the finite element method. *J Biomech*.35:803-11. 2002.
54. Yamawaki T, Shimokawa H, Kozai T, Miyata K, Higo T, Tanaka E, et al. Intramural delivery of a specific tyrosine kinase inhibitor with biodegradable stent suppresses the restenotic changes of the coronary artery in pigs in vivo. *J Am Coll Cardiol*.32:780-6. 1998.
55. Heldman AW, Cheng L, Jenkins GM, Heller PF, Kim DW, Ware M, Jr., et al. Paclitaxel stent coating inhibits neointimal hyperplasia at 4 weeks in a porcine model of coronary restenosis. *Circulation*.103:2289-95. 2001.

56. Xue L, Greisler HP. Biomaterials in the development and future of vascular grafts. *J Vasc Surg.*37:472-80. 2003.
57. Prager M, Polterauer P, Bohmig HJ, Wagner O, Fugl A, Kretschmer G, et al. Collagen versus gelatin-coated Dacron versus stretch polytetrafluoroethylene in abdominal aortic bifurcation graft surgery: results of a seven-year prospective, randomized multicenter trial. *Surgery.*130:408-14. 2001.
58. Hoerstrup SP, Zund G, Sodian R, Schnell AM, Grunenfelder J, Turina MI. Tissue engineering of small caliber vascular grafts. *Eur J Cardiothorac Surg.*20:164-9. 2001.
59. Pena TR. Vascular Tissue Engineering and the Advancement of an In Vitro Blood Vessel [MS in Engineering - Biomedical Engineering Biomedical and General Engineering, California Polytechnic State University, San Luis Obispo, 2009.
60. Malone JM, Brendel K, Duhamel RC, Reinert RL. Detergent-extracted small-diameter vascular prostheses. *J Vasc Surg.*1:181-91. 1984.
61. Lu H, Hoshiba T, Kawazoe N, Chen G. Autologous extracellular matrix scaffolds for tissue engineering. *Biomaterials.*32:2489-99.
62. Lichtenberg A, Tudorache I, Cebotari S, Ringes-Lichtenberg S, Sturz G, Hoeffler K, et al. In vitro re-endothelialization of detergent decellularized heart valves under simulated physiological dynamic conditions. *Biomaterials.*27:4221-9. 2006.
63. Liao J, Joyce EM, Sacks MS. Effects of decellularization on the mechanical and structural properties of the porcine aortic valve leaflet. *Biomaterials.*29:1065-74. 2008.
64. Konig G, McAllister TN, Dusserre N, Garrido SA, Iyican C, Marini A, et al. Mechanical properties of completely autologous human tissue engineered blood vessels compared to human saphenous vein and mammary artery. *Biomaterials.*30:1542-50. 2009.

65. Montoya CV, McFetridge PS. Preparation of Ex Vivo-Based Biomaterials Using Convective Flow Decellularization. *Tissue Engineering*.15:11. 2009.
66. Llewellyn BD. Nuclear staining with alum hematoxylin. *Biotech Histochem*.84:159-77. 2009.
67. Goldstein J, Newbury D, Joy D, Echlin P, Lyman C, Lifshin E. *Scanning Electron Microscopy and X-ray Microanalysis*. 3ed. 2003.
68. Alberts B, Johnson A, Lewis J, Raff M, Roberts K, Walter P. *Molecular Biology of The Cell*. 5th ed. New York: Garland Science; 2008.
69. Schweitzer J. *Scanning Electron Microscope*. 2010.
70. Smith W, Hashemi J. *Foundations of Materials Science and Engineering*. 4 ed: McGraw-Hill; 2006. pp. 217-27.
71. Roy S, Silacci P, Stergiopoulos N. Biomechanical Properties of Decellularized Porcine Common Carotid Arteries. *American Physiological Society*.289:10. 2005.
72. Reichlin T, Wild A, Durrenberger M, Daniels AU, Aebi U, Hunziker PR, et al. Investigating native coronary artery endothelium in situ and in cell culture by scanning force microscopy. *J Struct Biol*.152:52-63. 2005.
73. Dahl SL, Koh J, Prabhakar V, Niklason LE. Decellularized native and engineered arterial scaffolds for transplantation. *Cell Transplant*.12:659-66. 2003.
74. Berglund JD, Nerem RM, Sambanis A. Viscoelastic Testing Methodologies for Tissue Engineered Blood Vessels. *Journal of Biomedical Engineering*.127:9. 2005.
75. Lally C, Reid AJ, Prendergast PJ. Elastic Behavior of Porcine Coronary Artery Tissues Under Uniaxial and Equibiaxial Tension. *Annals of Biomedical Engineering*.32:10. 2004.
76. Rabkin E, Schoen FJ. Cardiovascular tissue engineering. *Cardiovasc Pathol*.11:305-17. 2002.

77. Hirschi KK, Rohovsky SA, D'Amore PA. PDGF, TGF-beta, and heterotypic cell-cell interactions mediate endothelial cell-induced recruitment of 10T1/2 cells and their differentiation to a smooth muscle fate. *J Cell Biol.*141:805-14. 1998.
78. Verma S, Li SH, Wang CH, Fedak PW, Li RK, Weisel RD, et al. Resistin promotes endothelial cell activation: further evidence of adipokine-endothelial interaction. *Circulation.*108:736-40. 2003.
79. Cantarella G, Lempereur L, Presta M, Ribatti D, Lombardo G, Lazarovici P, et al. Nerve growth factor-endothelial cell interaction leads to angiogenesis in vitro and in vivo. *FASEB J.*16:1307-9. 2002.
80. Seifalian AM, Tiwari A, Hamilton G, Salacinski HJ. Improving the clinical patency of prosthetic vascular and coronary bypass grafts: the role of seeding and tissue engineering. *Artif Organs.*26:307-20. 2002.
81. Leifer SM. Design and Optimization of a Blood Vessel Mimic Bioreactor System for the Evaluation of Intravascular Devices in Simple and Complex Vessel Geometries [Masters of Science in Engineering - Biomedical engineering Biomedical Engineering and General Engineering, California Polytechnic State University, San Luis Obispo, 2008.
82. Arts CH, De Groot PG, Atteveld N, Heijnen-Snyder GJ, Verhagen HJ, Eikelboom BC, et al. In vivo transluminal microvascular endothelial cell seeding on balloon injured rabbit arteries. *J Cardiovasc Surg (Torino).*45:129-37. 2004.
83. Carosi JA, Eskin SG, McIntire LV. Cyclical strain effects on production of vasoactive materials in cultured endothelial cells. *J Cell Physiol.*151:29-36. 1992.
84. Conte MS, Choudhury RP, Shirakowa M, Fallon JT, Birinyi LK, Choudhry RP. Endothelial cell seeding fails to attenuate intimal thickening in balloon-injured rabbit arteries. *J Vasc Surg.*21:413-21. 1995.

85. Conte MS, VanMeter GA, Akst LM, Clemons T, Kashgarian M, Bender JR. Endothelial cell seeding influences lesion development following arterial injury in the cholesterol-fed rabbit. *Cardiovasc Res.*53:502-11. 2002.
86. Kent KC, Oshima A, Whittemore AD. Optimal seeding conditions for human endothelial cells. *Ann Vasc Surg.*6:258-64. 1992.
87. Yazdani SK, Watts B, Machingal M, Jarajapu YP, Van Dyke ME, Christ GJ. Smooth muscle cell seeding of decellularized scaffolds: the importance of bioreactor preconditioning to development of a more native architecture for tissue-engineered blood vessels. *Tissue Eng Part A.*15:827-40. 2009.
88. Williams C, Wick TM. Endothelial cell-smooth muscle cell co-culture in a perfusion bioreactor system. *Ann Biomed Eng.*33:920-8. 2005.
89. Balcells M, Martorell J, Olive C, Santacana M, Chitalia V, Cardoso AA, et al. Smooth muscle cells orchestrate the endothelial cell response to flow and injury. *Circulation.*121:2192-9.
90. Key Facts. In: Organization WH, ed. *Cardiovascular Diseases (CVDs)*2011.
91. Foundation CD. Facts. In: Foundation CD, ed. *Facts*2009.
92. James CM. Assessment of Electrospinning as an In-House Fabrication Technique for Blood Vessel Mimic Cellular Scaffolding [Masters of Science - Biomedical Engineering Biomedical and General Engineering, California Polytechnic Stat University, San Luis Obispo, 2009.

Appendix A – Abbreviations:

BAECs – Bovine Aortic Endothelial Cells

BVM – Blood Vessel Mimic

CABG – Coronary Artery Bypass Grafting

CAD – Coronary Artery Disease

CVD – Cardiovascular Disease

ECs – Endothelial Cells

ECM – Extracellular Matrix

ePTFE – Expanded Ploy(tetrafluoroethylene)

HUMVECs – Human Umbilical Microvessel Endothelial Cells

HUVSMC – Human Umbilical Vein Smooth Muscle Cell

PGA – Polyglycolic Acid

PTFE – Polytetrafluorethylene

PAD – Peripheral Artery Disease

TEVG – Tissue Engineered Vascular Grafts

SEM – Scanning Election Microscope

SDS – Sodium doecyl Sulfate

SMCs – Smooth Muscle Cells

Appendix B – Protocols and Experimental Details:

B.1 Determining the Optimal Concentration for Decellularizing Porcine Arteries:

Purpose:

To decellularize porcine arteries and optimize the decellularization process. Concentrations of 0%, 0.075%, 0.1%, and 0.125% SDS were evaluated for their ability to fully differentiate the tissue.

Materials

- Daigger orbital shake table (model SH 06050597)
- 10% liquid SDS
- Several Clean 50 mL conicals
- Razor blade
- Milli-Q water
- Sterile forceps
- Histochoice

Decellularization Procedure:

1. Samples were removed from the -80°C freezer and placed in the 37°C water bath (make sure the cap is screwed on tightly).
2. Once defrosted (in a malleable state), the vessel was cut with a razor blade. The vessel sample was cut into 5 pieces about 5cm in length.
3. Samples were placed in individual 50mL tubes labeled with the proper corresponding sample numbers.

4. **Note: To mix the solution, all work should be done in the hood to keep all materials sterile. Concentrations of 0%, 0.075%, 0.1%, and 0.125% sodium dodecyl sulfate (SDS) decellularization solution were measured.

a. A total volume of 20 mL of solution will be needed for the decellularization in a 50mL tube. The SDS stock solution used is purchased as concentrated amount of 10% SDS in Mill-Q. The various concentrations of SDS were calculated using the following formulas:

Equation 1:

Final % SDS in solution (decimal form) * 20mL of total solution = The volume of a pure SDS solution

Equation 2:

The volume of pure SDS (from eqn 1)* 10 (dilution of SDS) = The volume of SDS to be used in the mix

Example calculation for .075% SDS in a 75mL of solution:

Equation1: $0.00075 * 20mL = 0.015mL$

Equation 2: $0.015mL / 0.10 = 0.15mL$ of 10% SDS

For a 20mL SDS solution; 0.15mL of the SDS solution is added to 19.85mL of PBS water.

5. The tissues will remain on the bench top and not be placed in the hood.
6. 20mL of SDS solution at 0%, 0.075%, 0.1%, and 0.125% concentrations was poured into their respective 50mL conical, along with the previously cut vessel sample.
7. The conicals were anchored to an orbital shake table.
8. The shake table was turned on to 100rpm to shake the tissues in solutions for 15 hours.
9. After 15 hours samples were removed from the shake table and the SDS solution was poured down the drain.
10. The decellularized tissue was rinsed 5 times for 10 minutes with sterile PBS.

- a. Using sterile forceps, the decellularized tissue was transferred to a conical with 20 mL of sterile PBS.
 - b. Samples were placed on the shake table for 10 minutes.
 - c. This process was repeated 5 times, for a total of 50 min and 5 rinse steps.
11. Decellularized tissues were transferred to a 15mL conical with 10-12mL of Histochoice. for each sample. .
- *Note: This is a dangerous material, be sure to use gloves and eye protection when pouring.
12. Samples were left in Histochoice overnight at room temperature allowing for fixation to occur.
13. Fixed samples were embedded in paraffin wax blocks evaluated using hematoxylin and eosin staining.

B.2 Perfusion Decellularization:

Purpose:

To decellularize porcine vessels using a perfusion system to keep the lumen open.

Materials:

- Daigger orbital shake table (model SH 06050597)
- 10% liquid SDS
- Several Clean 50 mL conicals
- Razor blade
- Milli-Q water
- Sterile forceps
- Histochoice
- Thermo Fisher Scientific Masterflex L/S 3 roller peristaltic pump (model 7519-05)
- Male and Female luer lock barbs

Procedure:

Samples were kept in a -80°C freezer until you need to use them (no known time limit).

1. Samples were defrosted in a 37°C water bath. Samples were defrosted when the entire sample was malleable and warm. If the sample is fresh, ignore this step.
2. Mix the .075% SDS decellularization solution. The perfusion system uses a total of 75 mL of solution. The SDS stock solution being used (Invitrogen Corporation's catalog number 15553-027) is a concentrated amount of 10% SDS in PBS. The following formula will obtain the volume of SDS in the solution:

Equation 1:

Desired % of SDS in the final solution (decimal form) * 75mL the total volume = the volume of a pure SDS solution

Equation 2:

The volume of pure SDS (eqn1) / 0.10 (the percent dilution of SDS) = The volume of SDS needed to be used

Example calculation for 0.075% SDS in a 75mL of solution:

$$\text{Equation1: } 0.00075 * 75\text{mL} = 0.05625\text{mL}$$

$$\text{Equation2: } 0.05625\text{mL} / 0.10 = 0.56\text{mL of 10\% SDS}$$

For a 75mL solution, 0.56mL of the SDS solution is added to 74.4mL of PBS water.

3. An end male lure lock barb that screws on to the 50mL tubes prepared with tubing was located. The male lure lock barb was required to be the right size for the vessel lumen diameter to fit over.
4. Samples were cut using a razor blade into sections approximately 5cm in length.
5. The proper lure lock barbs were then inserted into the lumen of the vessel and sutured tightly.
6. The barb and vessel were then screwed into place in the 50mL conical with tubing.
7. The tubing conical was placed on the peristaltic pump. The pump is set for fluid to be pushed through the sample side of the tube.
8. The 50mL conical was filled with the 0.075% SDS solution.
9. The tubing was perfused to remove most of the bubbles. The sample needed to be completely submerged in the SDS solution.
10. The pump was run at 140mL/min for 15 hours.
11. After 15 hours samples were removed from the shake table and the SDS solution was poured down the drain.
12. The decellularized tissue was rinsed 5 times for 10 minutes with sterile PBS.
 - Using sterile forceps, the decellularized tissue was transferred to a conical with 20 mL of sterile PBS.
 - Samples were placed on the shake table for 10 minutes.

- This process was repeated 5 times, for a total of 50 min and 5 rinse steps.

13. Decellularized tissues were transferred to a 15mL conical with 10-12mL of Histochoice. for each sample. .

*Note: This is a dangerous material, be sure to use gloves and eye protection when pouring.

14. Samples were left in Histochoice overnight at room temperature allowing for fixation to occur.

15. Fixed samples were embedded in paraffin wax blocks evaluated using hematoxylin and eosin staining.

B.3 Final Perfusion Decellularization:

Purpose:

To decellularize porcine vessels using a perfusion system to keep the lumen open.

Materials:

- Daigger orbital shake table (model SH 06050597)
- 10% liquid SDS
- Several Clean 50 mL conicals
- Razor blade
- Milli-Q water
- Sterile forceps
- Histochoice
- Thermo Fisher Scientific Masterflex L/S 3 roller peristaltic pump (model 7519-05)
- Male and Female luer lock barbs

Procedure:

Samples were kept in a -80°C freezer until you need to use them (no time limit).

1. Samples were defrosted in a 37°C water bath. Samples were defrosted when the entire sample was malleable and warm. If the sample is fresh, ignore this step.
2. Mix the .075% SDS decellularization solution. The perfusion system uses a total of 75 mL of solution. The SDS stock solution being used (Invitrogen Corporation's catalog number 15553-027) is a concentrated amount of 10% SDS in PBS. The following formula will obtain the volume of SDS in the solution:

Equation 1:

Desired % of SDS in the final solution (decimal form) * 75mL the total volume = the volume of a pure SDS solution

Equation 2:

The volume of pure SDS (eqn1) / 0.10 (the percent dilution of SDS) = The volume of SDS needed to be used

Example calculation for 0.075% SDS in a 75mL of solution:

$$\text{Equation1: } 0.00075 * 75\text{mL} = 0.05625\text{mL}$$

$$\text{Equation2: } 0.05625\text{mL} / 0.10 = 0.56\text{mL of 10\% SDS}$$

For a 75mL solution, 0.56mL of the SDS solution is added to 74.4mL of PBS water.

3. An end male lure lock barb that screws on to the 50mL tubes prepared with tubing was located. The male lure lock barb was required to be the right size for the vessel lumen diameter to fit over.
4. Samples were cut using a razor blade into sections approximately 5cm in length.
5. The proper lure lock barbs were then inserted into the lumen of the vessel and sutured tightly.
6. The barb and vessel were then screwed into place in the 50mL conical with tubing.
7. The tubing conical was placed on the peristaltic pump. The pump is set for fluid to be pushed through the sample side of the tube.
8. The 50mL conical was filled with the 0.075% SDS solution.
9. The tubing was perfused to remove most of the bubbles. The sample needed to be completely submerged in the SDS solution.
10. The pump was run at 20mL/min for 20 hours with the shake table at 30 rpm.
11. After 20 hours samples were removed from the shake table and the SDS solution was poured down the drain.
12. The decellularized tissue was rinsed 5 times for 10 minutes with sterile PBS.
 - a. Using sterile forceps, the decellularized tissue was transferred to a conical with 20 mL of sterile PBS.
 - b. Samples were placed on the shake table for 10 minutes.

c. This process was repeated 5 times, for a total of 50 min and 5 rinse steps.

13. Decellularized tissues were transferred to a 15mL conical with 10-12mL of Histochoice. for each sample. .

*Note: This is a dangerous material, be sure to use gloves and eye protection when pouring.

14. Samples were left in Histochoice overnight at room temperature allowing for fixation to occur.

15. Fixed samples were embedded in paraffin wax blocks evaluated using hematoxylin and eosin staining.

B.4 Histological Staining:

Purpose:

To stain paraffin embedded section with hematoxylin and eosin for collagen and nuclei.

Methods:

Blocks were sectioned at 6µm and mounted on slides. Slides were placed in a slide rack and then placed into glass dishes. Slides were dipped in the following order for the stated duration of time.

- 3 min – xylene *Performed in fume hood*
- 3 min – xylene *Performed in fume hood*
- 3 min – xylene *Performed in fume hood*
- 2 min – 100% EtOH
- 2 min – 100% EtOH
- 2 min – 95% EtOH
- 1 min – air dry
- 4 min – Hematoxlin
- 1 min – Water Distilled
- 30 – 45 sec – Clearifier
- 1 min – Water Distilled
- 1 min – Bluing
- 1 min- Water Distilled
- 1 min – 95% ETOH
- 1 min 30 sec – Eosin
- 1 min - 100% EtOH
- 1 min - 100% EtOH

- 1 min - 100% EtOH
- 3 min – xylene *Performed in fume hood*
- 3 min – xylene *Performed in fume hood*
- 3 min – xylene *Performed in fume hood*

While the slide rack remained in the last xylene dish, while each slide was individually pulled out and cover slipped using mounting glue. Slides were left to dry for 48 hours.

B.5 SEM Preparation:

Purpose:

To prepare the vessel scaffold for imaging with a scanning electron microscope.

Materials:

- Gluteraldehyde
- Distilled Water
- Ethanol (at 25%, 50%, 70%, 95%, and 100%)

Methods:

1. Excise the sample from its given treatment
2. Place sample in the glutaraldehyde for at least 30 minutes
3. Rinse sample in distilled water 4 times
4. Place sample in 25% ethanol for 5 minutes
5. Place sample in 50% ethanol for 5 minutes
6. Place sample in 70% ethanol for 5 minutes
7. Place sample in 95% ethanol for 5 minutes
8. Place sample in 100% ethanol for 5 minutes
9. Let air dry
10. Mount the sample to a coverslip so that it as flat as possible. Double stick tape can be used to adhere the sample to the coverslip.
11. Image with the SEM

B.6 Tensile Testing Protocol:

Purpose:

To ensure all tensile tests are repeated in the same manner, in order to ensure reproducible results

Procedure:

1. Samples warm to room temp and not soaking wet.
2. Using the palm pilot tap on the “Inspect” icon
3. Prepare to load the sample:
 - a. Cut open the sample longitudinally
 - b. Measure the width of the sample (w)
 - c. Measure the thickness of the sample (t)
4. Load sample:
 - d. Place proximal end into the clamp that remains stationary.
 - e. Tighten the clamp on a small edge of the sample, clamp enough of the sample to hold it in place
 - f. Repeat clamping process with the distal end into the movie clamp
 - i. Move the clamps into position, switch the machine into jog and in the direction desired, until location is reached
5. Measure the gauge length. When the sample is taught (has some load), measure the gauge length (the length between the two clamps) (l_0).
6. Begin testing
 - g. Switch to toggle and the right direction
 - h. Push start on the palm pilot
 - i. Push the green button on the machine
7. Watch the palm pilot to reach a max load and look for the sample to break.

8. Stop the palm pilot and push the green button on the machine.
9. A window to save will open on the palm pilot (save whatever name you wish.
10. Remove the sample by releasing the clamps and pulling the remains of the sample away.
11. Repeat for all samples.
12. To get the data off the palm pilot, first turn on the computer (password 4bmge).
13. On the palm pilot find the “Hot sync” icon, press on it. A new page will load, press the logo in the center.
14. The computer will automatically begin to work (it will beep when done).
15. On the computer open the file “hand held” (this will convert the palm pilot data files into the file type desired).
16. Make sure the Series XI is clicked on.
17. Open the file from the palm pilot.
18. Click on save as and determine a location that you want to save as. Save as a .txt file.
19. Then shut off the machine and put the palm pilot away.
20. Then use the tensile testing macro to determine the elastic modulus and the critical yield

B.7 Burst Pressure Protocol:

Purpose:

To test the scaffold for its mechanical integrity post decellularization, with specific regard to the radial compliance.

Materials:

- Pressure Transducer
- Data Acquisition software
- Male and Female Barbs
- Blood pressure arm cuff
- Capped Male Luer

Procedure:

Calibration:

1. The blood pressure arm cuff was located
2. The pressure transducer was attached on either side of the tubing of the blood pressure cuff
3. The data acquisition software started recording (1)
4. The arrow just above the input for the data was clicked on and the bridge pod was selected.
5. The arm cuff was quickly pumped to the max pressure (remember this number)
6. Units was selected on the min and max screen
7. The lowest pressure seen was equal to zero
8. The highest pressure seen was equal to the max pressure from the arm cuff
9. 'Ok' was pressed several times for the calibration of the transducer

Set-up:

Ordering: end piece => female piece that will to the sample => another fitting to the sample and the male barb => transducer => fitting to transducer and tubing => tubing => stop cock for syringe (seen in Figure B.1).

Testing:

1. Place the sample in between the fittings
2. Unlock the end cap
3. Connect the syringe and perfuse the lumen with fluid
4. Replace the end cap to the end
5. Begin recording
6. Slowly increase the pressure until the vessel bursts

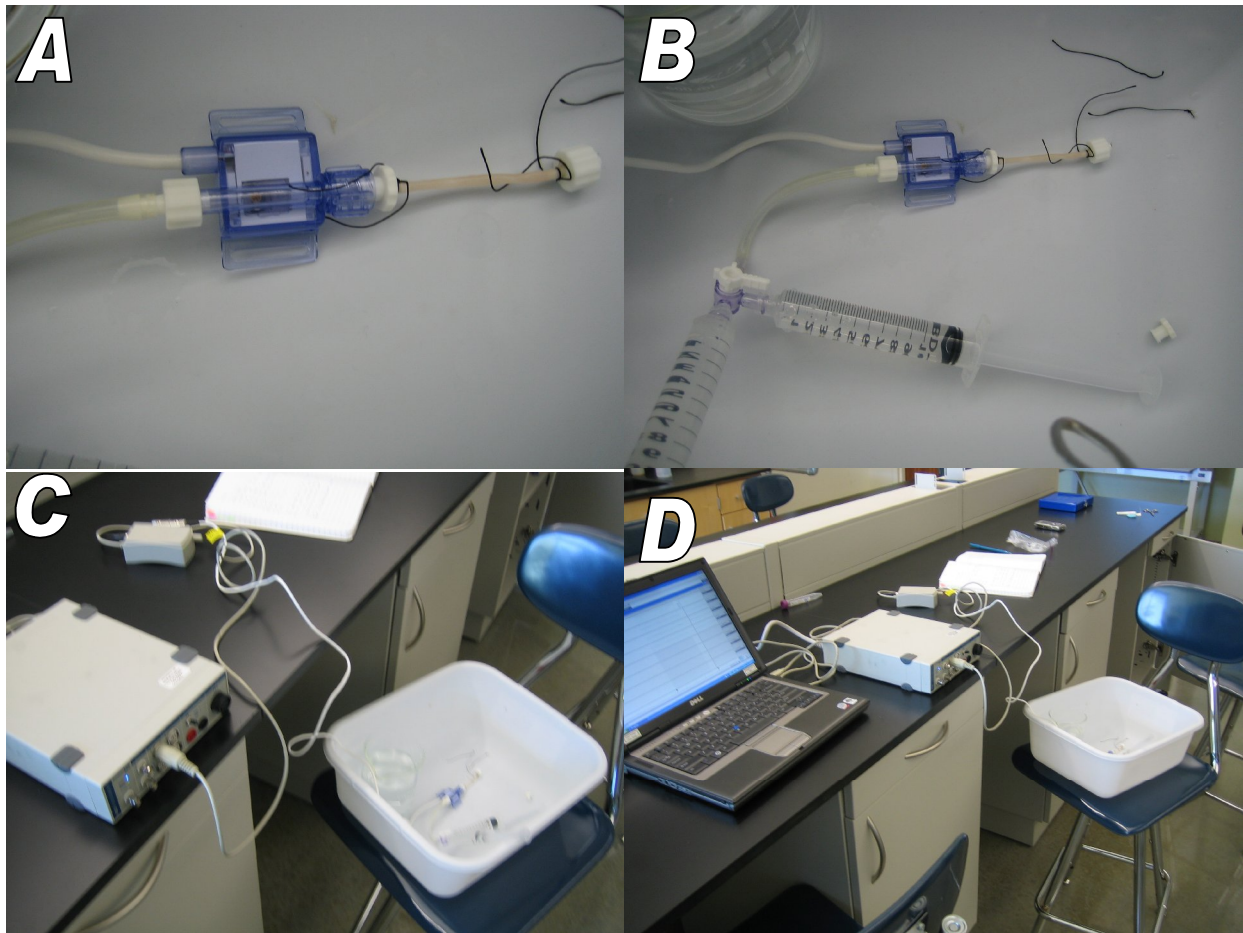


Figure B.1. Burst Pressure Images set up. Barbs and pressure transducer set up on a scaffold (A). The syringe ready to apply force in the lumen of the scaffold (B). The connection with the bridge pod and data acquisition connection (C). The completed set-up with all components (D).

B.8 Bacterial Evaluation:

Purpose:

To test scaffold for bacterial content post harvesting and post decellularization. This will also look at the potential for the Penicillin: Streptomycin, contained in cell culture media, to prevent contamination

Materials:

- Lysogeny Broth (LB)
- Tryptic (Trypticase) Soy Agar plates
- Glass beads
- Penicillin:Streptomycin (Penstrep)
- Sterile DCF-PBS

Methods:

1. Decellularize a vessel using the perfusion protocol in Appendix A.3
 - a. Cut the vessel sample in half: one part for decellularization and one part to be used as a control
2. Place 1 mL of LB into test tube
3. Place sample into the test tube with LB
4. Vortex for 1 minute
5. Add penstrep to the desired plates to see if bacteria are resistant to the concentration of the antibiotic used in the media.
 - a. Media contains 1% antibiotic
 - b. Agar is 15 mL volume
 - c. Add .15 mL of penstrep to the plate
6. Add glass beads

7. Shake glass beads back and fourth in a crossing motion to move the penstrep solution around the whole plate
8. Transfer the 0.1mL of the LB solution to the agar plate
9. Shake the beads again
10. Add 4 mL of brother to the LB tubes to increase the total volume to 5 mL (although 0.1 mL was taken out for the agar plate, we assume the sample displaces about that much volume)
11. Add 0.05 mL (50 μ L) of penstrep to the desired LB tubes to make a 1% solution of antibiotics

Place samples (both agar plates and LB tubes) on an orbital shaker at 37°C for at least 12 hours. Then evaluate the plates for the presence of bacterial colonies on the plate. For the broths, evaluate the clarity of the liquids; where the more clear, the less bacteria.

B.9 Tensile Test Evaluation:

Purpose:

To evaluate the raw data given by tensile testing

Methods – this is the Macro That is Run to Summarize the Tensile Testing Analysis:

```
'Sub TensileTestMacro()'
```

```
'February 23, 2009'
```

```
k = 0
```

```
d = InputBox ("How many tests would you like to analyze?")
```

```
If d > 3 Then
```

```
    For k = 4 To d      'you didn't type in a number'
```

```
        Worksheets.Add
```

```
    Next
```

```
End If
```

```
For j = 1 To d
```

```
    m = 0
```

```
    Max = 0
```

```
    sumofx = 0
```

```
    sumofy = 0
```

```
    sumofxy = 0
```

```
    sumofxx = 0
```

```
    sumofxsquared = 0
```

```
    Delta = 0
```

```
    a = 0
```

```
    b = 0
```

```
    c = 0
```

```
    l = 0
```

```
Filename = InputBox("Where is the location of the data file")
```

```
Name = InputBox("What test is this?")
```

```
a = InputBox("What is the gauge of the sample?")
```

```
b = InputBox("What is the width of the sample?")
```

```
c = InputBox("What is the thickness of the sample?")
```

```

Worksheets(j).Name = Name           'you kept hitting cancel didn't you?'
Worksheets(Name).Cells(1, 1).Value = "Time"
Worksheets(Name).Cells(1, 2).Value = "Extension"
Worksheets(Name).Cells(1, 3).Value = "Load"
Worksheets(Name).Cells(1, 4).Value = "Strain"
Worksheets(Name).Cells(1, 5).Value = "Stress"
Worksheets(Name).Cells(1, 7).Value = "Linear Strain"
Worksheets(Name).Cells(1, 8).Value = "Linear Stress"
Worksheets(Name).Cells(1, 10).Value = "Critical/Yield Stress"
Worksheets(Name).Cells(1, 11).Value = "20% Yield Stress"
Worksheets(Name).Cells(1, 12).Value = "50% Yield Stress"
Worksheets(Name).Cells(1, 13).Value = "Slope"
Worksheets(Name).Cells(1, 14).Value = "y-intercept"

```

Open Filename For Input As #j 'Typed the filename wrong/file doesn't exist/you've already opened it this session'

```
i = 0
```

```
Do Until EOF(j)
```

```
Input #j, x, y
```

```
  If i = 0 Or i = 1 Then
```

```
    Worksheets(Name).Cells(i + 1, 1).Value = x
```

```
    Worksheets(Name).Cells(i + 1, 1).Value = y
```

```
    i = 1 + i
```

```
  Else
```

```
  If (x >= 0) And (y > 0) Then
```

```
    i = i + 1
```

```
    Worksheets(Name).Cells(i - 1, 1).Value = (i - 2)
```

```
    Worksheets(Name).Cells(i - 1, 2).Value = y
```

```
    Worksheets(Name).Cells(i - 1, 3).Value = x
```

```
    Worksheets(Name).Cells(i - 1, 4).Value = y / a
```

```

'need to delete the
'first two lines of
'the notepad file
'(only data points

```

Worksheets(Name).Cells(i - 1, 5).Value = x / (b * c) 'no words) or you messed up typing a
value into the size of the sample

t = y / a

u = x / (b * c)

If u > Max Then

Max = u

timestop = (i - 2)

End If

Worksheets(Name).Cells(2, 10).Value = Max

e = (0.2) * Max

f = (0.5) * Max

Worksheets(Name).Cells(2, 11).Value = e

Worksheets(Name).Cells(2, 12).Value = f

End If

End If

Loop

g = 0

r = 0

p = 1

For m = 1 To (i - 2)

g = g + 1

o = Worksheets(Name).Cells(g, 1).Value

h = Worksheets(Name).Cells(g, 5).Value

n = Worksheets(Name).Cells(g, 4).Value

If h >= e And h <= f And o <= timestop Then

p = p + 1

```
Worksheets(Name).Select
Cells(g, 4).Select
Selection.Font.Bold = True
Cells(g, 5).Select
Selection.Font.Bold = True
```

```
Worksheets(Name).Cells(p, 7).Value = n
Worksheets(Name).Cells(p, 8).Value = h
```

```
End If
Next
```

```
Worksheets(Name).Cells(8, 1).Select
```

```
Charts.Add
```

```
With ActiveChart
```

```
.ChartType = xlXYScatterSmoothNoMarkers
.SetSourceData Source:=Sheets(Name).Range("D:E"), PlotBy:=xlColumns
.Location Where:=xlLocationAsObject, Name:=Name
```

```
End With
```

```
With ActiveChart
```

```
.HasTitle = True
.ChartTitle.Text = "Stress-Strain Curve"
.Axes(xlCategory, xlPrimary).HasTitle = True
.Axes(xlCategory, xlPrimary).AxisTitle.Characters.Text = "Strain"
.Axes(xlValue, xlPrimary).HasTitle = True
.Axes(xlValue, xlPrimary).AxisTitle.Characters.Text = "Stress"
.HasLegend = False
```

```
End With
```

```
Worksheets(Name).Cells(16, 6).Select
```

```
q = p - 1
```

```
Charts.Add
```

```
With ActiveChart
```

```
.ChartType = xlXYScatter
.SetSourceData Source:=Sheets(Name).Range("G:H"), PlotBy:=xlColumns
.Location Where:=xlLocationAsObject, Name:=Name
```

```
End With
With ActiveChart
    .HasTitle = True
    .ChartTitle.Text = "Linear Stress"
    .Axes(xlCategory, xlPrimary).HasTitle = True
    .Axes(xlCategory, xlPrimary).AxisTitle.Characters.Text = "Strain"
    .Axes(xlValue, xlPrimary).HasTitle = True
    .Axes(xlValue, xlPrimary).AxisTitle.Characters.Text = "Stress"
    .HasLegend = False
End With
ActiveChart.SeriesCollection(1).Select
ActiveChart.SeriesCollection(1).Points(q).Select
ActiveChart.SeriesCollection(1).Trendlines.Add(Type:=xlLinear, Forward:=0, _
    Backward:=0, DisplayEquation:=True, DisplayRSquared:=True).Select

Next

End Sub
```


B.10 Original Sodding Protocol:

Purpose:

The purpose of this protocol was to seed an ePTFE scaffold with cells to create a monolayer of cells throughout the length of the lumen.

Materials:

- Blood Vessel Model setup
- Cells to seed with
- Conditioning, cell, and bioreactor Media
- Syringes
- ePTFE scaffold

*** Please note, this work is based off of Dr. Cardinal's original protocol for seeding a scaffold.

Some blanks are purposely left blank to be filled out and tailored to a specific experiment.

Procedure:

Prep 1 week prior

1. Gas sterilize biochambers and 2-port reservoirs
2. Determine target number of cells and passage schedule, then thaw cells
3. Cut grafts, mount on fittings, and suture
4. Autoclave grafts, flasks, and forceps

Prep the day before

5. Make media:
 - a. Bioreactor Media (Human Complete w/o ECGS w/ antibiotics)
 - b. Conditioning Media (1:6 solution of FBS:M199 + antibiotics)
6. Denucleate grafts (using filtered EtOH)
 - a. 15 min 70% EtOH

- b. 15 min 100% EtOH
- c. Leave in degassed Conditioning Media in incubator overnight

Set-up day: BVM conditioning

7. Warm up media (Bioreactor Media and Conditioning Media)
8. Fill chamber with media
9. Insert sterile grafts into biochambers
10. Using a syringe, flush lumen with Conditioning Media to prime graft
 - a. Clamp lumen and continue to prime graft
 - b. Repeat for all vessels
11. Place small WM pump in hood
12. Prime 2-port reservoirs with Conditioning Media
13. Attach primed biochamber to 2-port reservoir and condition graft for 10 min
 - a. Flow through lumen first to remove air, then clamp lumen and condition transmurally on 150rpm setting
14. Leave primed biochambers in large incubator until ready for sodding step
15. Prime 2-port reservoirs with Bioreactor Media
 - a. Prepare one for each vessel
 - b. Be sure that drip is visible and outlet is submerged
 - c. Clamp tubing and leave in big incubator

Set-up day: BVM sodding

16. Take corresponding number of primed biochambers and reservoirs to hood
17. Attach outlet of reservoir to inlet stopcock of biochamber
 - a. Leave reservoir inlet unattached and biochamber outlet facing trough
18. Record BVM numbers (or chamber ID):

19. Harvest cells

a. Apply Trypsin, deactivate with media

b. Take 100uL from total _____mL cells

Counts:

20. $X =$ _____ $\times 2000 \times (\text{cell mL} \times .10)$

total number of cells =

21. Pellet cell suspension (on 4 for 4 min)

22. Resuspend in _____mL Bioreactor Media

23. Sod each graft with _____mL cell solution

a. Cells per graft =

b. Sodding density = _____ cells/cm²

24. Chase with 1-3mL Bioreactor Media

25. Attach biochamber outlet to reservoir inlet

26. Bring BVMs to large incubator

27. Place on small WM pump - leave lumen clamped!!

28. Immediately begin transmural flow at 7rpm, and maintain for 1 hour

a. Started on pump at: _____ (time)

29. Unclamp lumen and maintain 7rpm luminal flow for 1 hour

30. Increase flow to 11rpm

31. Increase flow to 15rpm; leave overnight

The next day and beyond

32. Increase flow by 10-15rpm at a time to reach 90rpm by the end of the day

33. BVM maintenance: replace media reservoirs every 3rd day Check CO₂!

B.11 Acute 3T3 Sodding:

Procedure:

The purpose of this protocol was to develop a protocol for the sodding of a decellularized scaffold with 3T3 fibroblasts.

Materials:

- Blood Vessel Model setup
- 3T3 Fibroblasts
- 3T3 Fibroblast media
- Syringes
- Porcine scaffold

Procedure:

Prep 4 Days Prior

1. Set up cell passage schedule
 - a. Day 0: thaw the vial of fibroblasts (this case is with p8 cells) and put them into a T75 with 20 mL of fibroblast media
 - b. Day 1: Pass the fibroblasts 1:3 into a T225. The T225 is prepared with 36 ml of media. To pass 3 mL of trypsin used to detach the cells and then 3 mL of fibroblast media.
 - c. Day 3: Will be time to isolate the cells. The cells will be centrifuged to make a pellet and be used in sodding
2. Start the cells passage (day 0)
3. Pass the cells (day 1) into a T225

Prep the day before

4. Start decellularization (day 2), use the normal perfusion decellularization system

- a. Prior to the start of decellularization, suture the fittings to each end of the vessel corresponding to how they need to fit into the BVM

Prep the day of

5. Stop decellularization and continue with the rinse process (day 3)
 - a. On the 4th rise start to warm up the fibroblast media

Harvest Cells

6. During the 5th rise (day 3)
 - a. Trypsinize cells with 9 mL of trypsin
 - b. Deactivate the trypsin with 9mL of fibroblast media
 - c. With the 18 mL, put it in a 50 mL conical
 - d. Put the conical into the centrifuge, and spin down for 4 min (on setting 4)
 - e. Fill the biochamber with Fibroblast media
 - f. Stop the rinse cycle
 - g. Put the vessel in the bioreactor, trying to keep it straight and fairly tight
 - h. Perfuse the system with fibroblast media (lumenally and transmurally)
 - i. Prime the media reservoir and the tubing with fibroblast media
 - j. Remove conical from centrifuge and pipette off all the media except the cell pellet
 - i. About 6 million cells were cultured
 - ii. $\text{Cells/cm}^2 = \text{Total Number of Cells/Surface Area}$
 - k. Then add 4 mL of fibroblast media per scaffold to the conical
 - l. Mix the conical to break up the pellet and create a mixed, homogenous cell solution
 - m. Get two 10 mL syringes (one with 4 mL of fibroblast media and one with the 4 mL of the cell solution)
 - n. Put a trough at the distal portion of the bioreactor

- o. Close off the distal luminal stop cock
 - p. Put the syringe of the cell solution on the proximal side- inserting into stopcock
 - q. Then inject cell solution through syringe
 - r. Then attach the syringe with the 4mL of media and flush transmurally as a chaser to force the cells into the lumen of the vessel
7. Then attach the media reservoir tubing in line with the bioreactor
 8. Put the bioreactor on the 8-roller pump
 9. Set the flow at 10 rpm for 1 hour transmurally
 10. To take down – cut the vessel out of the chamber, keeping track of proximal and distal ends
 11. Put the vessel in the histochoice
 12. Wait one day before cutting and getting ready for BBI

The next day and beyond

13. Cut a middle of the vessel into a thin cross-section
14. Cut the proximal and distal portions longitudinally into top and bottom
15. Put the samples into the BBI previously wrapped in foil because of its the light sensitivity
16. Image 3 sections on each part of the vessel along the lengths and around the cross-section
17. Count the number of cells per image
18. Process and embed the sample for histology

B.12 Making the BBI Stain:

Purpose:

To image the cells after they have been sodded to quickly and easily identify the cell density and consistency throughout the scaffold.

Materials:

- Histochoice
- Milli-Q
- Bisbenzimidide (BBI, a Hoechst Stain Kit 33258)

Procedure:


- 1) Put portions of scaffold in histochoice for 24 hours
 - a. ** Be careful to leave this as steady as possible as to not disrupt the cell adhesion
- 2) Make a solution of BBI (1:1000):
 - a. 30 μ L of BBI with 15 mL of Milli-Q
 - b. Mix well
 - c. Cover in Foil
- 3) Carefully move scaffold from histochoice to BBI solution
- 4) Incubate at room temperature for 30 min
- 5) Image


B.13 Procedure for (BBI) Evaluation of Cell-Sodded Scaffolds:

Purpose:

To visualize cells on a scaffold

Methods:

1. Put on safety glasses. Cut samples with blade or scissors, being careful to not disrupt cell lining inside lumen (squeezing, touching, and scraping can all disrupt lining and ruin experiment).
2. Use washed forceps to place samples in corresponding 15-mL conicals that contain BBI solution. Carefully keep track of samples. Leave foil on conicals.
 - a. Let samples soak for at least 15 minutes (longer is better).
3. Put away extra stock solution. Clean up preparation area.
4. With permission or help from Dr. Cardinal, use fluorescent microscope to obtain *en face* images. Take forceps to use at microscope. See Figure A.2 for pictures of steps below.
 - a. Log into notebook (fluorescence; initials; date; time and lamp hours).
 - b. Turn turret to setting 4.
 - c. Turn on Olympus lamp (green switch).
 - d. Turn on Optiscan wheels (black switch).
 - e. Turn on camera (black switch).
 - f. Set filter wheel 1 to 1, and set filter wheel 2 to 1.
 - g. Open shutter: 
 - h. Set Prior keypad to shutter S1.
 - i. Dial objectives to desired magnification (typically 4x and 10x for BBI images).
 - j. Set thin bar to icon of eye and camera.

- k. Sign into computer by clicking Kristen's account (password can be obtained from Kristen).
- l. Click QCapture Pro (on desktop).
- m. Click camera icon at top of QCapture Pro window: 
- n. Place slide on microscope. Place sample on slide.
- o. See Figure A.3.
- p. Manually adjust microscope to clarify image.
- q. If scaffold is too wet, carefully blot end of scaffold on Kim wipe.
- r. Take pictures. Save pictures if desired (labeled with sample info, initials, and magnification).
- s. Shut down system by switching off Olympus lamp, Optiscan wheels, and camera (on top of microscope).
- t. Log out of notebook.

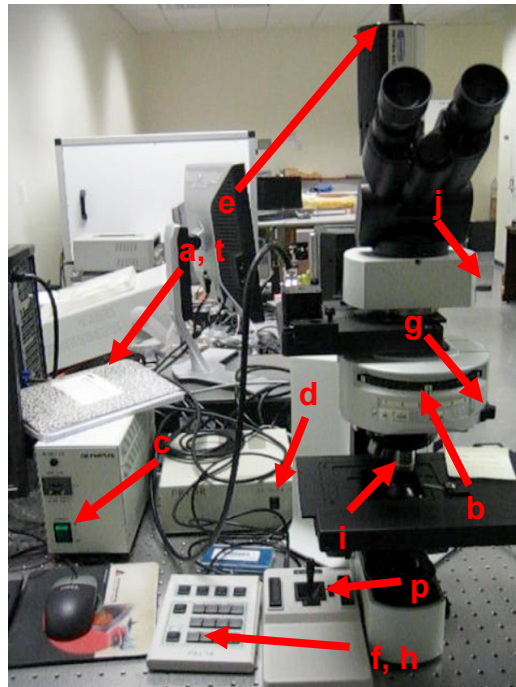


Figure B.2. Microscope anatomy. Letters correspond to step 6 in protocol.

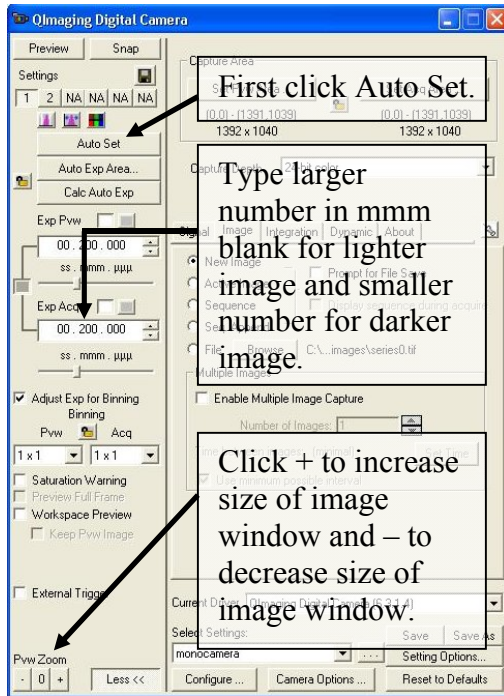


Figure B.3. QCapture Pro control panel.

B.14 Long-Term Testing of Decellularized Vessels with hUVSMCs:

Purpose:

To test to see if the decellularized scaffold can house SMCs for a longer time frame. The decellularized vessel will be seeded with SMCs for 1, 3, and 7 day time points. Hopefully the vessel houses the SMCs as the start to integrate with the scaffold wall and form a unique layer.

Materials:

- Blood Vessel Model setup
- Human Umbilical Vein Smooth Muscle Cells (hUVSMCs)
- HUVMC media
- Syringes
- Porcine scaffold
- Vessel A: Length = 3.4 cm, Inner Diameter = 0.322 cm
- Vessel B: Length = 3.4 cm, Inner Diameter = 0.429 cm
- Vessel C = Length = 3.4 cm, Inner Diameter = 0.49 cm

Protocol:

Prep 1 week prior

1. Gas sterilize biochambers and 2-port reservoirs
2. Determine target number of cells and passage schedule, then thaw cells
3. Autoclave grafts, flasks, and forceps

Prep the day before

4. Make media:
 - a. Bioreactor Media (Human Complete w/o ECGS w/ antibiotics)
 - b. SMC Media

5. Decellularize grafts
 - a. 0.1% SDS with PBS
 - b. Place in reservoir chamber
 - c. Perfuse at 20mL/min for 20 hours with the shake table at 33 rpm
 - d. Have both ends sutured to respective barb

Set-up day: BVM conditioning

6. Rinse the grafts with sterile Milli-Q 5X 10 min
7. Warm up media (Bioreactor Media and SMC Media)
8. Fill chamber with BR media
9. Insert rinsed grafts into biochambers
10. Using a syringe, flush lumen with SMC Media to prime graft
 - a. Clamp lumen and continue to prime graft
 - b. Repeat for all vessels
11. Prime 2-port reservoirs with SMC Media
12. Attach primed biochamber to 2-port reservoir and condition graft for 10 min
 - a. Flow through lumen first to remove air, then clamp lumen and condition transmurally on 150rpm setting
13. Leave primed biochambers in large incubator until ready for sodding step

Set-up day: BVM sodding

14. Take corresponding number of primed biochambers and reservoirs to hood
15. Leave reservoir inlet unattached and biochamber outlet facing trough
16. Record BVM numbers (or chamber ID):
17. Harvest cells
 - a. Apply Trypsin, deactivate with media

- b. Record confluency of flasks and number/size of flasks used for each vessel:
18. Pellet cell suspension (on 4 for 4 min)
 19. Resuspend in 12 mL Bioreactor Media
 20. Sod each graft with 4 mL cell solution
 - a. Cells per graft = 6 million
 - b. Sodding density = 1.5million cells/cm² (average)
 21. Chase with 1-3mL SMC Media
 22. Attach biochamber outlet to reservoir inlet
 23. Bring BVMs to large incubator
 24. Place on pump - leave lumen clamped!!
 25. Immediately begin transmural flow at 7rpm, and maintain for 1 hour
 - a. Started on pump at: _____ (time)
 26. Unclamp lumen and maintain 7rpm luminal flow for 1 hour
 27. Increase flow to 11rpm for 1 hour
 28. Increase flow to 15rpm; leave overnight

The next day and beyond

29. Increase flow by 10-15rpm every 30 min until reaching 90rpm
30. BVM maintenance: replace media reservoirs every 3rd day
 - a. Check CO2!

B.15 Long-Term Testing of Decellularized Vessels with hUVECs:

Purpose:

To look at the potential hUVECs have for creating an endothelial lining on decellularized porcine arteries. Pressure Sodding hUVECs should suffice for a monolayer of endothelial cells to create a physiologic model of a native blood vessel. Also cell tracker will be used to identify the hUVECs with in the vessel. Using the cell tracker in the case provides a proof of concept that the cell tracker is a simple dye that can be used for dual Sodding on vessels, to monitor any cell types placed in the scaffold.

Materials:

- Blood Vessel Model setup
- Human Umbilical Vein Smooth Muscle Cells (hUVECs)
- HUVEC media
- Syringes
- Porcine scaffold
- Vessel A: Length = 3.89 cm, Inner Diameter = 0.59 cm
- Vessel B: Length = 4.3 cm, Inner Diameter = 0.48 cm

Protocol:

Prep 1 week prior

1. Gas sterilize biochambers and 2-port reservoirs
2. Determine target number of cells and passage schedule, then thaw cells
3. Autoclave grafts, flasks, and forceps

Prep the day before

4. Make media:
 - a. Bioreactor Media (Human Complete w/o ECGS w/ antibiotics)

- b. HUVEC Media
5. Decellularize grafts
 - a. 0.1% SDS with PBS
 - b. Place in reservoir chamber
 - c. Perfuse at 20mL/min for 20 hours with the shake table at 33 rpmHave both ends sutured to respective barb

Set up Day: Applying Cell Tracker

6. Make Stock Solution: Add 1.8 μ m of DMSO to the 50 μ g of cell tracker,
7. Add 9.5 μ l of Stock solution and 19mL of serum free media
8. Vortex the working solution
9. Remove media on the cells
10. Rinse with DCF-PBS
11. Add working cell tracker solution to the flask of 3T3's
12. Incubate for 30 min
13. Remove working solution
14. Rinse with DCF-PBS
15. Fill with normal cell media
16. Incubate for 30 min

Set up Day: Static Culture

17. Rinse the grafts with sterile Milli-Q 5X 10 min
18. Warm up media (HUVEC Media)
19. Place stop-cocks on both ends of the vessel
20. Put 10 mL of HUVEC media in a trough
21. Using a syringe, flush lumen with HUVEC Media to prime graft

- a. Clamp lumen and continue to prime graft
- b. Repeat for all vessels

22. Leave vessels in the trough for sodding

Set-up day: BVM Culture

23. Rinse the grafts with sterile Milli-Q 5X 10 min

24. Warm up media (Bioreactor Media and HUVEC Media)

25. Fill chamber with BR media

26. Insert rinsed grafts into biochambers

27. Using a syringe, flush lumen with HUVEC Media to prime graft

- a. Clamp lumen and continue to prime graft
- b. Repeat for all vessels

28. Prime 2-port reservoirs with HUVEC Media

29. Attach primed biochamber to 2-port reservoir and condition graft for 10 min

- a. Flow through lumen first to remove air, then clamp lumen and condition transmurally on 150rpm setting

30. Leave primed biochambers in large incubator until ready for sodding step

Set-up day: BVM sodding

31. Pellet cell suspension (on 4 for 4 min)

32. Resuspend in 8 mL HUVEC Media

33. Sod each graft with 4 mL cell solution

- c. Cells per graft = 6 million cells
- d. Sodding density = 0.91 million cells/cm² (average)

Static set up:

34. Rotate the vessel 45° ever 15 min for 1 hour

35. Take down vessel after 1 hour and evaluate

BVM set up:

36. Chase with 1-3mL HUVEC Media Attach biochamber outlet to reservoir inlet

37. Bring BVMs to large incubator

38. Place on pump - leave lumen clamped!!

39. Immediately begin transmural flow at 7rpm, and maintain for 1 hour

a. Started on pump

b. Rotating 45° every 15 min for an hour

40. Unclamp lumen and maintain 7rpm luminal flow for 1 hour

41. Increase flow to 11rpm; leave overnight

The next day and beyond

31. Take down the vessel after 3 days

BVM Analysis

34. To view the cells, the cell tracker can be highlighted via setting on the fluorescence microscope

a. Green: Turret-4, S1, FW1-3, FW2-2

b. Red: Turret-4, S1, FW1-4, FW2-3

B.16 Cell Tracker Staining:

Purpose:

To stain cells Multiple colors for dual sodding

Materials:

- 5-20 μL pipette and sterile head (usually in the hood in 209)
- 3 ml Syringe with Needle tip
- DMSO 100mL bottle from the corner cupboard (Sigma-Aldrich) catalog number 276855 (anhydrous)
- Cell tracker Red CMPX (Invitrogen; Carlsbad, CA) catalog number C34522
- Cell Tracker Green CMFDA (5- Chloromethyl Fluorescein Diacetate; Invitrogen; Carlsbad, CA) catalog number C 7025
- Sterile Serum-free Media (for whatever cell type you are using)
- 1 – 25 ml pipettes (the regular ones we use)

Procedure:

- 7) Warm media in the water bath
- 8) Use a needle tip and syringe to pull out 1 mL of DMSO and placed in a 15mL conical
- 9) Use micropipette to pull out 10.8 μL of DMSO from the 15mL conical
- 10) Add the DMSO to the vial of Cell Tracker – attempt to get most of the powder cell tracker dye in with the DMSO. This is a 10mM concentration of **stock solution**, via the following equations:

$$M = \frac{\text{moles}}{L} \quad \text{mole} = \frac{g}{w} = \frac{.05g}{464.86} = 1.08 \times 10^{-4} \text{ moles}$$
$$0.01M = \frac{1.08 \times 10^{-4} \text{ moles}}{L} \quad L = 1.08 \times 10^{-2} L = 10.8 \text{ mL}$$

11) Dilute to the desired concentration for the cell tracker dye to create the **working solution**

Use the equation $c_1v_1 = c_2v_2$ (where $c_1 = 10\text{mM}$ – from the stock solution, $v_1 =$ is unknown,

$c_2 =$ the desired concentration – in this case $5\mu\text{M}$, and $v_2 =$ the final volume needed)

$$10\text{mM}(x) = 5\mu\text{M}(19\text{mL})$$

a. $10000\mu\text{M}(x) = 5\mu\text{M}(19\text{mL})$

$$x = .0095\text{mL} = 9.5\mu\text{L of Stock solution}$$

12) Vortex the working solution for use

a. Solution can be stored in the fridge for up to one week

13) Remove the media from the cell culture

14) Add your working solution of the Cell Tracker Dye to the cell culture

a. Cell Tracker Green should be incubated on the cells for 30 min

b. Cell Tracker Red should be incubated on the cells for 15 min

15) Remove the Cell Tracker Dye working solution from the cell culture

16) Add cell media back onto the cell culture

17) Incubate for at least 30 minutes

18) Cells are now dyed (**dyed cells**) and able to be used as you wish – i.e. pressure sodding described below

a. The dyed cells can be used for about 1 week (different concentrations will produce different intensities, as characterized by the graph below) as the dyed cells proliferate either through passages or sodding.

B.17 Analyzing Cell Tracker Images:

Purpose:

To easily, consistently, and quickly count cells that had been successfully stained with fluorescent dyes.

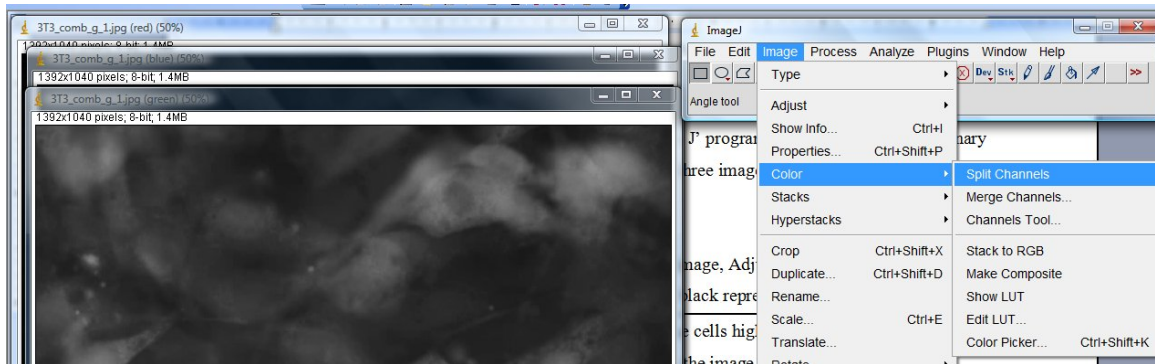
Materials:

- Images of the cells
- ImageJ analysis program

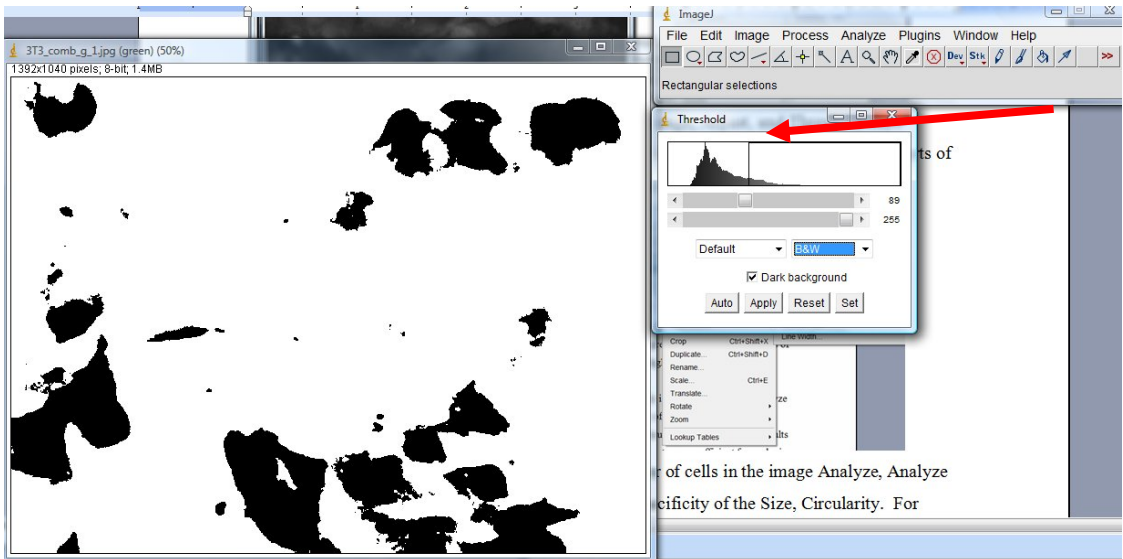
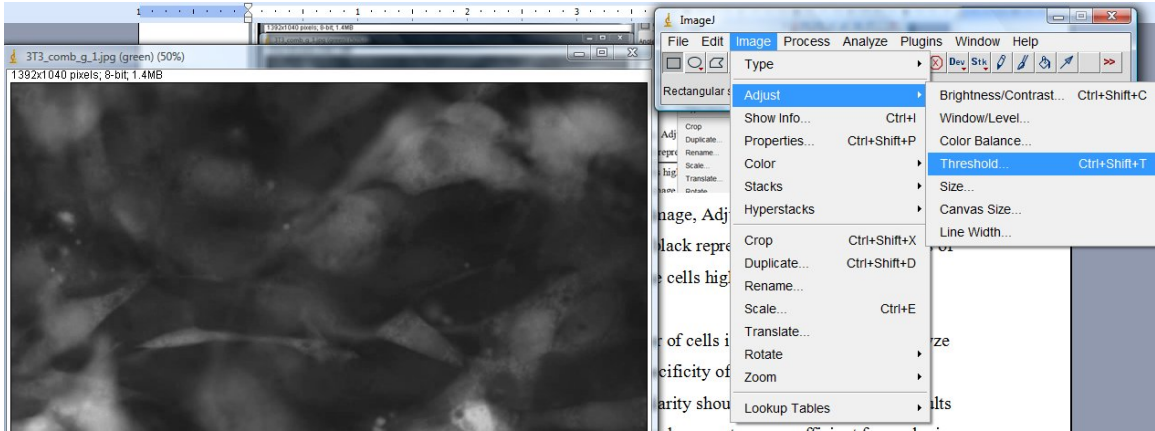
Procedure:

Counting the cells

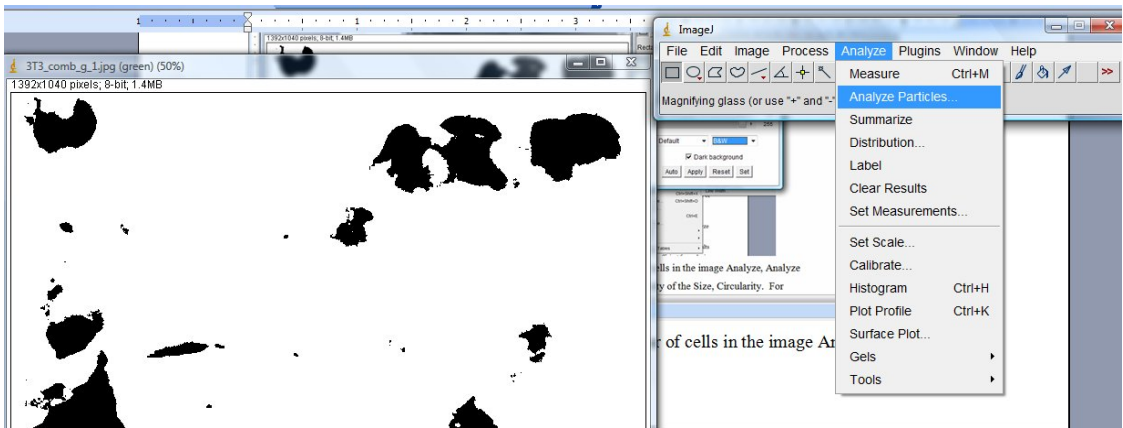
Images were opened and analyzed in the 'Image J' program. The image was made binary by going to Image, Color, split channels. This created three images in grey scale of red, green, and blue.



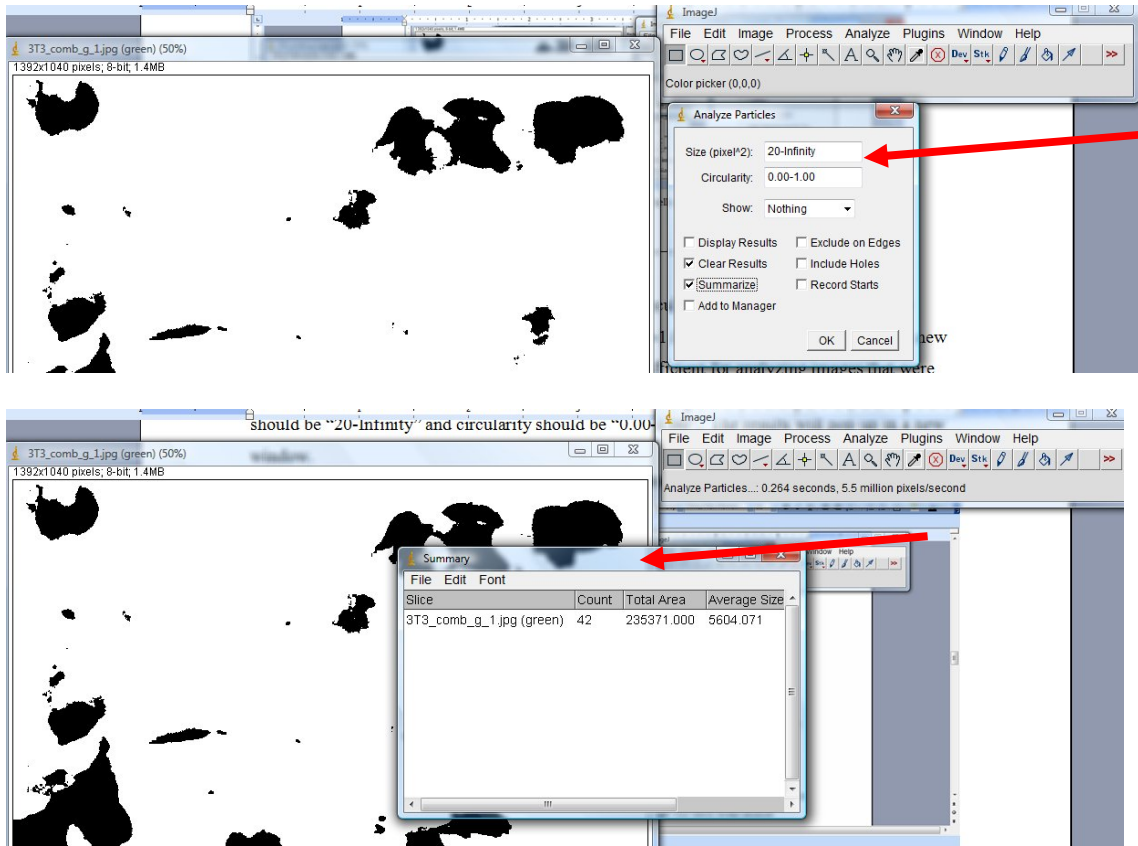
The grey scale of the green image was selected. Next Image, Adjust, and Threshold were selected to change the image to black and white where black represents the most intense parts of the image (be sure to press dark background to make the cells highlighted in black).



To tabulate the average area of each cell and the number of cells in the image Analyze, Analyze Particles was selected.

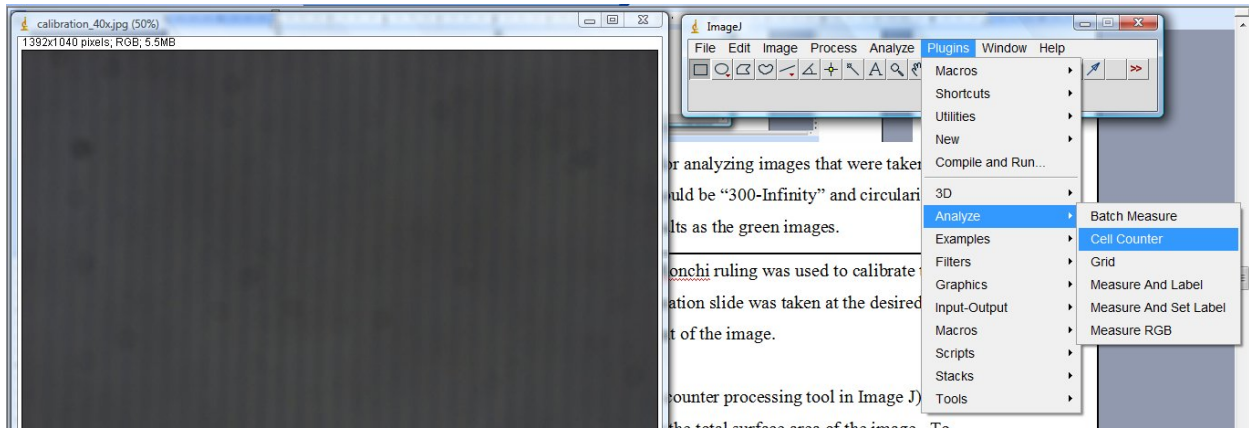


A screen emerges asking for specificity of the Size, Circularity. For green images the size should be “20-Infinity” and circularity should be “0.00-1.00”. The results will pop up in a new window.

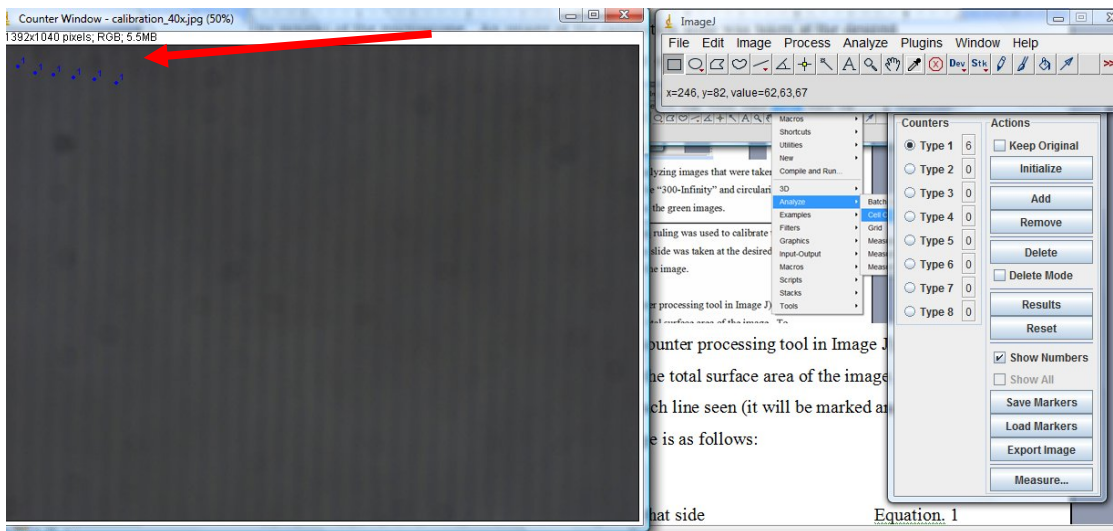


The previously mentioned parameters are sufficient for analyzing images that were taken with Cell Tracker Red as well. For red images the size should be “300-Infinity” and circularity should be “0.50-1.00”. This will produce similar results as the green images.

To determine the amount of cells per mm² a Ronchi ruling was used to calibrate the view (by pixels) of the microscope. An image of the calibration slide was taken at the desired magnification where vertical lines were the focal point of the image.



By counting how many lines (through the use of cell counter processing tool in Image J) span the width of the image, a ratio can be found to determine the total surface area of the image. To use cell counter: initialize and press type one, then click each line seen across the width of the image (it will be marked and counted).



To calculate the size of one edge of an image is as follows:

$$\frac{\text{Number of Lines Spanning the Image}}{\text{Number of Pixels in the x direction}} = \text{the length of that side} \quad \text{Equation. 1}$$

Example 1: 135 lines on the width of the image.

$$\frac{135}{1392} = .9mm$$

The ratio calculation can be seen as follows, where x is the length the other side:

$$\frac{\text{Length of side 1}}{\text{Pixels on side 1}} = \frac{x}{\text{Pixels on side 2}} \quad \text{Equation. 2}$$

Example 2: Known side is .9mm on 1392, the other side has 1040 pixels.

$$\frac{.9mm}{1392 \text{ pixels}} = \frac{x}{1040 \text{ pixels}} \rightarrow x = .67mm$$

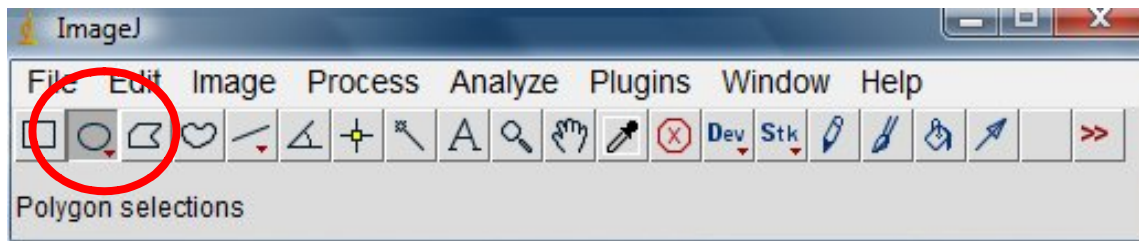
Once each side of the image has a calculated length, the sides can be multiplied together to find the surface area of the image (.9mm x .67mm = .603mm).

Combination of the Green and Red Images

Using Image J the individual combination images can be overlaid to produce an image which best represents the cells present on the vessel. Open both green and red images in Image J. Then combine by selecting Image, Color, Merge channels. A screen with pop up to select the image that represents the color channels (i.e. the title of the red image should be displayed on the red option and the green title should be under green). Finally, ensure create a composite image is checked at the bottom and push ok. This will produce a new composite image titled RGB 50%. Intensities may be adjusted to produce the most vivid picture via selecting Image, Adjust, Color Balance. Then save this image as a new composite for later use and evaluation.

Calculating the Intensity of the Image

Images were opened and analyzed in the 'Image J' program. The images were made binary, by selecting Image, Color, split channels. This created three images in grey scale of red, green, and blue select and the color of the image can be selected. Then click on the circular button:



This tool was used to circle a single cell on the image and then Analyze, Histogram was selected. The histogram will have a mean number, which is the mean intensity of the area circled. This process was repeated for five cells in the image and the numbers were averaged to get the relative intensity of all the cells.

Appendix C - Extra Data

C.1 Higher Magnification Decellularization Pictures

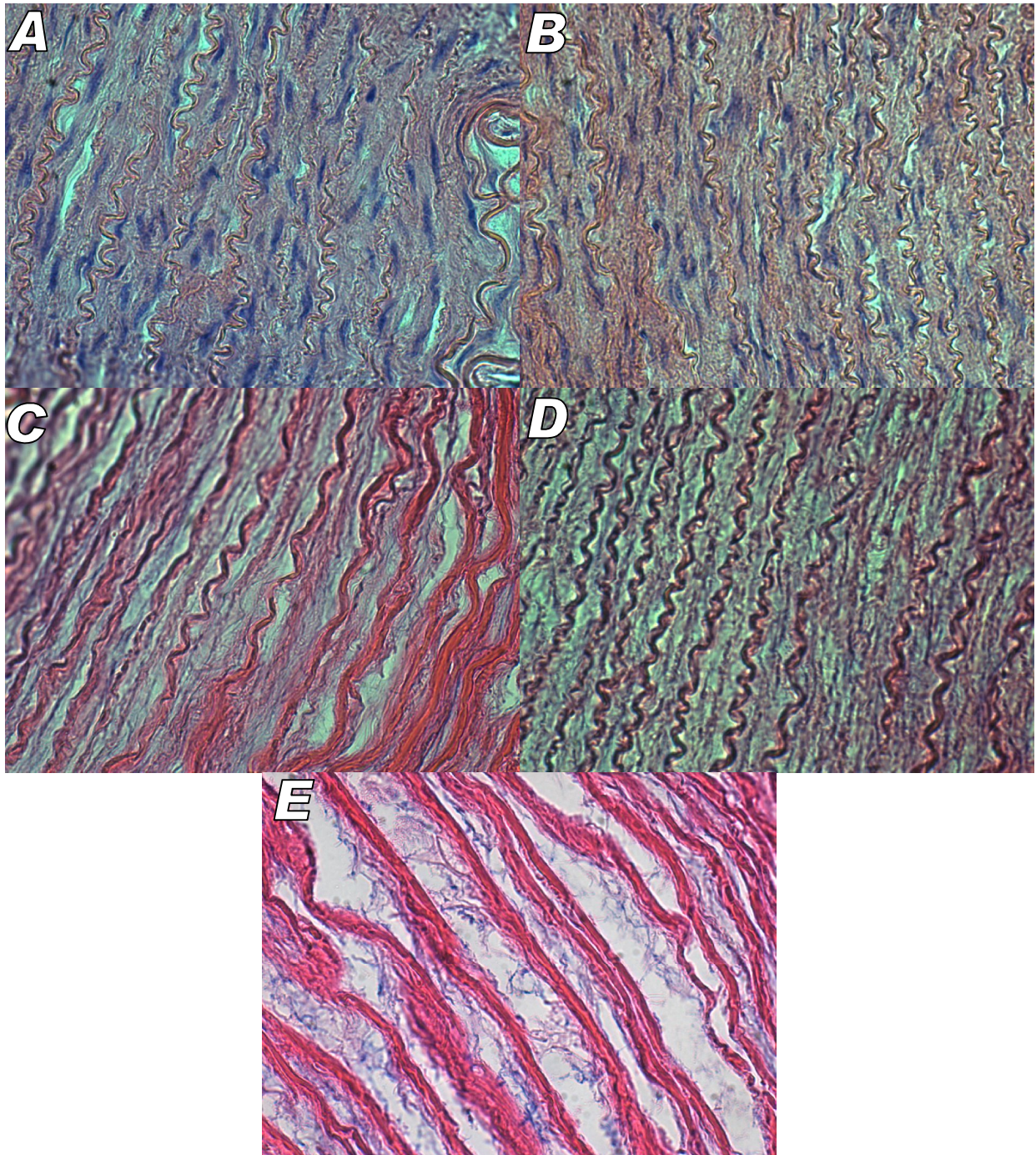


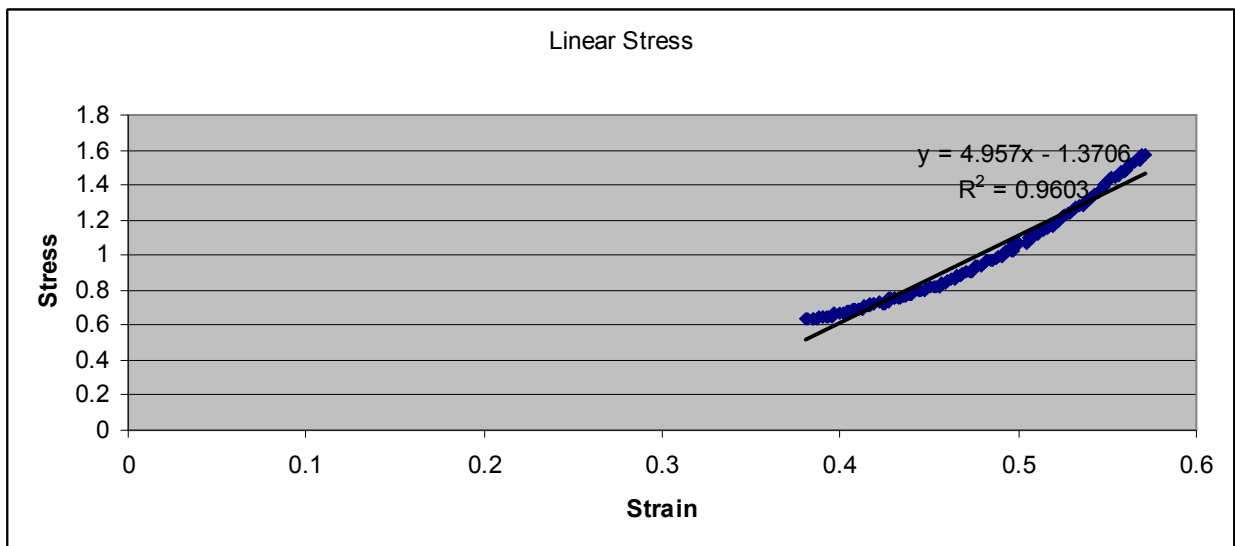
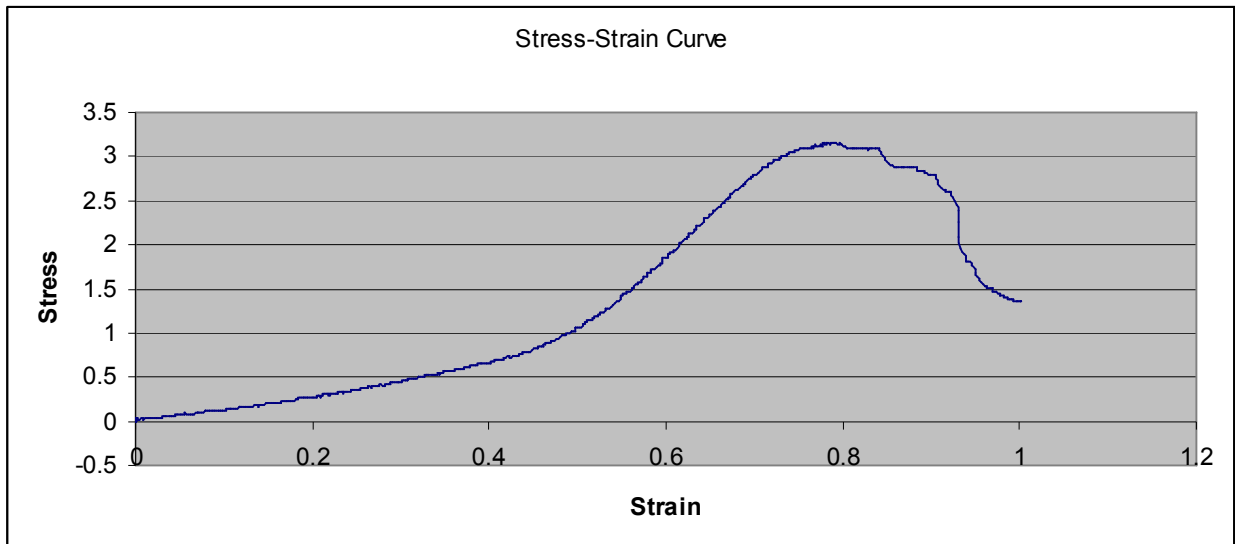
Figure C.1. Higher magnification of decellularization. Native (A), 0% SDS (B), 0.075% SDS (C), 0.01% SDS (D), and 0.0125% SDS (E). Most degradation in (E) with the most amount of SDS.

C.2 Sample Tensile Testing Data:

The original parameters are recorded then the stress and strain curve and linear elastic modulus graphs are shown directly below.

1. Por5-a (decellularized)

- a. $L_0 = 13.42\text{mm}$
- b. $W = 11.43\text{mm}$
- c. $T = 0.79\text{mm}$
- d. $D_0 = 4.11\text{mm}$



Youngs: 4.957 Mpa
Critical: 3.147311 Mpa

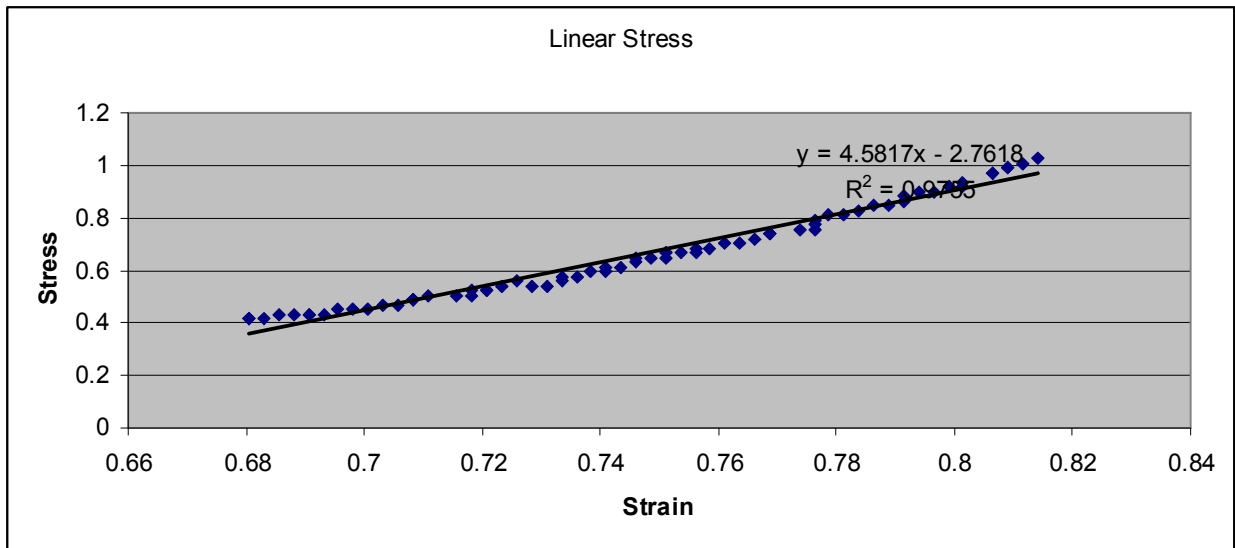
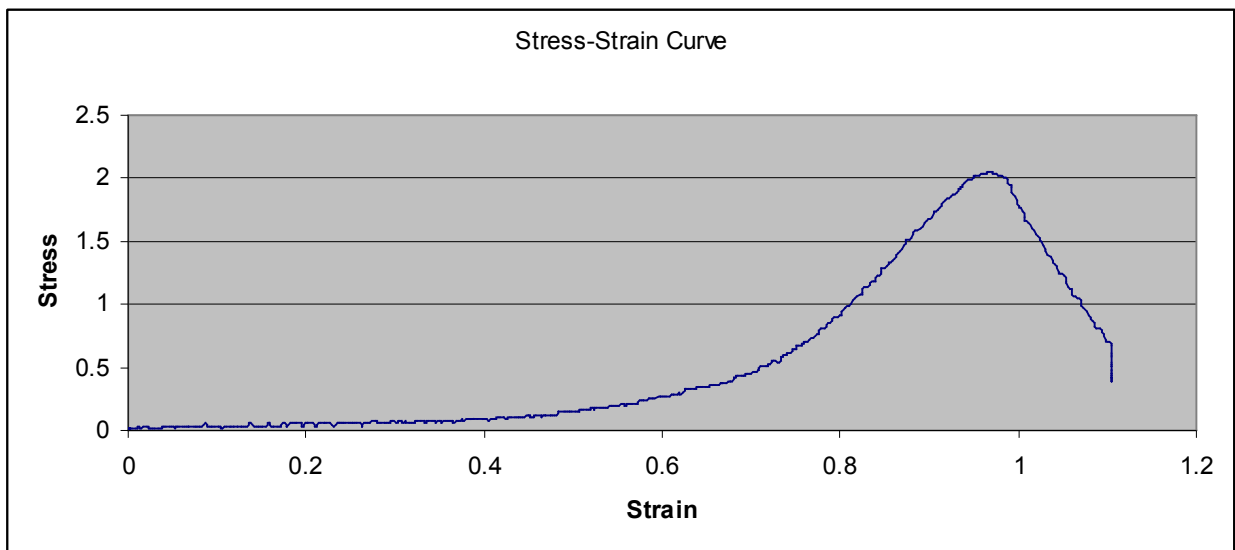
2. Por5-b (control)

e. $L_0 = 8.94\text{mm}$

f. $W = 8.14\text{mm}$

g. $T = 0.81\text{mm}$

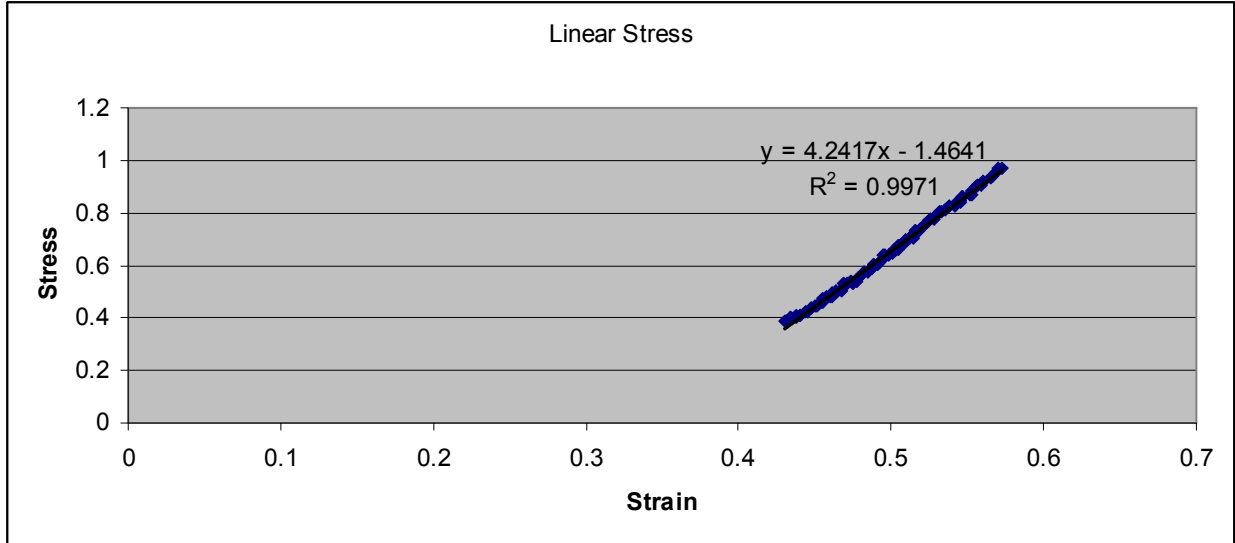
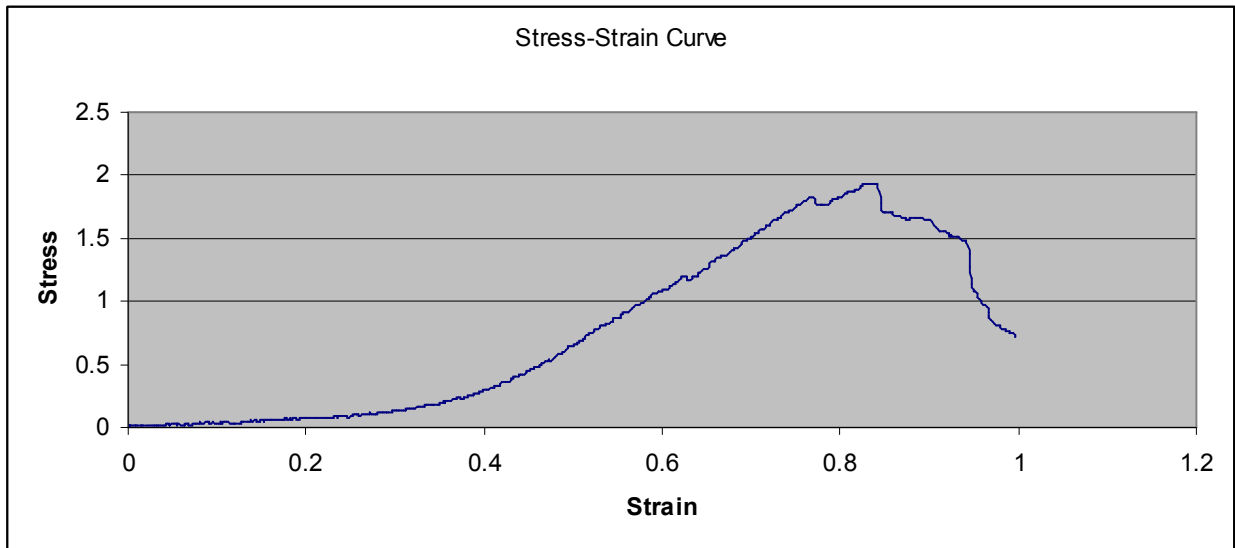
h. $D_0 = 4.14\text{mm}$



Youngs: 4.5817 Mpa
Critical: 2.05595

3. Por5-c (decellularized)

- i. $L_0=11.564\text{mm}$
- j. $W= 11.43\text{mm}$
- k. $T =0.88\text{mm}$
- l. $D_0=5.2\text{mm}$



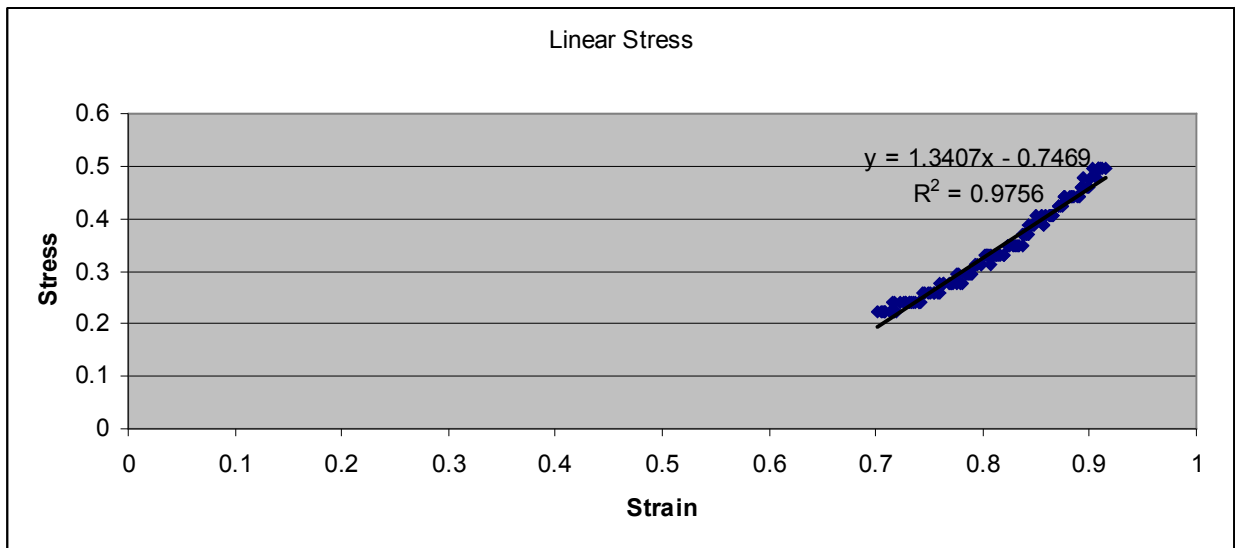
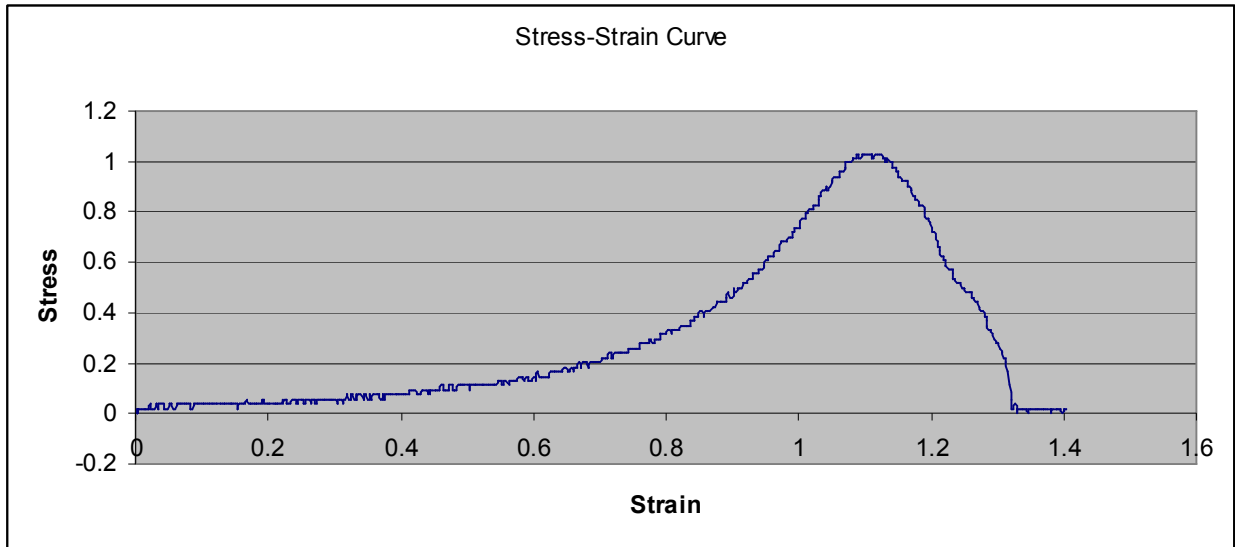
Youngs: 4.2417Mpa
Critical: 1.937376Mpa

4. Por5-d.1(control) ** Not sure if it worked on this one, was tested twice

- m. $L_0=10.17\text{mm}$
- n. $W= 9.1\text{mm}$

o. $T = 0.71\text{mm}$

p. $D_o = 4.0\text{mm}$



Youngs: 1.3407Mpa
Critical: 1.031347Mpa

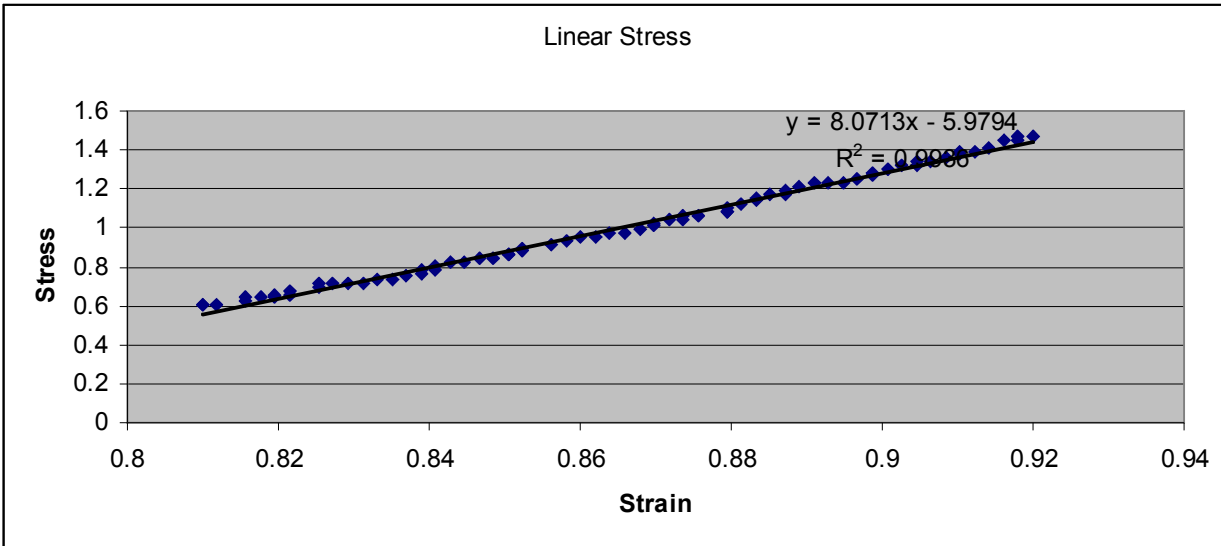
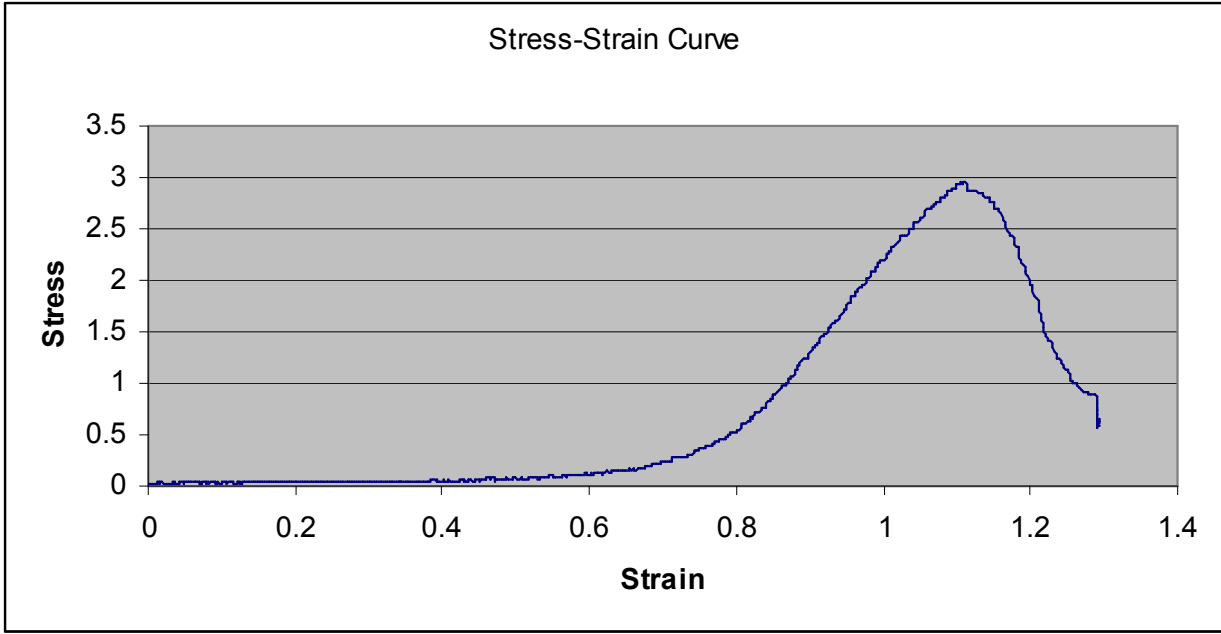
5. Por5-d.2 (control) **This was tested as well

q. $L_o = 11.67\text{mm}$

r. $W = 9.1\text{mm}$

s. $T = 0.71\text{mm}$

t. $D_o = 4.0\text{mm}$



Youngs: 8.0713 MPa
Critical: 2.961121 MPa

C.3 Summary Table of Raw Tensile Testing Data:

Table C.1. Summary of Young's Modulus and Critical Yield for Tensile Tests

Size	Treatment	Critical Yeild (Mpa)	Youngs (Mpa)
Small	Native	2.22	3.4
Small	Native	2.22	3.41
Small	Native	3.855	8.5395
Small	Native	4.5199	8.9296
Medium	Native	2.05595	4.5817
Medium	Native	1.27	8.0713
Small	decell	3.02	7.868
Small	decell	1.27	2.352
Small	decell	2.36	5.4421
Small	decell	1.23	5.1969
Small	decell	0.9814	3.262
Medium	decell	1.937376	4.957

C.4 Images and Average Cell Counts for 3T3 Sodding:

Pictures of BBI were all taken at 4x, the later the letter in the alphabet, the further distal the picture was take. Also note, that top and bottom were not specifically noted at the time of removal of the vessel.

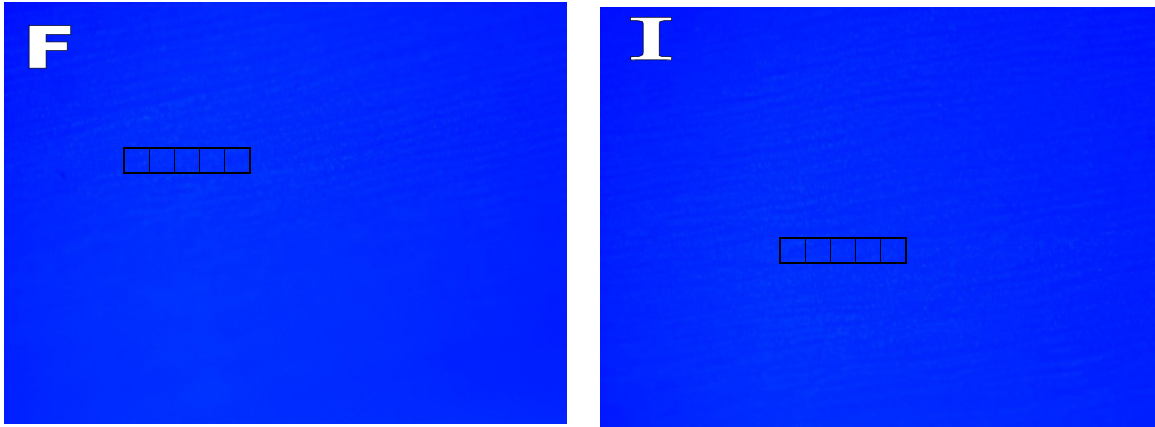


Figure C.2. Bottom A: These two pictures had the most cells, but you can clearly see that there are ridges displaying more cells

Bottom A						Avg Per square	Avg Per mm ²
	1	2	3	4	5		
A	5	13	17	13	17	13	1300
B	5	9	10	9	10	8.6	860
C	3	4	1	3	3	2.8	280
D	9	14	32	15	20	18	1800
E	6	5	9	9	8	7.4	740
F	14	14	10	17	13	13.6	1360
G	10	9	5	11	8	8.6	860
H	9	18	12	12	12	12.6	1260
I	13	13	8	12	16	12.4	1240
J	3	4	3	3	4	3.4	340
K	15	19	11	13	11	13.8	1380
						Average	1038.18182

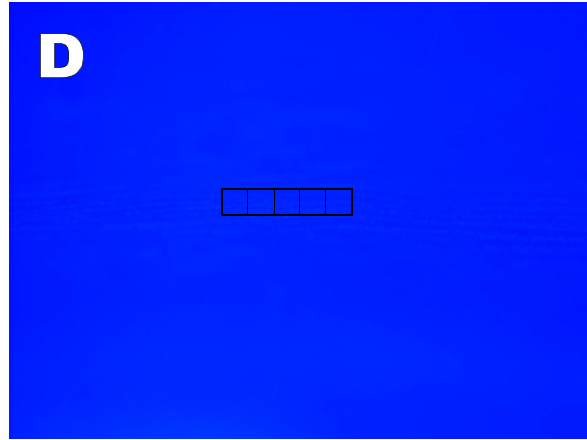
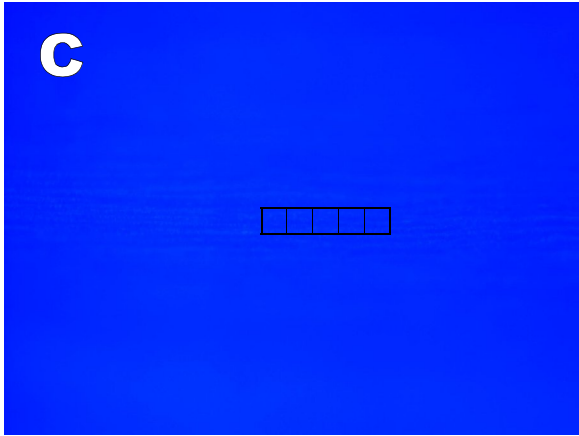


Figure C.3. Top A: These pictures were the ones with the most visible cells, the ridges are again visible with the highlighted cells.

Top A

	1	2	3	4	5	Avg Per square	Avg Per mm ²
A	4	7	10	6	8	7	700
B	15	18	15	19	7	14.8	1480
C	10	13	12	12	10	11.4	1140
D	15	17	12	10	10	12.8	1280
E	10	10	10	10	6	9.2	920
F	14	15	9	20	12	14	1400
G	9	4	10	13	5	8.2	820

Average 1105.71429

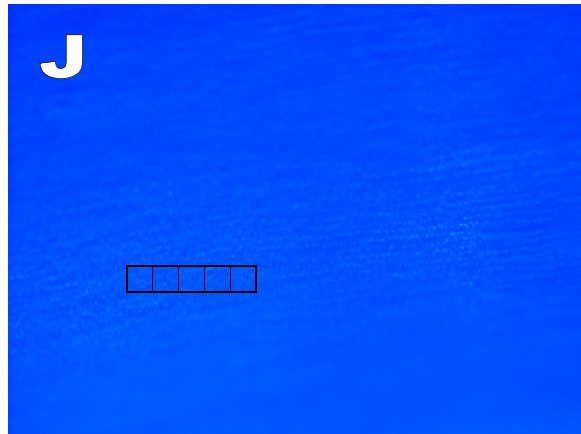
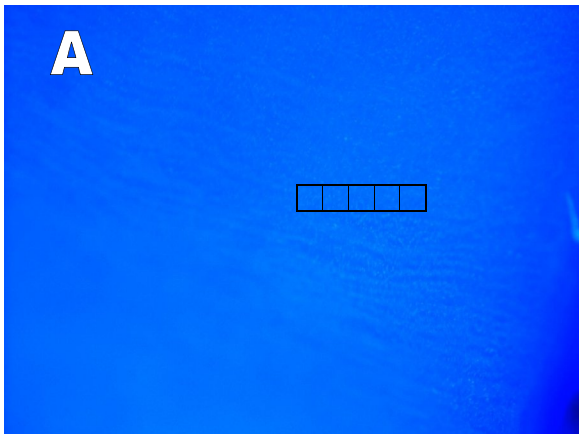


Figure C.4. Bottom B: Much more of a visible cell lining, random cell orientation

**Bottom
B**

	1	2	3	4	5	Avg Per square	Avg Per mm ²
A	25	16	26	8	19	18.8	1880
B	19	9	23	16	24	18.2	1820
C	18	16	12	20	14	16	1600
D	7	11	10	11	12	10.2	1020
E	14	14	12	20	12	14.4	1440
F	14	16	17	17	18	16.4	1640
G	14	15	21	16	13	15.8	1580
H	18	17	15	10	6	13.2	1320
I	12	18	16	13	11	14	1400
J	24	17	27	20	13	20.2	2020
K	12	12	13	12	12	12.2	1220
J	12	9	10	7	9	9.4	940
Average						1490	

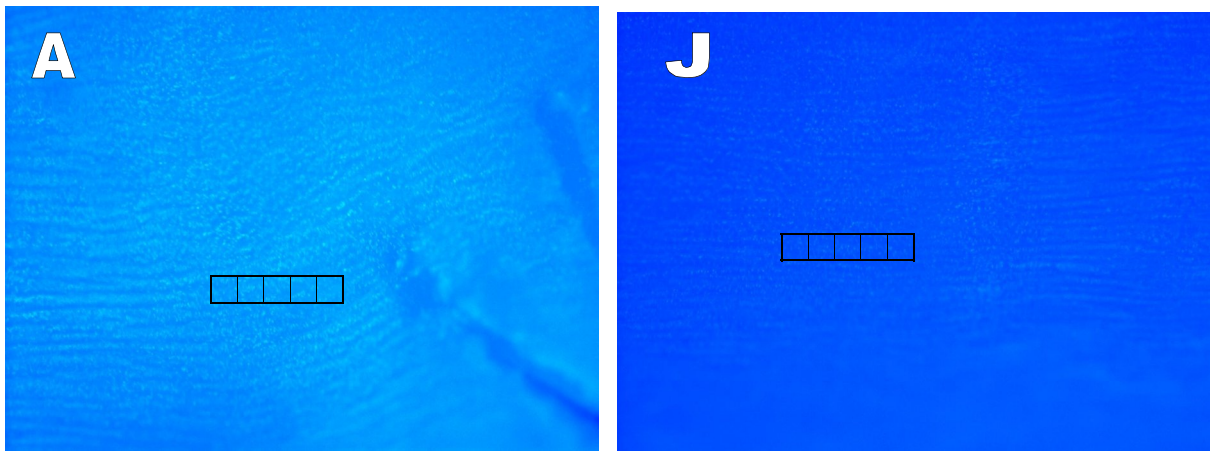


Figure C.5. Top B: Again lots of cells more randomly dispersed

Top B

	1	2	3	4	5	Avg Per square	Avg Per mm ²
A	25	21	20	24	21	22.2	2220
B	14	16	18	25	12	17	1700
C	14	12	16	15	11	13.6	1360
D	18	25	23	19	18	20.6	2060
E	13	16	9	13	10	12.2	1220
F	20	20	17	24	29	22	2200
G	18	16	11	17	15	15.4	1540
H	16	13	18	17	17	16.2	1620
I	3	9	8	6	5	6.2	620
J	19	25	22	20	17	20.6	2060
K	17	13	22	18	21	18.2	1820
Average						1674.54545	

Appendix D – CIRM Translational Project

Development of a Decellularized Aorta Coating to Improve ePTFE Polymer-Cell Interface

Aubrey Smith, Chris Miracle, and Dr. Kristen Cardinal

D1.1 Introduction

The current BVM system can utilize both polymer (ePTFE or PLGA) and biologic scaffolds, however none of which present the ideal model. The polymer scaffolds do not mimic the natural compliances and lack native biological components to encourage cell adhesion. Biologic scaffolds, such as the decellularized construct described here, cannot be consistently reproduced and limits the capacity for a high throughput system. The ideal scaffold would contain the best of each scaffold; one that is consistent in size and strength, has the capacity to mimic native compliances, and has biologic components. Several of these improvements are possible by using the decellularized material as a complex tissue specific biological coating on a polymer scaffold. This combination utilizes the polymer scaffold as a high throughput model and when coated with the extracellular matrix (ECM) from a decellularized artery, the unique biological components to aid in cell adhesion.

As a California Institute of Regenerative Medicine (CIRM) intern, the opportunity arose to be immersed in cutting edge stem cell research. Dr. Christman's lab at the University of California, San Diego is focused on designing scaffolds for cardiac tissue engineering. The lab has a particular interest in decellularized tissues as a naturally derived matrix for cell cultivation. These decellularized tissues contain the appropriate chemical and biological components to mimic the native environment and incorporate a diverse range of proteins. Dr. Christman's lab has shown preliminary results for the matrix's ability to naturally differentiate stem cells using a decellularized tissue matrix as an extracellular matrix coating for cell culture substrates. The ultimate goal of the research during the internship was to enhance stem cell differentiation into

cardiac lineages using decellularized tissue matrices. Dr. Chrisman et al. have done several experiments and published on numerous uses for the decellularize materials. It is from the work done in this internship that the coating method can be used as a translation project with the BVM system.

Most recently, DeQuach et al. were able to see cell maturation of committed skeletal myoblast progenitors when cultured on muscle-specific ECM (1). The decellularized composed of a complex mixture of peptides from a variety of collagens and proteoglycans such as decorin, dermatopontin, heparan sulfate, and lumican. In addition, a Blyscan assay for glycosaminoglycan (GAG) content measured $16.8 \pm 0.1 \mu\text{g}$ of GAG/mg of ECM. Proteoglycans and GAGs are known to play an important role in binding growth factors *in-vivo*. Preliminary data demonstrates that the decellularized skeletal muscle can be processed into an soluble, and retains a complex mixture of ECM components (1). *In-vitro*, skeletal muscle matrix has shown to enhance differentiation of C2C12 skeletal myoblasts compared to the standard collagen coating (Figure D.1). Skeletal myoblasts were also shown to preferentially migrate towards the skeletal matrix compared to controls of collagen alone, fetal bovine serum (FBS, a known chemo-attractant), and pepsin using a trans-well migration assay. Migration towards the matrix was also tissue specific, with myoblasts migrating towards skeletal versus the similarly processed cardiac and brain matrix. This *in-vitro* data demonstrates that this soluble form of skeletal matrix can both attract and enhance differentiation of skeletal muscle progenitors (2). This complex composition varies between tissue types thus, providing a unique advantage over other more simple coatings.

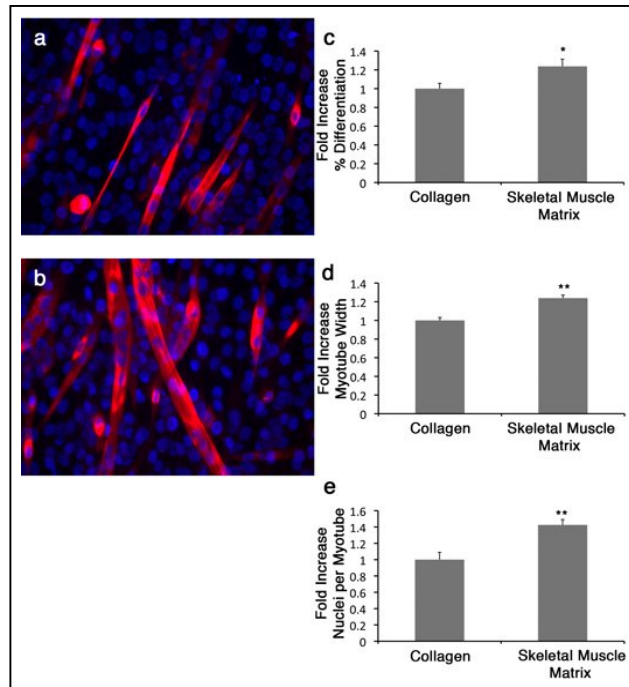


Figure D.1. The improvement of Skeletal Myoblasts on Decellularized Skeletal Matrix. A shows myoblasts on collagen and B are myoblasts on Skeletal Muscle Matrix, labeled by myosin heavy chain (red) and Hoechst (blue). C. is the percent differentiation, D is the change in width of the myotube, and E is the number of nuclei per myotube (2).

The work done by DeQuach et al., provided the motivation of this proof-of-principle experiment, to evaluate coating the decellularized ECM from pig aortas on polymer scaffold to improve the polymer-cell interface. To assess the effectiveness and potential benefits of applying a porcine ECM coating onto the scaffold, sodding efficiency and cell viability assays were performed. The efficiency assay determined the number of cells incorporated into the scaffold as a percentage of the total initial cell-sodding count. The viability assay used a live and dead stain analysis to calculate the percentage of live cells remaining on the scaffold after three days.

D.2 Methods

D.2.1 Decellularization Coating

Aorta ECM was isolated by decellularizing porcine aorta. The vascular tissue was decellularized (see Figure D.2) using a techniques modified from the originally published methods from Singeliyn et al. for myocardial matrix (3). Briefly, the freshly excised tissue was chopped into 2 mm pieces; then the tissue was washed in millipore water. The tissue was then agitated in 1% sodium dodecyl sulfate (SDS) and 1% penstrep in phosphate buffered saline (PBS) solution at 100 mg per 1000 mL for 20 hours (Figure D.2). Finally, decellularized vascular tissue was rinsed in millipore water to remove the SDS for 10 minutes 5 times. The decellularized ECM was desiccated (Figure D.2) and then milled to create a powder, followed by enzymatic digestion using pepsin, creating a solubilized vascular matrix (Figure D.2). Pepsin (SIGMA, St. Louis, MO) was dissolved in 0.01 M hydrochloric acid (HCl) to make a concentration of 1 mg/mL. Approximately 10 mg of the ECM was digested in 1 mL of pepsin solution under constant stirring. After approximately 56 hours, the matrix was diluted using 0.1 M acetic acid to make a 1–2.5 mg/ml concentration of decellularized aorta coating. This solution was used to the coat ePTFE scaffold for 1 h at 37°C, followed by rinsing with PBS (2). Each scaffold was denucleated and sterilized with EtOH prior to ECM coating. Each scaffold was placed in 70% EtOH for 15 min and then in 100% EtOH for 15.

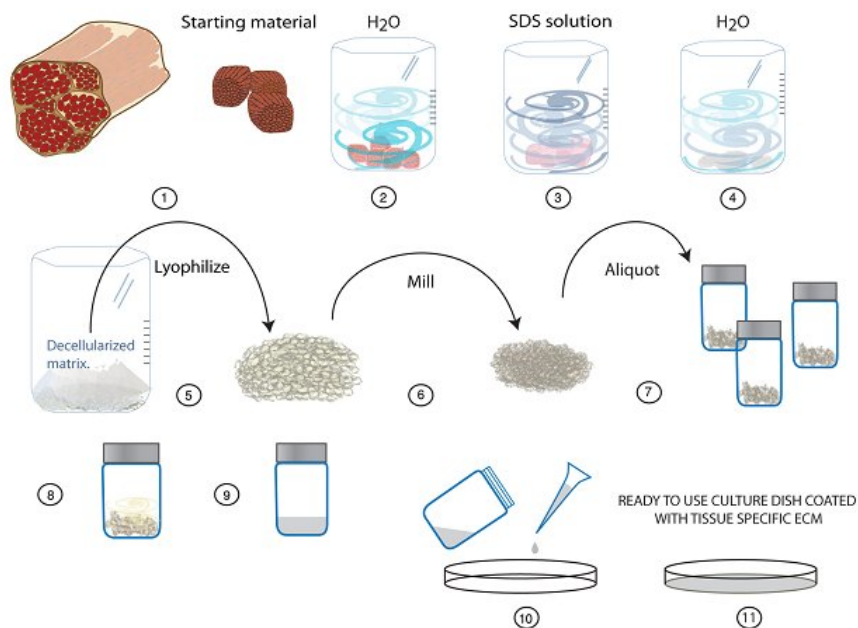


Figure D.2. The procedure for creating the decellularized coating matrix. 1) Harvest the muscle and removed the excess connective tissue. 2) Rinse with deionized water to remove blood and debris. 3) Decellularize with SDS solution for 20 hours. 4) Remove detergent by rinsing with deionized water. 5) Lyophilize the decellularized tissue. 6) Mill the decellularized tissue to create a white powder. 7) Aliquot the ECM powder was stored at -80°C for later use. 8) The ECM power digested in pepsin for 48 hours (with agitation at 60 rpm). 9) Dilute the ECM/pepsin solution in 1.0 M acetic acid to 1 mg/ml. 10) Coat the culture surface for culture for 1 hour at 37°C . 11) The surface is now ready for culture.

D.2.2 Sodding Scaffolds

A total of two BVM systems were set up with the following conditions: (1) an ePTFE scaffold that was conditioned with media, and (2) an ePTFE scaffold with the decellularized aorta coating. The denucleated scaffold (BVM setup 1) was placed in a 15ml conical with Conditioning Media (M199 and 10% Fetal Bovine Serum) in the incubator at 37°C overnight. BVM setup 2 was coated with the decellularized coating for 1 hour at 37°C and was then rinsed

several times with PBS. After each scaffold was prepared, they were inserted into the BVM system. The bioreactor was filled with Bioreactor Media, approximately 200-300 mL. A syringe was used to flush the lumen with Conditioning Media to prime the scaffold. The 2-port media reservoir was also primed with Conditioning Media. The assembled BVM system was attached to a peristaltic pump and primed with transmural flow at 150 rpm.

One week prior to set up, 10 million hUVECs were cultured for each scaffold, about one T225 flask at 80% confluency. Cells were trypsinized to detach from the culture plate and the cell suspension was spun down. The supernatant was aspirated from the cell pellet. The cells were resuspended in 4 mL of Bioreactor Media and were pressure sodding into the lumen of the scaffold. This was done by clamping the distal end of the scaffold and using a syringe, the cells were slow injected with transmural flow into the lumen. After the cells were sodded, 4 mL of Bioreactor Media was injected in a similar fashion to ensure the scaffold was pressure sodded.

The BVM system was then connected with the peristaltic pump at 7 rpm with the distal end of the scaffold clamped for transmural flow. After one hour of transmural flow, flow was redirected for luminal flow at a low flow rate. One hour post luminal flow, the media reservoir was replaced with a new conical containing HUVEC media. The bioreactor media in the original reservoir was saved for analysis in the sodding efficiency assay. The rpm of the pump was then slowly ramped up to 90 rpm in increments of 10-15 rpm every hour and was left running at 90 rpm until day 3.

D.2.3 Analysis

A sodding efficiency assay was developed to investigate the capacity for a coated scaffold increase cell adhesion during the pressure-sodding process. The sodding efficiency analysis was done using a Trypan Blue stain and a hemocytometer. Trypan Blue is a common staining agent used to calculate the number of live and dead cells in suspension. The cell counts

were taken from various solutions at three points during the experimentation: (a) the cell solution prior to sodding $\{C_i\}$, (b) the reservoir media after being switched one hour post luminal flow $\{C_r\}$, and (c) all of the media within the system at the point of take down $\{C_t\}$. The efficiency assay takes a 150 μl sample of the cell suspension and transfers it to a microcentrifuge tube containing 50 μl of Trypan Blue. 10 μl of this Trypan Blue-cell solution was pipetted onto a hemocytometer. Cell counts were taken from at least 5 squares, the following equation is used to calculate the approximate number of cells in the solution:

$$\text{Total Cell Count} = \left(\frac{\text{Total Cells Counted}}{\text{Number of Squares Counted}} \right) \times (\text{Dilution Factor}) \times (10^4) \times (\text{Cell Suspension Volume})$$

To determine the sodding efficiency, the following equation is used:

$$\text{Sodding Efficiency} = \frac{C_i - (C_t + C_r)}{C_i} \times 100$$

Once the culture was complete, the scaffolds were carefully removed from the BVM system. Using a blade, each end of the scaffold was cut from the barbs. Extra care was taken to ensure the scaffold was not compressed and the cell monolayer was altered. Once excised from the BVM, the scaffolds were cut into 4 sections (Figure D.3). Sections A and C were analyzed with bisbenzimidazole nuclear stain to identify cell consistency and distribution on the lumen of the scaffold. Then the sections were embedded for H&E analysis of the cellular monolayer as a cross section. Sections B and D were assessed using a live and dead staining on the scaffold wall as a viability assay. The assay was performed on Sections B and D to evaluate the viability of the cell population remaining on the scaffold post culturing.

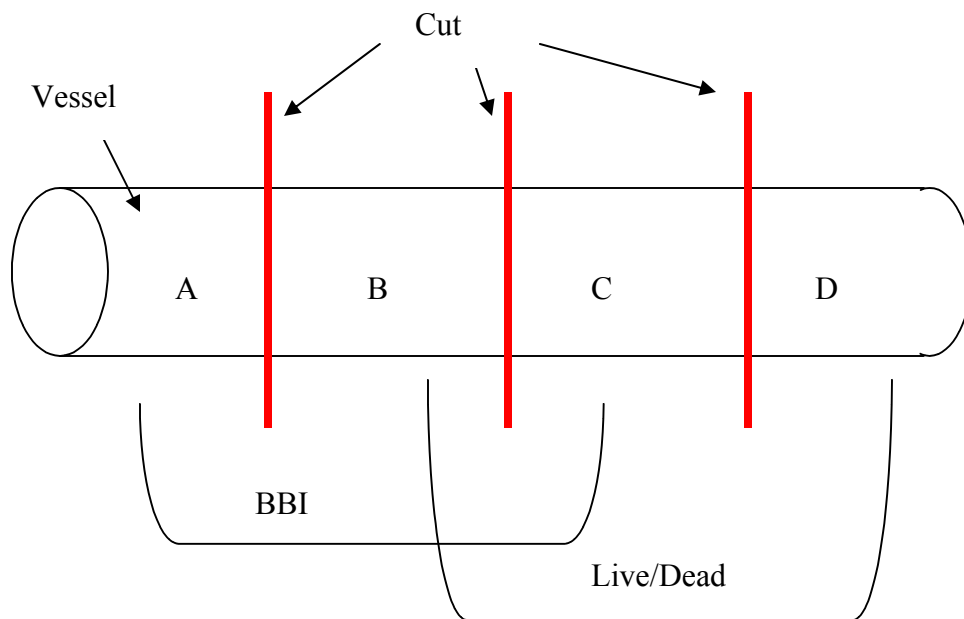


Figure D.3. Scaffold sections. A and C were imbedded for H&E analysis. B and D were assessed using a live/dead stain.

Staining Methods

The BBI stain, is a nuclear dye that attaches within the chromosomes of the cell. This is a very quick stain that is used here to simply identify the presence of cells. Sections A and C of the scaffold were fixed in 10% formalin for at least 24 hours. The scaffolds were dipped in a 1:1000 concentration of the BBI dye, diluted in Millipore water. The scaffolds were left in the solution for 15 minutes, in the dark. After staining, the scaffold was placed in covered Millipore water until imaged. After sections A and C were imaged with the BBI stain, they were processed and embedded in paraffin wax. The blocks were then cut into 6 μm sections and stained with H and E to identify the cellular lining on the scaffold.

The viability assay was developed by using a live and dead stain as a means of identifying the cell population remaining on the scaffold post culturing. The scaffold portions were fixed in histochoice for at least 30 minutes. Then the scaffolds were gently dunked into a PBS solution to rinse prior to staining. A 2 μM solution of Calcein AM and a 1 μM solution of EthD-1 was

prepared for the live and dead stain. The sections were incubated in the solution for 30 minutes in dark conditions. Once again the scaffolds were placed into PBS for imaging. The BBI and live and dead stains were performed as whole mount stains on the lumen of sections from the scaffold. Scaffolds were imaged using an Olympus BX41 microscope at 100 times magnification.

Statistical Analysis

Statistical analysis was performed using 2-sample T-tests. The difference between the original cell counts were determined by comparing the number of cells/ cm² from the coated and uncoated scaffold. Difference in sodding efficiency was determined for the coated and control groups by comparing the final sodding density (cells/cm²) based off of the results from the efficiency assay. Any difference in cell viability between the coated and control group was determined by comparing the percentage of live cells on the BVM calculated in the cell viability assay.

D.3 Results

The efficiency of the pressure sodding HUVEC into the lumen of a ePTFE scaffold was determined using the Trypan Blue stain and a hemocytometer. The cells were counted: (a) prior to being pressure sodded, (b) post luminal flow, (c) at the time of take down. The efficiency was calculated as previously mentioned. The percentage of cells remaining adhered to the scaffold post sodding and culturing was significantly increased on the coated scaffold (p-value = 0.002). The non-coated scaffold had a 35% efficiency, where as the coated scaffold had a 78% percent efficiency (Figure D.4)

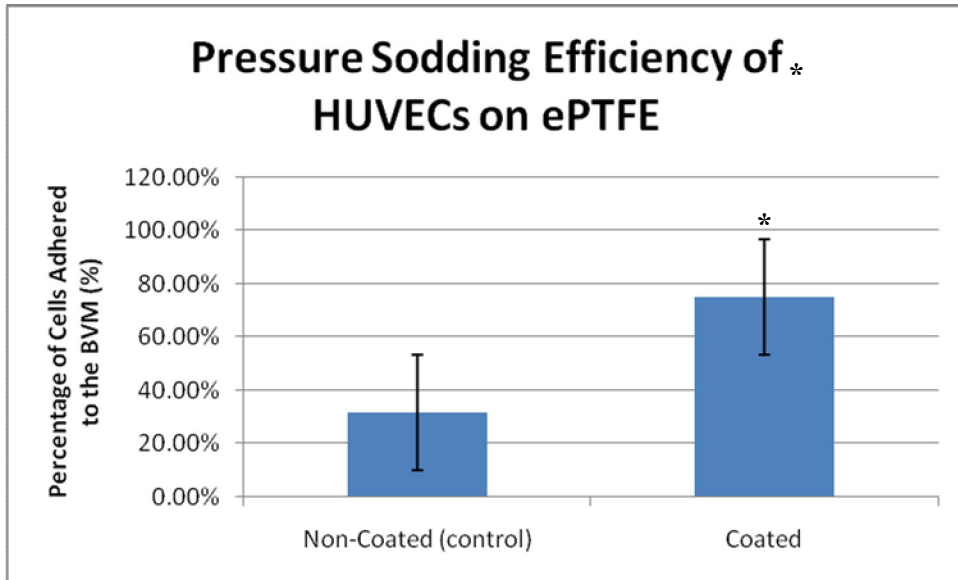


Figure D.4 Pressure sodding efficiency of HUVECs on ePTFE. The coated scaffold had a significantly greater ability to retain cells on the lumen of the scaffold (p-value = 0.002).

Sections A and C from each treatment was embedded in paraffin wax for further analysis. The scaffolds were sectioned and stained with H&E (Figure D.5). A pink lining was visualized on both scaffold, indicated cell matrix or the decellularized ECM coating remained on the lumen of the scaffold. However, there are very few identifiable purple nucli on the lumen of the scaffold. Although, as seen by the efficiency assay and confirmed with BBI staining, cells must be maintained within the scaffold. From qualitative analysis, the lining of the scaffold does not appear altered between the two treatments. To further verify the ability of the coated scaffold to increase cell adhesion, BBI stains were analyzed. The BBI stain identifies the cells and their relative location on the surface of the lumen (Figure D.6 and D.7). The primary function was to evaluate the cell consistency and disribution throughout the length of the scaffold. Figure D.6 and D.7 displays a consistent monolayer throughtout the length of both coated and non-coated ePTFE scaffolds. Additionally, these images were used to count cell density on the scaffold, as a means to quantiatively compare the treatments. There was a significant increase in the number of cells remaining on the lumen of a coated scaffold compared to the non-coated (control) scaffold (p-value = 9.54 E-5). Figure D.8 illustrates the difference in cells/cm² between each treatment.

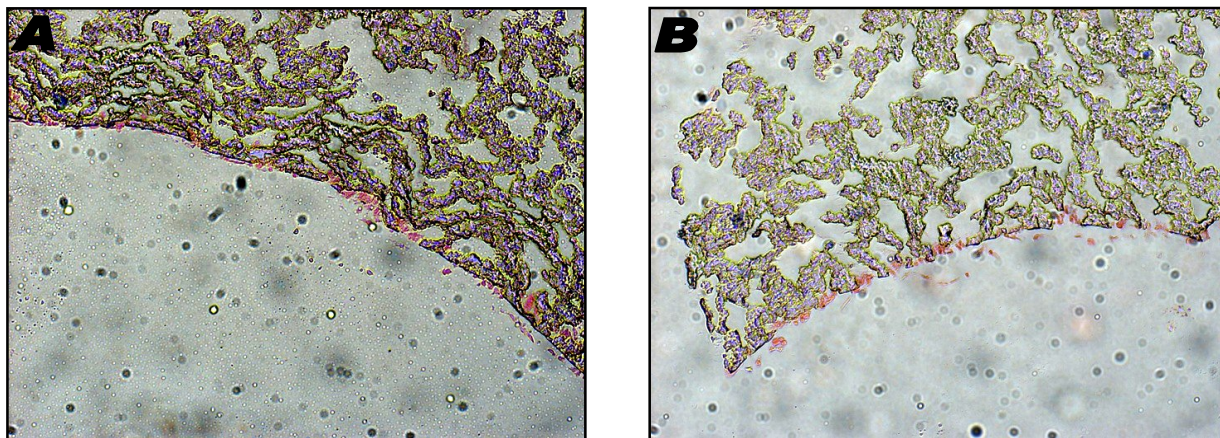


Figure D.5. H and E images of the cellularized ePTFE scaffold. Left is the control (A) and Right is the coated scaffold (B).

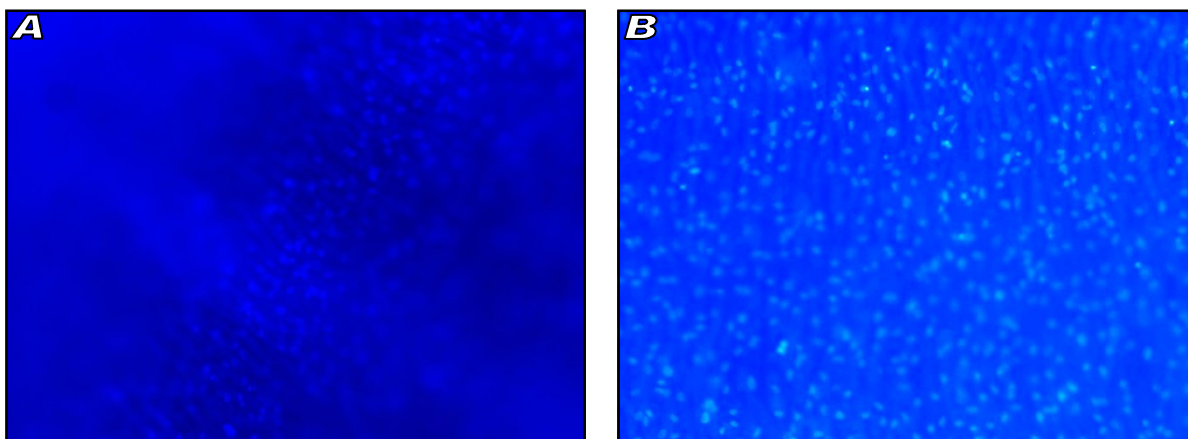


Figure D.6. BBI images of the non-coated scaffold; proximal (A) and distal (B)

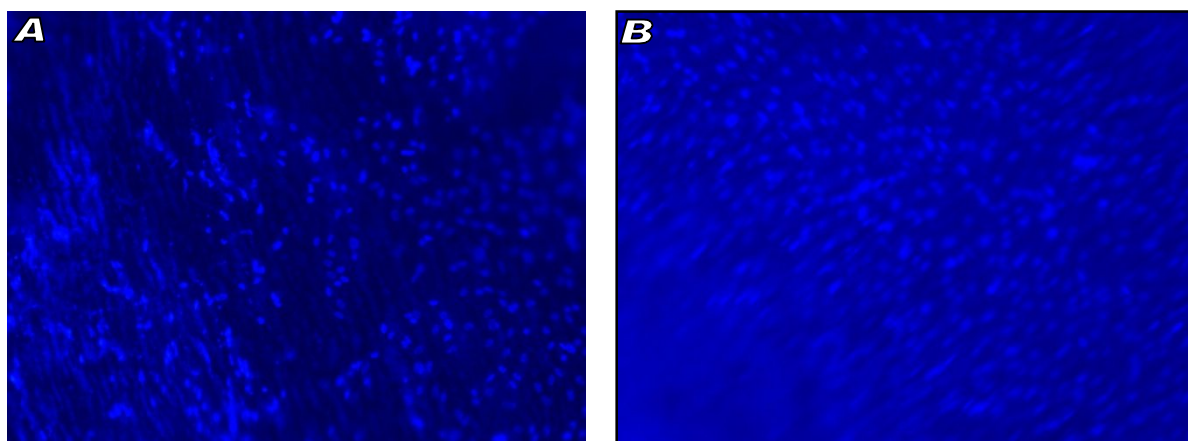


Figure D.7. BBI images of the coated scaffold; proximal (A) and distal (B)

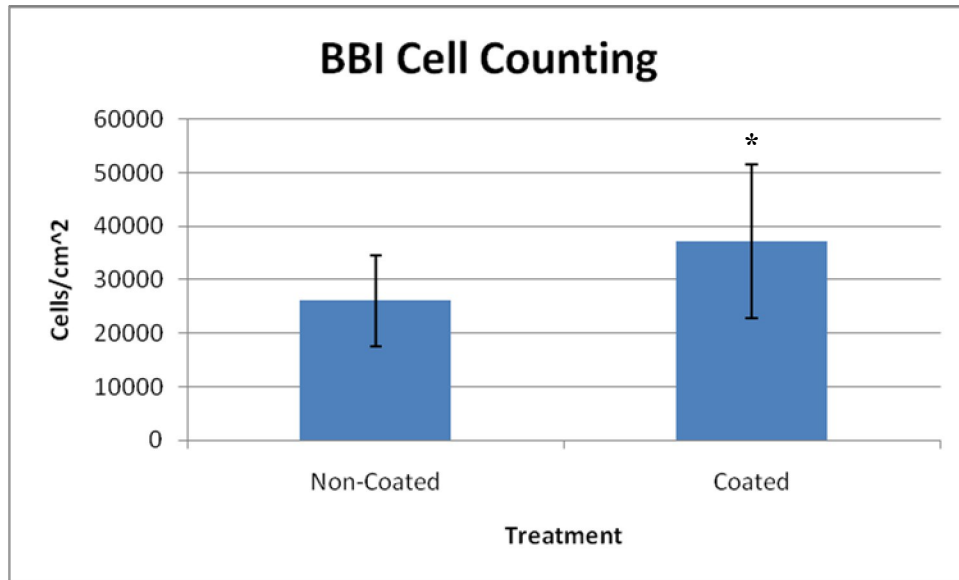


Figure D.8. BBI cell counting. Significant increase in cell numbers on the coated ePTFE scaffold (p-value = 9.54 E-5).

The live and dead stain was the last analysis performed on the scaffolds. Calcein AM and EthD-1 were used to identify the live and dead cells. Live cells were identified with Calcein AM and a green fluorophore, while EthD-1 identified dead cells with a red fluorophore. Figure D.9 are sample images from the whole mount live dead stains. With qualitative analysis, the uncoated scaffold has an increased number of red cells on the lumen of the scaffold, indicating a higher instance of cell death, compared to the coated scaffold. Additionally, these live and dead cells in these images were used to quantitatively identify the differences in cell numbers visually seen. Figure D.10 quantitatively compares the amount of live and dead cells between each the coated and non-coated ePTFE scaffolds. On both sections B and D of the scaffold, there was a significant increase in the number of live cells on the lumen of the scaffold (p-value section B = 0.041 and section D = 0.045).

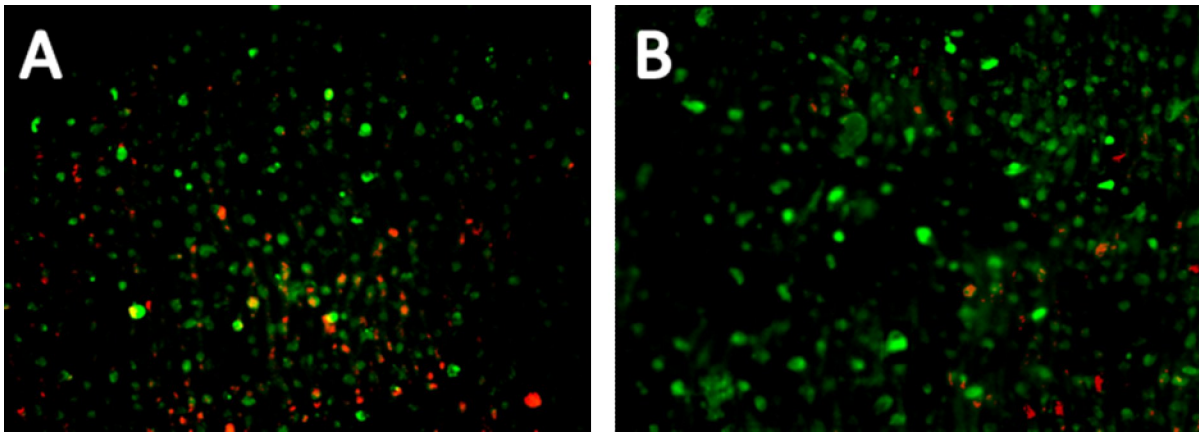


Figure D.9. Live and dead stains on the ePTFE scaffolds. Calcein AM indicated a live cell with a green fluorophor, EthD-1 identified dead cells with a red fluorophor; uncoated scaffold (A) and coated scaffold (B)

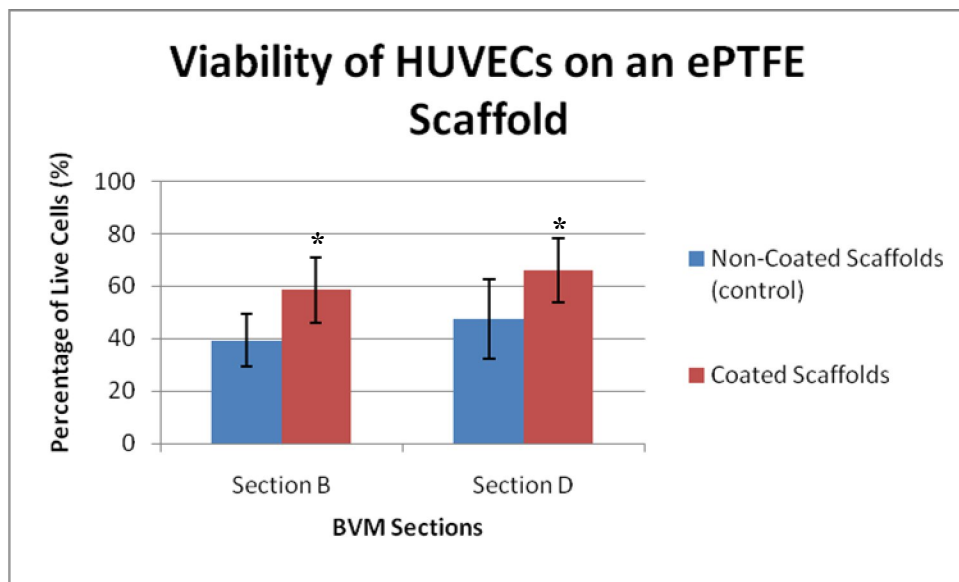


Figure D.10. Viability comparison of live HUVECs on ePTFE. P-value for section B = 0.041 and section D = 0.045.

D.4 Discussion

The BVM has been developed to bridge the gap between *in-vitro* and *in-vivo* preclinical testing of intravascular devices. To mimic a native artery, a polymer scaffold has been utilized and to recreate an endothelium, a monolayer of cells coats the lumen of the scaffold. The

polymers used in the BVM are ePTFE and PGLA; both are biocompatible and have a consistent structure. However, the scaffolds are composed of polymers and lack any biological components; which impedes with cellular adhesion properties. To improve the polymer-cell interface, protein coatings have been introduced to the polymer-cell interface. As seen from this work, a decellularized coating can be used to provide a complex combination of tissue specific proteins to the polymer. The addition of the decellularized coating was found to improve the sodding efficiency of the pressure sodding process, increase the number of cells on the lumen of the scaffold, and improve the viability of the cells which remained on the ePTFE. Indicating, the addition of the decellularized aorta coating stands to improve the polymer-cell interface of the BVM model

The sodding efficiency was assessed using Typan Blue and counting the number of cells at specific time point throughout the culture. The decellularized coating allowed more cells to be retained during the pressure sodding procedure as well as throughout the culture. There was a two fold increase in the percentage of cell remaining on the scaffold after 3 days of culture. The non-coated scaffold had approximately 38% of its original cells on the lumen; while the decellularized aorta coated scaffold retained approximately 75% of the cells. This trend was confirmed using the standard counting method of BBI staining. Rather than evaluating the percentage of cells lost during culture, the number of cells which remained on the lumen of the scaffolds was counted. Again a significant increase in the number of cells was seen on the coated scaffold with approximately 37,000 cells/cm² verses 26,000 cells/cm² observed on the non-coated scaffold. These results indicated the use of a decellularized coating on ePTFE scaffolds improves cellular adhesion.

Additionally, a viability assay was developed to asses if the decellularized coating altered the amount of live and dead cells seen on the scaffold. To create the decellularized coating,

pepsin, HCL, and acetic acid were used. The use of these harsh chemicals may have negatively affected the polymer-cell interface, by leaving residual chemicals on the scaffold. Any chemically residue would have a poor interaction with the cells, causing a decrease in cell viability. In order to prevent this from occur, after the scaffold was coating, it was rinsed several times in sterile PBS to ensure only the proteins of the decellularized matrix remained adhered to the scaffold. Live and dead staining was preformed of the cells which remained on the lumen of the scaffold after three days of culture. The staining revealed there was a significant increase in the percentage of live cells on the decellularized coating. The non-coated scaffold had approximately 43% viability, while the decellularized coating improved the viability to about 65%.

The previously discussed results are very promising however there are some limitations to the work. This was a very short proof-of-principle work that should be expanded to investigate the repeatability of the procedure and results. Additionally, this procedure should be modified to incorporate the use of PLGA scaffolds. This experimentation intended to use PLGA scaffolds in addition to the ePTFE scaffolds; however the PLGA did not interact with the decellularized coating well. As mentioned, the decellularized coating was created with the use of several harsh chemicals and the interaction with the PLGA cause the immediate dissolving of the scaffold. Thus, the PLGA scaffold was not included in this experimentation. However, the solution can be neutralized to attempt this coating experiment once more and to further investigate the utility of the decellularized coating.

These experiments have demonstrated the use of a decellularized aorta coating has the ability to improve cellular adhesion and viability on an ePTFE scaffold. The tissue specific, complex combination of proteins, proteoglycans, and glycosaminoglycans found in the decellularized aorta coating has improved the polymer surface to encourage cellular adhesion.

The increased number of cells found on the lumen improves the development of a consistent monolayer of cells on the lumen of the scaffold, thus mimicking the native endothelium.

Additionally, by enhancing the polymers ability to maintain more viable cells the ability to have a functional endothelium will be improved. In conclusion, the use of a decellularized coating has the potential to vastly improve the polymer-cell interface of the scaffolds used in the BVM system.

References:

1. DeQuach JA, Mezzano V, Miglani A, Lange S, Keller GM, Sheikh F, et al. Simple and high yielding method for preparing tissue specific extracellular matrix coatings for cell culture. PLoS One.5:e13039.
2. DeQuach J, Mezzano V, Miglani A, lange S, Keller G, Sheikh F, et al. Simple and High Yielding Method for Preparing Tissue Specific Extracellular Matrix Coatings for Cell Cuture. PloS One.5:11. 2010.
3. Singelyn JM, DeQuach JA, Seif-Naraghi SB, Littlefield RB, Schup-Magoffin PJ, Christman KL. Naturally derived myocardial matrix as an injectable scaffold for cardiac tissue engineering. Biomaterials.30:5409-16. 2009.